TECHNISCHE UNIVERSITÄT DRESDEN

Transport of *Enterococcus faecalis* JH2-2 through sandy sediments

A combined experimental and modelling approach

Cumulative Dissertation

by

Aparna Chandrasekar, M. Sc.

Faculty of Environmental Sciences

Technische Universität Dresden

TECHNISCHE UNIVERSITÄT DRESDEN

Institute of Groundwater Management and Institute of Hydrobiology

Faculty of Environmental Sciences, Technische Universität Dresden

Transport of *Enterococcus faecalis* JH2-2 through sandy sediments

A combined experimental and modelling approach

Cumulative Dissertation

to obtain the degree Doctor rerum naturalium (Dr. rer. nat)

at the Technische Universität Dresden.

Author:

Aparna Chandrasekar, M. Sc.

Born on 23 June 1991, at Srirangam, Tamil Nadu, India.

Committee Chair: Prof. Dr. rer. nat. habil. Thomas U Berendonk, Head of Institute, Institute of Hydrobiology, Technische Universität Dresden.

Principal Supervisor and Reviewer: Prof. Dr. habil. Rudolf Liedl, Former Head of Institute, Institute of Groundwater Management, Technische Universität Dresden.

Reviewer: Prof. Dr. Traugott Scheytt, Head of the Chair of Hydrogeology and Hydrochemistry, TU Bergakademie Freiberg.

Reviewer: Prof. Dr. Gertjan Medema, Chief science officer & Principal microbiologist at KWR Watercycle Research Institute, Part-time Chair on Water & Health at Delft University of Technology.

Date of Submission: 22 March 2022.

Date of Defense: 20 September 2022.

Keywords: Process model, rodeo, ecological models, wastewater reuse, column experiment, dissolved oxygen, *Enterococcus*, bacteria, R-software, risk assessment

Contents

List of Figures

List of Tables

List of Abbreviations

1-D	One-dimensional
ADE	Advection-dispersion equation
AR	Antibiotic Resistance
ARB	Antibiotic resistant bacteria
ARG	Antibiotic resistant gene
BATH	Bacterial Adhesion to Hydrocarbons
BHI	Brain Heart Infusion
C1	Condition 1
C2	Condition 2
C3	Condition 3
C4	Condition 4
CFU	Coliform units
DO	Dissolved oxygen
EU	European Union
FAO	Food and Agriculture Organisation
FIB	Faecal indicator bacteria
JRC	Joint Research Center
REV	Representative elementary volume
SCHEER	Scientific Committee on Health, Environmental and Emerging Risks
TWW	Treated waste water
UN	United Nations
VBNC	Viable but non-culturable
WHO	World Health Organization
WWTP	Wastewater treatment plant

List of Symbols

A	cross-sectional area of the column (cm^2)
α	longitudinal dispersivity (cm)
C	concentration in water phase ($mg\ L^{-1}$, $CFU\ mL^{-1}$)
C_o	concentration (microsphere or bacteria) at the start of the experiment ($mg\ L^{-1}$, $CFU\ mL^{-1}$)
C_R	normalised concentration in water phase (-)
C_{RS}	normalised Concentration in sediment phase (-)
C_s	concentration in sediment phase ($mg\ g^{-1}$, $CFU\ g^{-1}$)
d	diameter of column (cm)
d_p	diameter of particle (μm)
d_g	sediment grain diameter (mm)
Da_d	damkoehler number for decay process (-)
Da_r	damkoehler number for respiration process (-)
$Da_{att_{C1}}$	damkoehler number for attachment process for condition C1 (-)
$Da_{att_{C3}}$	damkoehler number for attachment process for condition C3 (-)
$Da_{g_{C2}}$	damkoehler number for growth process for condition C2 (-)
$Da_{g_{C4}}$	damkoehler number for growth process for condition C4 (-)
Da_{str}	damkoehler number for straining process (-)
F_{fast}	"fast" flow velocity represented by 0.13 $cm\ min^{-1}$
F_{med}	"medium" flow velocity represented by 0.078 $cm\ min^{-1}$
F_{slow}	"slow" flow velocity represented by 0.02 $cm\ min^{-1}$
K_{att}, K_{att}(C1),$K_{att_{C1}}$	attachment rate for condition C1 (min^{-1})
$K_{att_{O2}}$, K_{att}(C3), $K_{att_{C3}}$	attachment rate for condition C3 (min^{-1})
L	length of column (cm)
μ	dynamic viscosity
μ_d	decay rate (min^{-1})
μ_g, μ_g(C2), $\mu_{g_{C2}}$	growth rate for condition C2 (min^{-1})
$\mu_{g_{O2}}$, μ_g(C4), $\mu_{g_{C4}}$	growth rate for condition C4 (min^{-1})
μ_{gs} (C2), μ_{gs} (C4)	growth rate in sediment phase for condition C2 and C4 respectively (min^{-1})
μ_r	respiration rate rate (min^{-1})

Pe	peclet number (-)
pv	pore volume (-)
q, v_d	darcy velocity ($cm\ min^{-1}$)
Q	flow rate ($cm^3\ min^{-1}$)
Re	reynolds number (-)
REV	representative Elementary Volume (-)
ρ, ρ_b	bulk density ($g\ cm^{-3}$)
ρ_s	grain density ($g\ cm^{-3}$)
t	time (minutes)
t_o	time at the start of the experiment (t=0) (minutes)
θ_e	effective porosity (-)
θ_t	total porosity (-)
v	average linear flow velocity ($cm\ min^{-1}$)
W_i	dry weight of the sediment before filling column (g)
W_f	dry weight of the sediment after filling column (g)
x	discretised length (cm)
x_o	inlet point of the column (x=0) (cm)

Summary

The agricultural sector is one of the largest consumers of fresh water. With the ever-increasing problem of water scarcity, urbanization, over-population, and climate change, fresh water resources used by agriculture could be put to better use by redirecting it for drinking water purposes. In this context, many countries reuse treated urban waste water for irrigation, to overcome this problem. While this is a sustainable practice, the reuse of urban wastewater could facilitate the spread of pathogenic bacteria (or antibiotic resistant bacteria) in the subsoil region and consequently the groundwater. Since groundwater is one of the main sources of drinking water, the contaminants could pose a risk to human health. Furthermore, obtaining scientific data for emerging contaminants during water reuse is the need of the hour.

The objective of this work is to build a mechanistic model that can aid in the development of large-scale risk assessment models; thus facilitating the setup of water reuse regulations for the relevant pathogenic organisms. In the present study, process based models were developed and evaluated using lab scale results. Then, the relative time scales of the processes are compared, and the relative importance of the various process studies are assessed. When assessing time scales of the processes, it is kept in mind that processes with relatively fast time scales can be approximated using equilibrium models, relatively slow processes can be neglected, and only the rate limiting processes can neither be neglected or further simplified in further model development. Therefore, an idea of the rate limiting processes assessed in lab scale can serve as important tools facilitating model simplification when evaluating larger scale models.

A combined experimental and modelling approach has been used to study relevant transport and reactive processes during bacteria transport through sandy sediments. The mechanistic model contained transport processes which were implemented using the advective dispersive equation. An additional straining process was added using non-linear rate law. The biological processes of decay, respiration, attachment, and growth were expressed using linear rate laws. This mechanistic model was verified using data from fully water saturated, sediment packed lab-scale column experiments. Continuous injection of tracer, microspheres, and *Enterococci* (in water environments with and without dissolved oxygen and nutrients) was performed. The experiment was verified for three

flow velocities (0.13, 0.08 and 0.02 $cm\ min^{-1}$), and the parameter values were compared for these flow velocities using dimensionless numbers. The linear rate coefficients were converted to a dimensionless form (Peclet and Damkoehler numbers respectively) to facilitate the comparison of processes across the various flow velocities.

The results indicate that the processes of attachment and growth are flow dependent. Furthermore, in the presence of dissolved oxygen, attachment of bacteria to sediment was the most influential process. Sensitivity analysis showed that the parameters representing growth and respiration were influential, and care must be taken when using the results for field-scale experiments or models.

These processes and parameters add new knowledge on the impact of urban wastewater reuse on the spread of pathogenic bacteria (especially resilient species like *Enterococci*), and emphasizes the importance of research in this area. Future work could focus on obtaining data from culture independent methods and extension of the model framework, and include (where necessary) non-linear rate laws. This will provide a critical pathway to developing a decision support framework for use by regulatory frameworks, policy makers, stakeholders, local and global environmental agencies, World Health Organization, or the United Nations.

Zusammenfassung

Der Agrarsektor ist einer der größten Verbraucher von Süßwasser. Angesichts der zunehmenden Wasserknappheit, der Verstädterung, der Überbevölkerung und des Klimawandels könnten die von der Landwirtschaft genutzten Süßwasserressourcen besser genutzt werden, indem sie für Trinkwasserzwecke umgewidmet werden. In diesem Zusammenhang verwenden viele Länder aufbereitetes kommunales Abwasser für die Bewässerung, um dieses Problem zu lösen. Dies ist zwar eine nachhaltige Praxis, aber die Wiederverwendung von kommunalem Abwasser könnte die Ausbreitung pathogener Bakterien (oder antibiotikaresistenter Bakterien) im Untergrund und damit im Grundwasser fördern. Da das Grundwasser eine der Hauptquellen für Trinkwasser ist, könnten diese Schadstoffe eine Gefahr für die menschliche Gesundheit darstellen. Darüber hinaus ist es ein Gebot der Stunde, wissenschaftliche Daten über neu auftretende Verunreinigungen bei der Wasserwiederverwendung zu gewinnen.

Ziel dieser Arbeit ist es, ein mechanistisches Modell zu erstellen, das bei der Entwicklung groß angelegter Risikobewertungsmodelle behilflich sein kann und somit die Aufstellung von Vorschriften für die Wiederverwendung von Wasser für die relevanten pathogenen Organismen erleichtert. In der vorliegenden Studie wurden prozessbasierte Modelle entwickelt und anhand von Ergebnissen im Labormaßstab bewertet. Anschließend werden die relativen Zeitskalen der Prozesse verglichen und die relative Bedeutung der verschiedenen Prozessstudien bewertet. Bei der Bewertung der Zeitskalen der Prozesse wird berücksichtigt, dass Prozesse mit relativ schnellen Zeitskalen durch Gleichgewichtsmodelle angenähert werden können, relativ langsame Prozesse können vernachlässigt werden, und nur die ratenbegrenzenden Prozesse dürfen in der weiteren Modellentwicklung weder vernachlässigt noch vereinfacht werden. Daher kann eine Vorstellung von den ratenbegrenzenden Prozessen, die im Labormaßstab bewertet werden, als wichtiges Instrument zur Vereinfachung des Modells bei der Bewertung von Modellen in größerem Maßstab dienen.

Ein kombinierter experimenteller und modellierender Ansatz wurde verwendet, um relevante Transport- und reaktive Prozesse während des Bakterientransports durch sandige Sedimente zu untersuchen. Das mechanistische Modell enthielt Transportprozesse, die mit Hilfe der Advektions-Dispersions-Gleichung implementiert wurden. Ein zusätzlicher

Filtrationsprozess ("straining") wurde mit Hilfe nichtlinearer Ratengesetze hinzugefügt. Die biologischen Prozesse des Zerfalls, der Atmung, der Anhaftung und des Wachstums wurden durch lineare Ratengesetze ausgedrückt. Dieses mechanistische Modell wurde anhand von Daten aus vollständig wassergesättigten, sedimentgefüllten Säulenexperimenten im Labormaßstab verifiziert. Kontinuierliche Injektion von Tracer, Mikrosphären und *Enterokokken* (in Wasserumgebungen mit und ohne gelösten Sauerstoff und Nährstoffe) wurde durchgeführt. Das Experiment wurde für drei Strömungsgeschwindigkeiten (0,13, 0,08 und 0,02 $cm\ min^{-1}$) verifiziert, und die Parameterwerte wurden für diese Strömungsgeschwindigkeiten anhand dimensionsloser Zahlen verglichen. Die linearen Ratengesetze wurden in eine dimensionslose Form umgewandelt (Peclet- bzw. Damköhler-Zahlen), um den Vergleich der Prozesse bei den verschiedenen Strömungsgeschwindigkeiten zu erleichtern. Die Konzentrationen wurden in regelmäßigen Abständen sowohl am Einlass als auch am Auslass der Kolonnen gemessen. Die überprüften Prozesse waren Advektion, Dispersion, Filtration, Zerfall, Atmung, Wachstum und Anhaftung. Der Versuch wurde für drei Strömungsgeschwindigkeiten (0,13, 0,08 und 0,02 $cm\ min^{-1}$) wiederholt, und die verifizierten Parameterwerte wurden für diese Strömungsgeschwindigkeiten verglichen.

Die Ergebnisse zeigen, dass die Prozesse der Anhaftung und des Wachstums strömungsabhängig sind. Darüber hinaus war bei Vorhandensein von gelöstem Sauerstoff die Anhaftung der Bakterien an das Sediment der einflussreichste Prozess. Die Sensitivitätsanalyse zeigte, dass die Parameter, die das Wachstum und die Atmung repräsentieren, einflussreich sind, so dass bei der Verwendung der Ergebnisse für Experimente oder Modelle im Feldmaßstab Vorsicht geboten ist.

Diese Prozesse und Parameter liefern neue Erkenntnisse über die Auswirkungen der Wiederverwendung von kommunalem Abwasser auf die Ausbreitung pathogener Bakterien (insbesondere widerstandsfähiger Arten wie *Enterokokken*) und unterstreichen die Bedeutung der Forschung in diesem Bereich. Zukünftige Arbeiten könnten sich auf die Gewinnung von Daten aus kulturunabhängigen Methoden und die Erweiterung des Modellrahmens konzentrieren und (wo nötig) nichtlineare Parameter einbeziehen. Dies wird einen entscheidenden Weg zur Entwicklung eines Rahmens für die Entscheidungsfindung darstellen, der von Regulierungsbehörden, politischen Entscheidungsträgern, Interessengruppen sowie lokalen und globalen Umweltbehörden, der Weltgesundheitsorganisation oder den Vereinten Nationen genutzt werden kann.

Chapter 1

Introduction

1.1. Broad Scope

Climate change supplemented with an increase in population has put pressure on freshwater sources worldwide [Lavrnić et al., 2017]. The Sustainable Development Goals developed by the UN in 2015 elucidate the need for eradicating extreme poverty and hunger (Goal 1) and providing clean water and sanitation to all (Goal 6, [Assembly, 2015]), by the year 2030. Reusing treated wastewater (TWW) for irrigation and, or aquifer recharge is one way to achieve these goals. TWW passing through constructed wetlands or agricultural fields use the natural filtration process of the soil to filter out contaminants and recharge the groundwater table. Constructed wetlands consistently provide a reduction of 90–99% (1–2 log-removal) in the concentration of fecal indicators such as coliform bacteria and fecal streptococci [Ghermandi, Bixio, Traverso, et al., 2007]. Additional advantages of TWW reuse for irrigation lie in the high nutrient concentration (e.g., in urban wastewater), which serves as fertilization for crops, possibly eliminating or reducing the need for artificial fertilization [Ghermandi, Bixio, and Thoeye, 2007; Ghermandi, Bixio, Traverso, et al., 2007].

Knowledge on wastewater reuse is a concept accumulated with the history of humankind [Angelakis et al., 2018]. Records show that the ancient Greeks were among the first to use wastewater in agriculture [Angelakis et al., 2018]. Water reuse evolved from then and eventually declined in the late 19th century, owing to the development of intensified wastewater treatment methods [Angelakis et al., 2018]. However, with time, factors like population growth, high birth rates, climate change, and rapid technological advancement led to the rebirth of wastewater reuse around the 1900s [Angelakis et al., 2018]. Today, many countries have adopted the practice of reusing TWW for agriculture, industry, and managed aquifer recharge [Angelakis and Gikas, 2014; Bixio et al., 2006; Chanan and Woods, 2006; Jiménez and Asano, 2008; Khan and Anderson, 2018; Lavrnić et al., 2017; Salgot and Folch, 2018].

Countries like China [Chang and Ma, 2012; K. Smith et al., 2018], Japan [Asano and Levine, 1996], Australia [Chanan and Woods, 2006; Khan and Anderson, 2018; Radcliffe, 2006], Tunisia [Bahri and Brissaud, 1996], Israel [Haruvy, 1998], and USA [Asano, 2005] have adopted TWW for potable and non-potable water reuse. In Europe, the applications of TWW reuse are primarily in agricultural - in the Mediterranean region, and industrial sectors - in northern Europe [Bixio et al., 2005; Bixio et al., 2008; Brissaud, 2008; Consoli et al., 2012; Ghermandi, Bixio, and Thoeye, 2007; Janosova et al., 2006; Lavrnić et al., 2017; Lazarova et al., 2001; Mizyed, 2013; Molinos-Senante et al., 2011; Paranychianakis et al., 2015]. Water reuse projects have been successful in several Mediterranean countries where it serves as the only significant and low-cost alternative resource for irrigation [Ghermandi, Bixio, Traverso, et al., 2007]. It is estimated that by the year 2040, treated sewage effluent will become the main source of water for irrigation in Israel and the Palestinian autonomous regions, supplying approximately 70% of the water used for irrigation [Haruvy, 1998].

Various factors, including the risks resulting from pathogen exposure, nutrients, heavy metals, and salinity resulting from TWW reuse, have been widely addressed in guidance documents and regulations [Helmecke et al., 2020]. However, the hazards from organic micro-contaminants appear to be less in the spotlight [Helmecke et al., 2020]. With many water reuse projects gaining prominence in various sectors, there is a consistent lack of unified guidelines for the minimum water quality that is required for each type of reuse [Bixio et al., 2006]. The Joint Research Center (JRC) of the European Commission identified current significant knowledge gaps for organic micro-contaminants, specifically their role in agriculture, exposure pathways in the environment, and the impacts of long-term exposure on human health [Alcalde-Sanz and Gawlik, 2017]. A risk management approach was proposed to address these issues [Alcalde-Sanz and Gawlik, 2017]. This approach was also recommended in a report by the Scientific Committee on Health, Environmental and Emerging Risks (SCHEER), where antibiotic resistance was indicated as a contaminant of emerging concern [Rizzo et al., 2018].

The World Health Organization (WHO) and Food and Agriculture Organization (FAO) have provided specific guidelines of water quality criteria for contaminants that can be present in food crops [World Health Organisation, 2006; Ayers and Westcot, 1985]. However, these are not necessarily followed by each country [Brissaud, 2008]. For example, France, Tunisia, regions in Spain, and Sicily in Italy have adopted the water quality criteria suggested in the WHO guidelines [Brissaud, 2008]. In contrast, other countries like Cyprus, Italy, and Israel elaborated regulations or policies close to the more conservative California's Water Recycling Criteria [Asano, 1993; Brissaud, 2008].

Social and political challenges are vital in developing a common regulation for water quality standards for reuse [Cipolletta et al., 2021; Ricart and Rico, 2019]. While many countries want relaxed water quality standards for reuse, certain countries still cope with societal challenges in adopting TWW for potable or drinking water use [Fawell et al., 2016; Paranychianakis et al., 2015]. Therefore, a unified approach to determine minimum water quality standards based on scientific data for various contaminants in water reuse settings must be sought after [Angelakis et al., 1999; Cipolletta et al., 2021; Kellis et al., 2013; Shoushtarian and Negahban-Azar, 2020].

1.2. Hypotheses and Research objectives

Reuse of urban wastewater for irrigation could serve as a pathway for the spread of antibiotic resistance in the environment [Berendonk et al., 2015; Kampouris, Klümper, et al., 2021]. In this context, mechanistic models verified with processes relating to bacteria transport are instrumental [Berendonk et al., 2015]. Evaluating mechanistic models using data from controlled lab-scale experiments is the first step to understanding the risks of pathogen transport through the subsoil. Small-scale models can guide building processes and parameters (at larger scales) with correlated effects.
Bacteria disseminate in soil by advection and dispersion while being subjected to effects like filtration, adsorption, desorption, growth, decay, sedimentation, and chemotaxis [Abu-Ashour et al., 1994]. Although many species of microorganisms have been used in column experiments, very few studies have incorporated growth and decay terms into the mathematical model, probably owing to the considerable complexity of the numerical modeling due to the bacterial growth and decay term [Ding, 2010]. This study investigates the effect of water quality parameters on the processes related to bacterial migration through sandy sediments to fill in this knowledge gap. The factors considered essential for this study were dissolved oxygen (DO) concentration, nutrient concentration, and water flow velocity [Asano and Levine, 1996]. Based on this, three hypotheses were formulated and investigated within the scope of this work. They are:

1. The absence of dissolved oxygen plays a key role, even for facultative anaerobes.

2. Bacterial growth is not an important process when small concentrations of nutrients are present in the water.

3. Linear rate laws are sufficient to describe biological processes for laminar flow velocities.

A step-wise combined experimental and modeling approach is used to verify the aforementioned hypotheses. A flexible modelling framework is developed in *R* [R Core Team, 2020]. The model is verified using lab-scale sediment packed, water-saturated, continuous flow column experiments. The parameters for the biological processes (represented using linear rate laws) are compared for the various conditions and flow velocities studied. The four objectives formulated for this research study are:

1. Establish transport processes using salt tracers and microspheres;
2. Determine processes relating to *Enterococcus faecalis* JH2-2 under varying DO and nutrient concentrations;
3. Investigate and compare processes and process rates resulting from varying DO and nutrient concentration for three flow velocities, within laminar flow region; and
4. Conduct an uncertainty analysis to determine the influential parameters and assess the model's applicability for field-scale predictions.

This mechanistic model will serve as a starting point for risk assessment models that can be used to compare or predict field-scale scenarios qualitatively (as has been previously suggested by Abu-Ashour et al., 1994).

1.3. Outline of the work

The main results from this study are already published (Chapters 3 and 4) in two journal papers. The overall research study has been divided into five chapters.

Chapter 1: Introduction
The chapter illustrates the background of the work under the broad scope of wastewater reuse for agriculture and aquifer recharge. Water reuse as a means to combat water scarcity and improve food security has been emphasized. The need for scientifically backed reasoning to set guidelines for water reuse for various applications is needed. The research gaps are highlighted, and the objectives of the work are described.

Chapter 2: Concepts, Terminologies and Methodology
The chapter illustrates the concepts and terminologies used in this study. Column design standards, materials used, and the rationale for the same have been explained. The

transport and reactive processes studied and their context in wastewater reuse has been elaborated. Furthermore, the *R* packages that have been used in the model development have been described.

Chapter 3: Reactive-transport modelling of *Enterococcus faecalis* JH2-2 passage through water saturated sediment columns
The research article presented here [Chandrasekar et al., 2021b] probes into the combined experimental and modeling approach used to study the biological processes of attachment, respiration, growth, and decay when bacteria suspended in varying DO, and nutrient environments are injected into a water-saturated sediment column. A predictive model analyzing the risk of groundwater contamination in field-scale has been presented. In addition, an uncertainty analysis has been conducted, indicating influential parameters that must be carefully measured in field scenarios. The primary take-home message from this study is that changes in dissolved oxygen concentrations significantly impact bacteria survival in subsoil environments.

Chapter 4: Determining the impact of flow velocities on reactive processes associated with *Enterococcus faecalis* JH2-2
The research article presented here [Chandrasekar et al., 2021a] investigated the impact of flow rates (hydraulic loading rates) on the processes of straining, attachment, respiration, and growth. Flow rates determine the retention time of the bacteria in the subsoil or sediment. While first-order rate coefficients sufficiently describe the processes as mentioned earlier for relatively "fast" and "medium" flow rates, the "slower" flow rates often require an alternative model formulation for the process of growth. Beyond a specific flow rate, the processes are intensified for the growth process. The primary take-home message from this study is that flow velocities impact various biological processes in a non-linear manner, and parameters relating to each flow velocity must be carefully measured.

Chapter 5: Synthesis
In this chapter, the main findings are elucidated. The primary conclusions derived from both research works are explained. The state of the hypotheses is evaluated, and a critical review of the results and discussion are also presented. Based on the critique, pathways for future work are suggested.

Chapter 2

Concepts, terminologies, and methodology

2.1. Concepts and terminologies

2.1.1. Background

Groundwater constitutes 97% of freshwater sources available worldwide, with over 75% of EU inhabitants depending on groundwater as a drinking water source [European Commission and Directorate-General for Environment, 2009]. Reusing TWW for irrigation can enable crop yield, and recharge the groundwater table [Vergine, Lonigro, et al., 2017; Asano, 2005]. However, pathogenic bacteria could find their way into drinking water or food crops through this water reuse cycle (Figure 2.1, [Asano and Levine, 1996]) in turn causing a risk to human health. Specifically, the spread of antibiotic resistance [Alcalde-Sanz and Gawlik, 2017; Rizzo et al., 2018] in the water reuse cycle has gained importance, over the years [Alcalde-Sanz and Gawlik, 2017]. Since groundwater moves slowly through the subsurface, the impact of anthropogenic activities may last for a relatively long time [European Commission and Directorate-General for Environment, 2009]. Coupling transport processes with biological processes [Huertas et al., 2008; Sen et al., 2005] can be beneficial in quantitatively assessing the factors influencing pathogen transport.

Microbes are highly responsive to the environment around them. Therefore studying the environmental factors impacting the fate of pathogens during the wastewater reuse cycle could provide considerable insight into the microbial processes occurring during subsoil passage of these pathogenic bacteria [Holden and Fierer, 2005]. Some of the factors impacting microbes in the vadose zone are the availability of water [Stevik et al., 2004], terminal electron acceptors [Hornberger et al., 1992], nutrients [Cunningham et al., 2007; Stevik et al., 2004], pH, cell size and shape [Bai et al., 2016; Fontes et al., 1991;

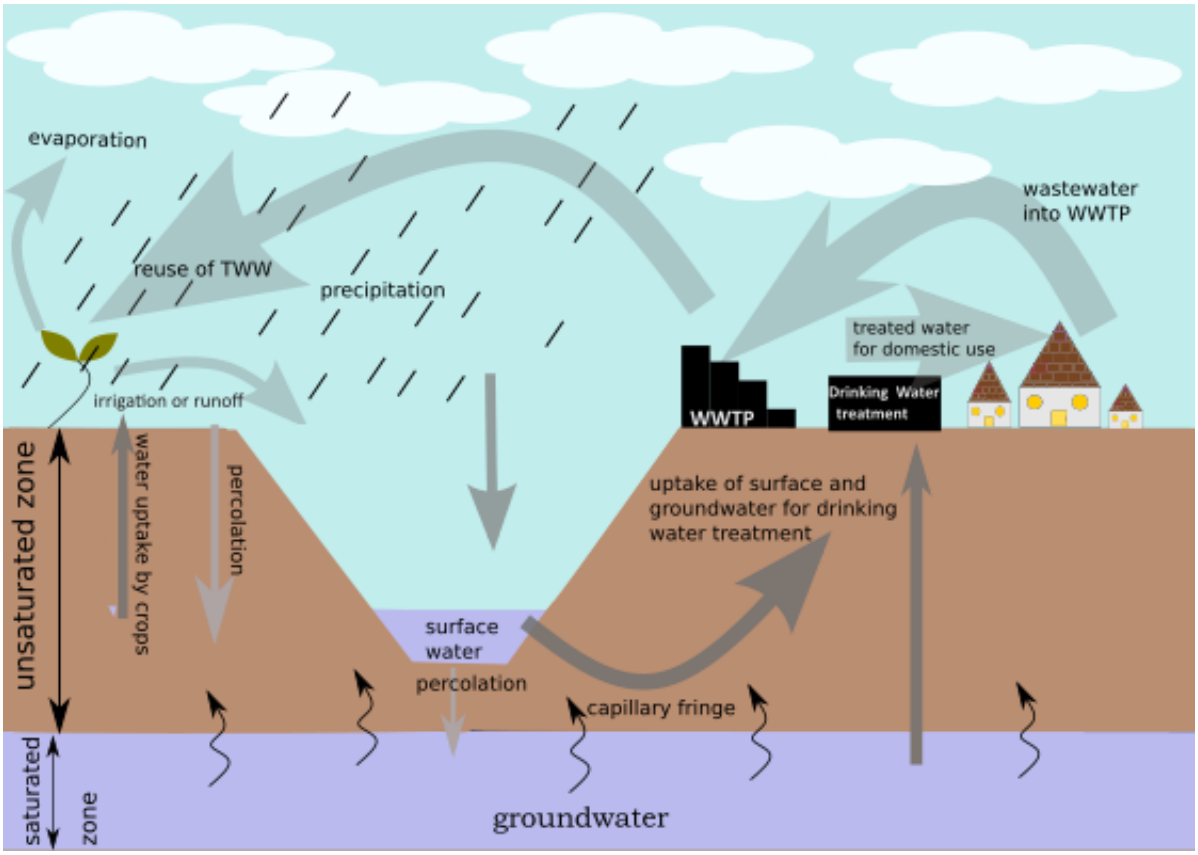

Figure 2.1: Wastewater reuse cycle adopted from Asano and Levine, 1996

Hornberger et al., 1992; McCaulou et al., 1994; Stevik et al., 2004; Weiss et al., 1995], soil characteristics [Bai et al., 2016; Fontes et al., 1991; Hornberger et al., 1992; McCaulou et al., 1994; Silliman et al., 2001; Stevik et al., 2004], presence of plants, microbial community of the soil, presence of other microorganisms, water flux, and temperature, to name a few [Abu-Ashour et al., 1994; Holden and Fierer, 2005; Jamieson et al., 2002]. The processes that are commonly modelled based on the aforementioned parameters are microbial inactivation, immobilisation [Hornberger et al., 1992], decay, filtration [Stevik et al., 2004], growth, attachment [Cunningham et al., 2007; Johnson et al., 1995; McCaulou et al., 1994], detachment [Johnson et al., 1995; McCaulou et al., 1994] and straining [Stevik et al., 2004]. The Section 2.2 elaborates all the processes that were investigated in the context of this study.

The surface of sediments can be very well aerated, with oxygen concentration being nearly equal to atmospheric concentrations as in the case of sandy sediments [Holden and Fierer, 2005]. However, deeper soil layers, especially layers closer to the groundwater table, could be anaerobic or anoxic [Holden and Fierer, 2005]. Nevertheless, various resilient pathogenic species could still survive in such harsh environments. Considering these factors, this study focuses on the risks posed by persistent bacteria in harsh

conditions.

2.1.2. The vadose zone

The study of water infiltration in sediment and soil environments has intrigued scientists and researchers for many decades [Šimůnek and van Genuchten, 2016]. More commonly known as the vadose zone, the subsoil area lies between the soil's surface and the groundwater table [Šimůnek and van Genuchten, 2016]. This zone hosts a variety of microbes that can be critical in determining the attenuation of the contaminants before reaching the groundwater [Šimůnek and van Genuchten, 2016; Feddes et al., 2004]. The vadose zone comprises the water-unsaturated or variably water-saturated zones [Šimůnek and van Genuchten, 2016]. The water-unsaturated or variably water-saturated zone is characterized by the pore space in the soil matrix comprising of both water and air (Figure 2.2a), with the volumetric water content possibly changing with time [Nimmo, 2006]. A fully water-saturated zone is characterized by the pore space being filled with water (Figure 2.2b). These anaerobic zones are usually found close to the groundwater table [Holden and Fierer, 2005]. The saturated zone (Figure 2.1) is characterised by the absence of air and is typically groundwater. High variability within soil matrices makes studying processes in the subsoil region very complex. Therefore, much data encompassing soil heterogeneity must be factored in when modelling biological processes. Especially, the interface between water-air could play a vital role in determining some critical rate-limiting processes for water-unsaturated and variably water-saturated media [Schäfer et al., 1998]. The setup of a steady-state flow and uniform water-unsaturated flow condition can be a considerable challenge [Schäfer et al., 1998]. Since the focus of this work was to study and set up biological processes, the hydraulic model and the corresponding experimental setup consider water-saturated conditions (Section 2.3).

2.1.3. Porosity and pore models

Porosity is an essential parameter for the characterization of packed sediment [Issaadi et al., 2018]. It corresponds to the volume of interstices that can contain fluid, related to the total volume of the material [Issaadi et al., 2018]. During contaminant transport in the vadose zone, water and solute flow through the pore space in the soil. The pore system, considered as a communicating or not communicating pores network, can be decomposed into several classes of porosity [Issaadi et al., 2018]. The communicating pores form the "effective" porosity, which is the porosity that takes into account the volume of accessible or connected pores [Issaadi et al., 2018]. On the other hand, the

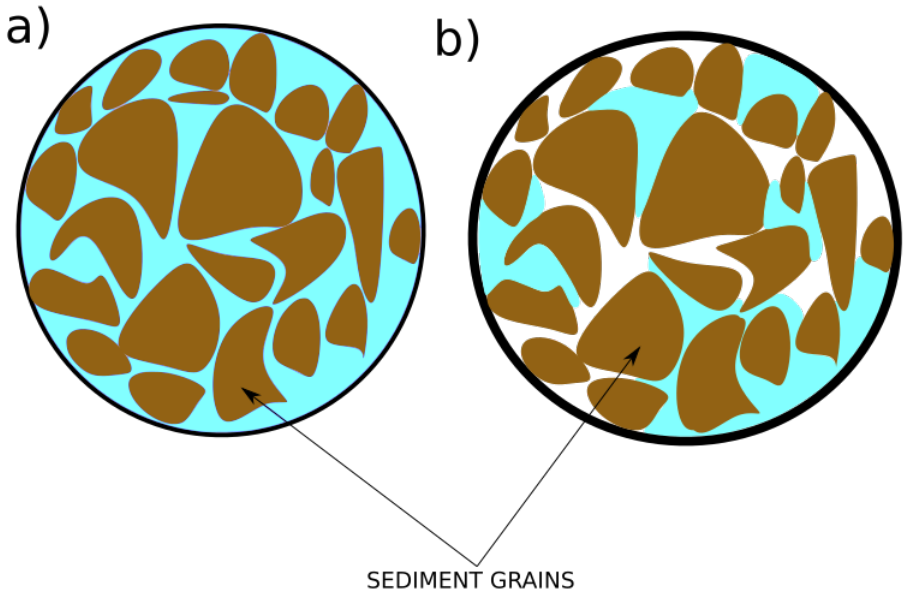

Figure 2.2: Representation of a horizontal cross-section of a pore space when it is (a) fully water saturated, and (b) unsaturated. Please note that the brown color represents the sediment grains, blue represents water and white represent air.

"residual porosity" constitutes the occluded pores, without communication with the rest of the pore spaces and the outside [Issaadi et al., 2018]. This type of porosity is not involved in the mass transfer phenomenon but does contribute towards the total porosity of the system [Issaadi et al., 2018].

Water and solute transport in fully water-saturated soils or sediments can be described using conceptual pore models. Single-porosity, dual-porosity (multi-porosity), and dual-permeability (multi-permeability) models can be used to describe the water-unsaturated or water-saturated zones [Figure 2.3, Šimůnek and van Genuchten, 2016]. Single-porosity models (Figure 2.3a, Šimůnek and van Genuchten, 2016) assume that a single pore system exists that is fully accessible to both water and solute. The single porosity model describes a pore space, where (assuming no solute-soil interactions) water and solute move together within the pore network at a uniform speed [Šimůnek and van Genuchten, 2016]. Here, there is a negligible difference between the effective and total porosity of the pore system. Dual-porosity and dual-permeability models assume that the porous medium consists of two interacting pore regions. Dual-porosity pore models assume that either only solute interacts with the immobile water (Figure 2.3b, Šimůnek and van Genuchten, 2016), or both solute and water interact with the immobile water (Figure 2.3c, Šimůnek and van Genuchten, 2016) contained in part of the pore space. Finally, a dual-permeability model consists of a network of pores where one or more (in the case of multi-porosity pore models) pore networks are associated with slower flower

velocities through which both water and solute move and, can be exchanged (Figure 2.3d, Šimůnek and van Genuchten, 2016). Dual-porosity and dual-permeability models can be extended into multi-porosity and multi-permeability models wherein many pore types and networks exist that interact with each other [Šimůnek and van Genuchten, 2016].

In a single porosity system, the porosity of the media could vary based on the type of sediment or soil being used. For example, figure 2.4 represents the relationship between the grain size of soil and the total porosity of the medium. In general, the total porosity reduces with increasing soil grain sizes.

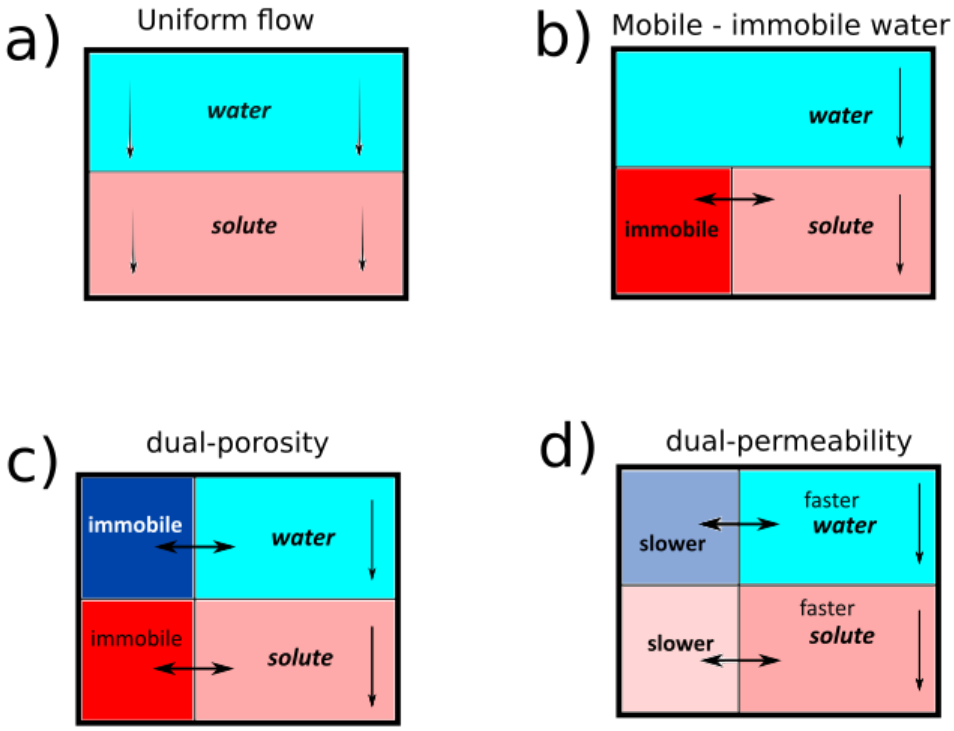

Figure 2.3: Conceptual models of water and solute flow, adopted from Šimůnek and van Genuchten, 2016

2.1.4. Darcy's law

Darcy's findings laid the foundation for the modern science of hydrogeology by quantifying the relationships between volumetric groundwater flow rate, driving forces, and aquifer properties [Arthur and Saffer, 2022]. Water saturation in sediments is an essential factor to consider when studying any contaminant transport in soils and sediments

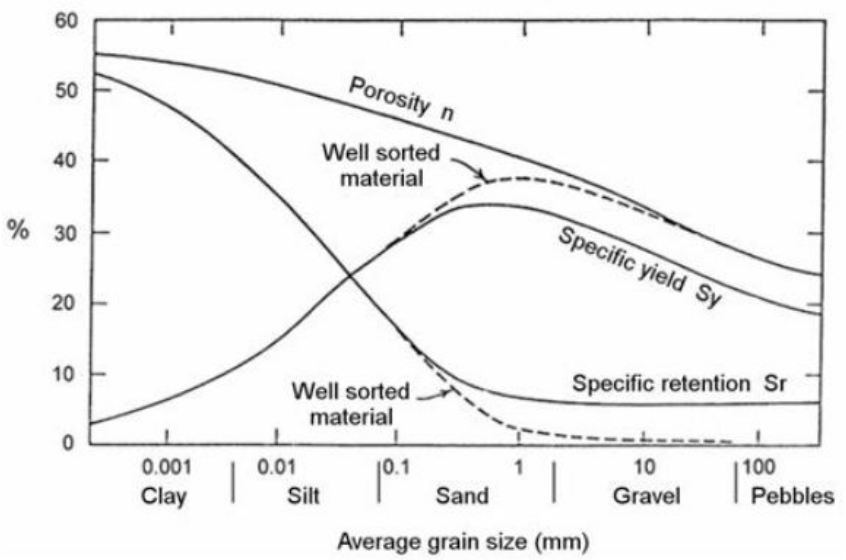

Figure 2.4: Porosity versus grain size, adapted with permission from Beretta and Stevenazzi, 2018. The figure has been previously adopted from Eckis, 1934. Please note that the y-axis represents the % porosity, and x-axis represents the grain size with resulting sediment characterisation.

[Manning, 2016]. Darcy's law, is given by a simple proportionality relationship (Equation 2.1 and 2.2), [Darcy, 1856; Manning, 2016]) between the instantaneous flux, and the cross-sectional area. The effect of gravitational forces on the flow of water is neglected [Manning, 2016].

Specifically, Darcy's experiments revealed proportionalities between the flux of water through the laboratory columns and different characteristics of the experimental system [Arthur and Saffer, 2022]. Note that in Darcy's Law, the other terms all describe the driving forces or geometry of the experimental system; none of them would change if the sand pack in the tube were changed to gravel, silt, or another material [Arthur and Saffer, 2022], and the change in the flow rate would correspond to the permeability of the media.

$$q = \frac{Q}{A} \tag{2.1}$$

$$q = -\frac{k}{\mu * L} * \Delta p \tag{2.2}$$

Where Q is the flow rate of water ($L^3\ T^{-1}$),
A is the cross sectional area of the column (L^2),
k is the medium's permeability (L^2),
μ is the fluid's dynamic viscosity ($M\ L^{-1}\ T^{-1}$), and
Δp ($M\ L^{-1}\ T^{-2}$) is the pressure drop over a given distance L (L).

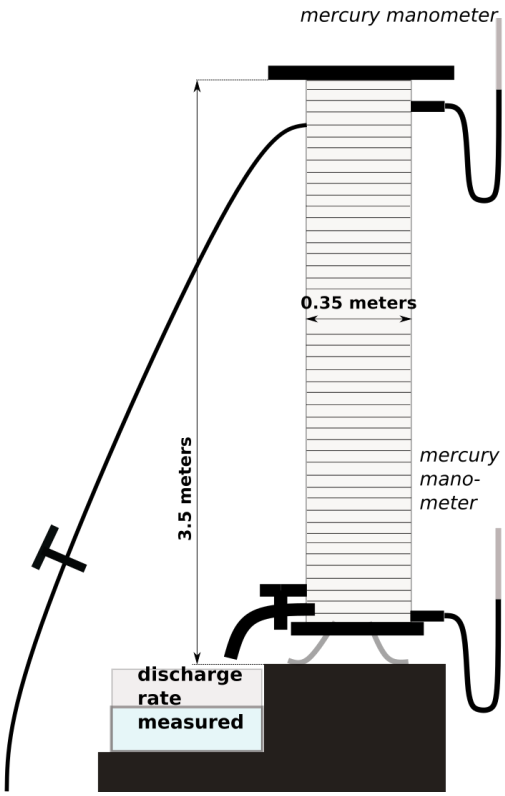

Figure 2.5: Experimental setup used by Darcy to verify Darcy's Law as adopted from Darcy, 1856

Experimental tests have shown that flow regime with Reynolds numbers up to 10 follow Darcy's Law [Manning, 2016] (Typically, any flow with a Reynolds number less than 2000 is laminar [Menon, 2014]). The Reynolds number (a dimensionless parameter, [Stokes et al., 1851]) for porous media flow is typically expressed as shown in Equation 2.3.

$$Re = \frac{\rho * v * L}{\mu} \tag{2.3}$$

Where:
Re is the Reynolds number;
ρ is the density of the fluid,
v is the Darcy flow velocity ($cm\ min^{-1}$);
L is the characteristic length of the column (cm), and
μ is the dynamic viscosity of the fluid ($g\ cm^{-1}\ min^{-1}$).
Please note that for the current experimental setup (Section 2.3), the Re is calculated before the experiment to ensure that the system follows Darcy's Law. The dynamic viscosity of water is 10^{-3} Pascal.second [Nagashima, 1977] or 0.6 $gcm^{-1}\ min^{-1}$. In this study, the Re for the highest flow velocity 0.13 $cm\ min^{-1}$ ($L = 15cm$, $\rho = 1.7g\ cm^{-3}$ (Refer to the bulk density values obtained empirically as shown in Table 4.3) is as shown

in Equation 2.4 below.

$$Re = \frac{1.7 * 0.13 * 15}{0.6} = 5.5 \tag{2.4}$$

Hence, even for the fastest flow velocity, it is ensured that the $Re < 10$ so that the system always follows Darcy's Law.

2.2. Bacteria strain used and Processes Studied

2.2.1. *Enterococcus faecalis* JH2-2

Antibiotic-resistant *Enterococci* have been isolated in various countries in Europe from the guts of healthy humans and food animals [Bourgeois-Nicolaos et al., 2006]. The persistence of *Enterococci* in the environment over other traditional fecal indicators like *Escherichia coli* (*E. coli*), have deemed them as better indicators of fecal contamination [Boehm and Sassoubre, 2014; Gilmore et al., 2002; Stuart et al., 2006]. Furthermore, a previous study conducted by Chen and Walker, 2012 observed a noticeable difference in the breakthrough patterns between *E. faecalis* and *E. coli*. This difference warrants a need to study processes associated with *E. faecalis* separately. The ability of the strains of *Enterococci* to exchange genetic material within them [Bourgeois-Nicolaos et al., 2006] deem them as interesting candidates in the context of antibiotic resistance. Processes associated with various *Enterococci* strains can be used to build models describing the spread of antibiotic resistance in the environment (e.g., horizontal gene transfer, selection pressure from antibiotics, or heavy metals promoting antibiotic resistance spread). *Enterococci* are gram-positive cocci that can occur singly, in pairs, or as short chains [Stuart et al., 2006]. They are facultative anaerobes possessing the ability to grow in the presence or absence of oxygen [Stuart et al., 2006]. Enterococcus species live in vast quantities ($10^5 - 10^8$ colony-forming units (CFU) per gram of feces) in the human intestinal lumen and, under most circumstances, cause no harm to their hosts [Stuart et al., 2006]. *Enterococcus faecalis* (*E. faecalis*), specifically, have been found more often related to human feces and can be suitable as fecal indicator bacteria (FIB) to identify anthropogenic influences in water environments [Boehm and Sassoubre, 2014]. In this context, the strain Enterococcus faecalis JH2-2, a non-pathogenic strain, was used in this study.

2.2.2. Advection and Dispersion

The advection and dispersion equation (ADE, Equation 2.5, Figure 2.6) is commonly used to describe water and solute transport through porous media [Runkel, 1996].

$$\frac{\partial C}{\partial t} = \alpha * v * \frac{\partial^2 C}{\partial x^2} - v * \frac{\partial C}{\partial x} \tag{2.5}$$

Where:
C is the concentration of the solute ($mg\ L^{-1}$ or $CFU\ mL^{-1}$),
t is the time passed since the start of the experiment (min),
α is the dispersivity (cm)
v is the flow velocity ($cm\ min^{-1}$), and
x is the length (cm)
Analytical solutions for the equation are widely available, along with the addition of an equilibrium coefficient [Ogata and Banks, 1961; Runkel, 1996; Thomann and Mueller, 1987]. Moreover, they have successfully described experimental results obtained from well-controlled laboratory studies in uniformly packed soil columns. However, when coupled with terms describing processes like adsorption or attachment (especially in non-equilibrium), the ADE only weakly describes the sorbed organic and inorganic compounds [Selim and Ma, 1998]. Nevertheless, the analytical solutions are beneficial to provide an exact solution and to check the accuracy of a numerical solution that is developed for complex cases [Runkel, 1996].

In the current study, a numerical solution for the ADE is used, which is solved using *R* software (Section 2.4). The numerical solution is verified using the exact solution obtained from the analytical solution before other processes were added to the system. To ensure reaching numerical solutions at minimized numerical dispersion, the discretization parameter values are set to $dx = 0.075$, and $dt = 0.1$. It is to be noted that the equation typically requires two boundary conditions for solving the particular equation. Since only one boundary condition is provided, the solution near the column's end could be inaccurate due to end effects. Therefore, to avoid these boundary condition effects, we solve the equation for a column twice as long as desired and only use the solution for our desired column length. Using this technique can 'correct' the possible inaccuracies caused due to the lower boundary conditions. The percentage error between the numerical solution developed in this study in *R*, (Section 2.4) and the analytical solution of the ADE was found to be of a maximum of 0.0001%. Therefore, the numerical solution was deemed accurate, based on which other processes can be built.

2.2.3. Straining

Physical straining of colloids (used as a proxy for bacteria) is an essential process that must be considered when studying their transport in porous media [Bradford, Simunek, Bettahar, Van Genuchten, and Yates, 2006; Dıaz et al., 2010]. Straining occurs in a fraction of the soil pore space that has a similar size to that of the particles [Foppen et al., 2007]. In this context, the two main models that have successfully determined the kinetics of the straining process are the colloid attachment theory [Bradford et al., 2003] and the colloid straining theory [Xu et al., 2006]. The colloid attachment theory implements combined attachment and degradation parameters; [Bradford and Bettahar, 2006; Bradford et al., 2004; Bradford et al., 2003], while the model proposed by [Porubcan and Xu, 2011; Xu et al., 2006; Xu and Saiers, 2009] employ more simplified model containing only two parameters [Porubcan and Xu, 2011; Xu et al., 2006; Xu and Saiers, 2009]. For this study, the more simplified model was employed (Figure 2.6). The grain size diameter of 0.1 to 0.4 cm was used in this study so that filtration effects can be neglected (filtration and straining are simultaneous processes and can often not be differentiated [Dıaz et al., 2010; Foppen et al., 2007]). The filtration effects were reduced in this study using sediments of relatively larger grain diameters (Section 2.3). The equation used to verify the straining process is as shown in Equation 2.6 [Xu et al., 2006], and later in Tables 3.2 and 4.2. Please note that only the right side of Equation 2.5 is used in Equation 2.6.

$$\frac{\partial C}{\partial t} = Equation\ 2.5 - k_{str}.C.e^{-C_s/\lambda} \tag{2.6}$$

Where:
k_{str} is the straining rate (min^{-1})
λ is the straining coefficient ($mg\ g^{-1}$)
C_s is the concentration of bacteria in the sediment phase ($mg\ g^{-1}$)

2.2.4. Microbial Decay and Respiration

Microbial decay is defined by the cell lysis of a bacteria cell occurring due to various environmental factors. Microbial respiration is the loss of bacterial cell concentration due to bacteria anaerobically respiring dissolved oxygen (from the water). Since this study is conducted in DO free and DO rich environments, the loss in bacteria cell concentration is attributed to DO free environments (refer to condition C1 in Chapters 3 and 4,

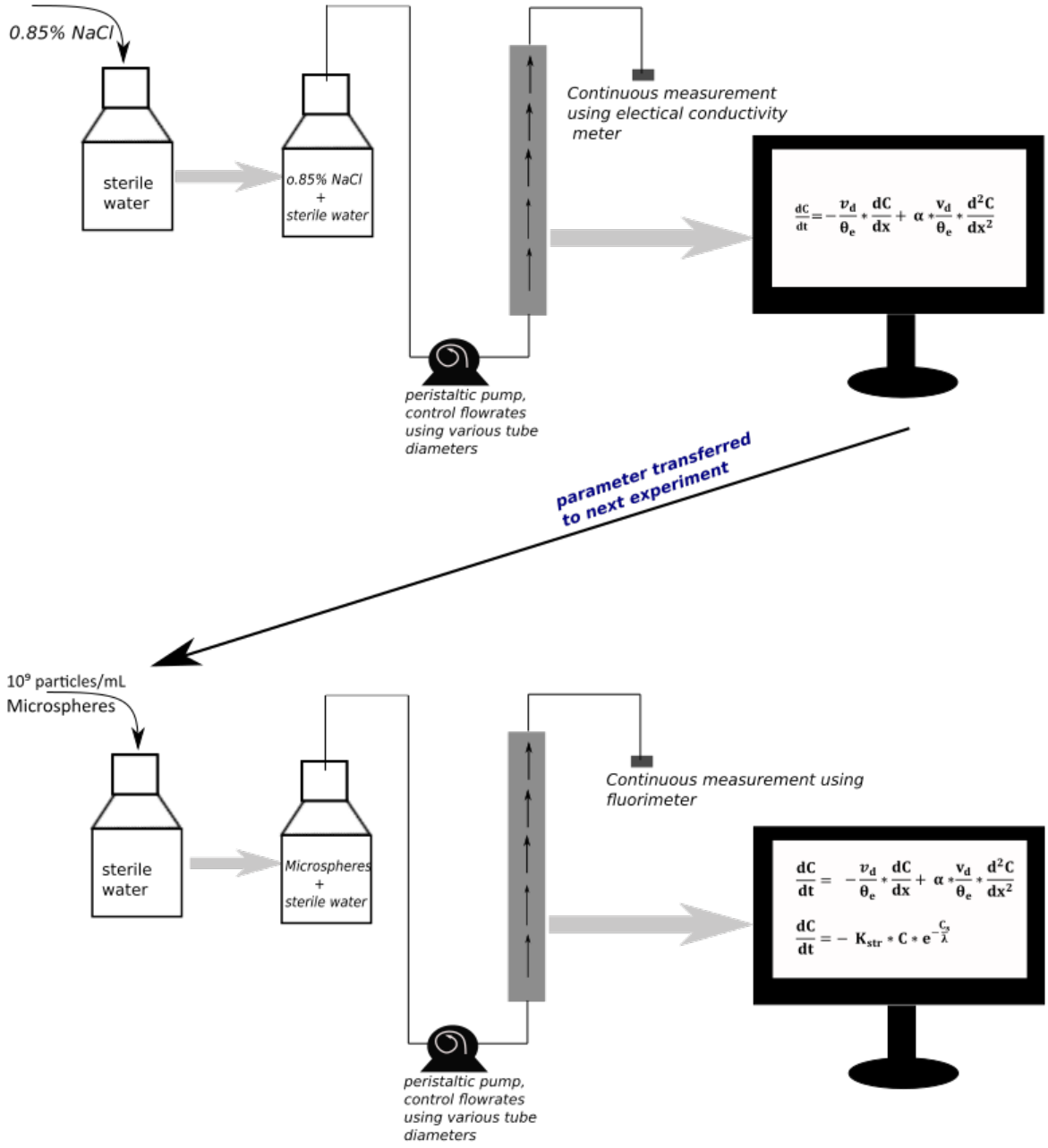

Figure 2.6: Approach used to set up the hydraulic model. Advection and dispersion are determined by continuously measuring the electrical conductivity of the saline tracers (top half of figure). These parameters then form the basis to determine and validate the model used to describe straining. Straining was quantified using a fluorimeter by continuously injecting microspheres in the column (bottom half of figure). Please note that the computer and the equations represent the numerical model verified using the experimental data obtained from the column experiments.

Figure 2.7), and respiration is attributed to DO rich environments, (refer to condition C3 in Chapters 3 and 4, Figure 2.7), respectively. However, these processes could be non-identifiable when combined with attachment or straining. For this purpose, these processes are studied using the reduction in concentration observed at the inlet solution injected into the column. The linear rate laws [Abu-Ashour et al., 1994; Corapcioglu and Haridas, 1985, Equation 2.7] were then transferred to the column studies where the attachment rate coefficients were then determined. Please note that only the right side of Equation 2.6 is used in Equation 2.7.

$$\frac{\partial C}{\partial t} = Equation\ 2.6 - \mu_d\ or\ \mu_r * C \tag{2.7}$$

Where:
μ_d is the decay rate (min^{-1})
μ_r is the respiration rate (min^{-1})

2.2.5. Microbial Attachment

Microbial attachment is defined as the attachment of the bacteria to the sediment grains due to electrostatic forces. When talking about microbial attachment, usually detachment must also be considered [McCaulou et al., 1994]. However, for simplicity and to ensure parameter identifiability, only the attachment process was studied in the context of this work. The microbial attachment like decay or respiration is represented using a linear rate law (Equation 2.8), and later in the Tables 3.2 and 4.2. The microbial attachment processes was determined separately for the conditions C1 and C3 (Refer Subsection 2.2.4, Chapters 3, 4, Figure 2.7). These values were unaltered when determining the growth rates in conditions C2 and C4, respectively. Please note that only the right side of Equation 2.7 is used in Equation 2.8.

$$\frac{\partial C}{\partial t} = Equation\ 2.7 - (K_{att_{C1}} * C\ or\ K_{att_{C3}} * C) \tag{2.8}$$

Where:
$K_{att_{C1}}$ is the attachment rate for condition C1 (min^{-1})
$K_{att_{C3}}$ is the attachment rate for condition C3 (min^{-1})

2.2.6. Microbial Growth

Microbial growth is defined as the increase in the concentration of bacteria in the presence of nutrients. The Monod equation [Monod, 1942] is the simplest solution used to express the nutrient-limited growth of bacteria [Corapcioglu and Haridas, 1985]. This model has provided an accurate description of the nutrient-limited growth rate of bacteria (for most bacteria strains). However, using the Monod model required the constant monitoring of the concentration of both the concentration of bacteria and nutrients. For this study, a simplified model using a linear rate law (refer conditions C2 and C4 in the Figure 2.7) [Corapcioglu and Haridas, 1985, Equation 2.9] was used to describe the growth kinetics of the bacteria in the column. Please note that only the right side of Equation 2.8 is used in Equation 2.9.

$$\frac{\partial C}{\partial t} = Equation\ 2.8 + (\mu_{g_{C2}} * C\ or\ \mu_{g_{C4}} * C) \tag{2.9}$$

Where: $\mu_{g_{C2}}$ is the growth rate for condition C2 (min^{-1}), and $\mu_{g_{C4}}$ is the growth rate for condition C4 (min^{-1})

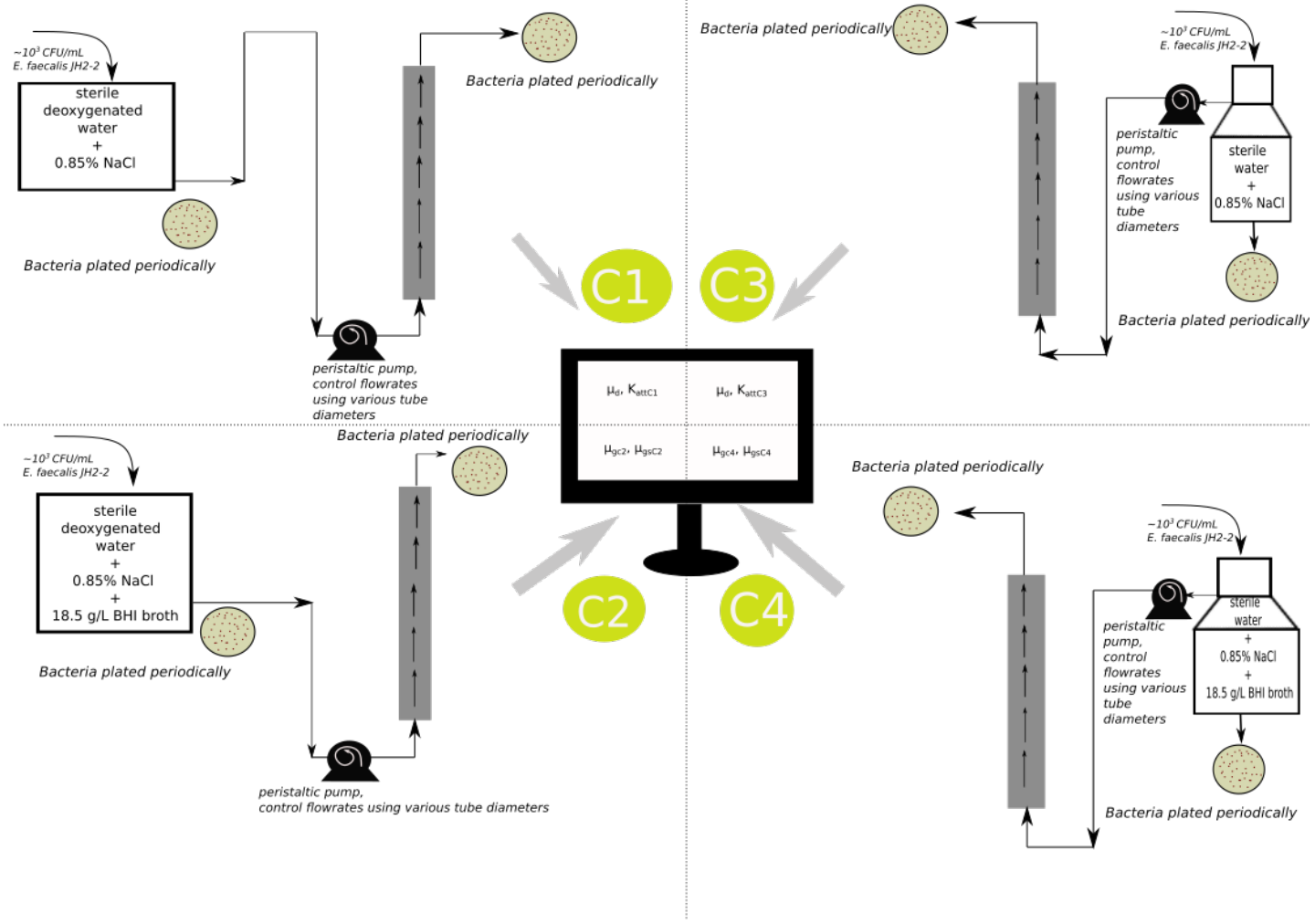

Figure 2.7: Combined approach for the biological model. Please note that this model is built using parameters obtained from the hydraulic model. In conditions C1 and C2, the inlet 'bag' is a collapsible sterile bag that does not allow any dissolved oxygen to enter through the surface. In conditions C3 and C4, the sterile bottle is fitted with a cork and two pipes allowing the flow of air (sterilised using a filter of 0.2 microns) into the bottle as the solution is pumped out. This ensures that the dissolved oxygen concentration at the inlet does not change with time.

2.2.7. Dimensionless numbers

Chemical non-equilibrium for flow systems occurs when the chemical reaction rate happens slower compared to the flow velocity [Selim and Ma, 1998]. Most processes in continuous flow setups may not have attained equilibrium, i.e., the processes do not occur within the residence time of the contaminants within the soil. In more complex cases, the processes could be co-occurring, thus requiring the model to differentiate the processes that are occurring [Šimůnek and Bradford, 2008]. Identifying simultaneously occurring processes remain one of the biggest challenges in modelling non-equilibrium flow and transport [Šimůnek and Bradford, 2008]. Flow velocities impact the processes as a faster flow velocity may mean that the reaction is bypassed or less critical as the solute is not given enough time to interact with the soil to perform the reaction. Conversely, a slower flow velocity may give the solute enough time to interact with the soil so that the reaction can take place and possibly attain equilibrium. Therefore the flow rate of a media could impact the process parameter rates in non-equilibrium flow models.

Normalization of variables is essentially developed to obtain approximate best estimate solutions for differential equations [Deen, 2012]. When done properly, the magnitudes of the various terms in an equation are revealed by the dimensionless parameters [Deen, 2012; Leal, 1992]. This approach can then compare the time scale of the reactions rather than looking at actual numbers. The scale of a variable is chosen such that it is an estimate of its maximum order of magnitude [Deen, 2012]. The variables are then normalised by their respective scales [Deen, 2012; Leal, 1992].

Normalising the variables give considerable insight into which rate processes are essential [Deen, 2012]. In this work (Chapter 4), the dimensionless numbers Peclet (Pe, Equation 2.10) and Damkoehler (Da, Equation 2.11) are used to compare transport and reactive time scales for various flow velocities.

$$Pe = \frac{L}{\alpha} \tag{2.10}$$

$$Da = \frac{M * L}{v} \tag{2.11}$$

Where:
M is a generalised rate coefficient (represented in Equations 2.6, 2.7, 2.8, 2.9)

Please note that normalisation procedure used to represent the results (C/C_o), and the time in terms of pv has been elaborated in Section 3.2.2 - Stepwise model fitting

approach, and briefly elaborated in the end of Section 4.2.2.

2.3. Experimental design

During the column experiments' design, various factors have been considered to ensure that it aids model development and represents field-scale setups (to aid future scale-up of the model). Thus, a reasonable compromise must be found between field-like conditions and an ability to control the conditions within the experiment.

The columns used for the experiments were made of acrylic glass. The columns were of length 15 cm and diameter of 3 cm (Figure 2.8a). The column was planked on each side with fibreglass filters to avoid leaking sediment during water flow through the sediment-packed column. Silicone tubes were used to connect the various parts of the setup (Figure 2.8e). A three-way pipe regulator (Figure 2.8c) was used at each connection point to ensure easy switching of flow pathways during the experiment and prevent contamination from entering the column during sampling. The guide used for materials chosen in the design of the experiments mainly was from [Gilbert et al., 2014]. Semi-natural sediments (lake sediments, cleaned and sieved) were used in the column and had a grain diameter of 1 to 4 mm. The classification of the sediment is coarse sand to fine gravel (Figure 2.4). Sediment with larger grain size was used to eliminate processes like physical filtration, thus facilitating the study of processes like straining and attachment (Subsection 2.2.3). A vacuum pump is used for degassing the sterile saline water (also removing DO) to study the processes of decay and growth under anoxic conditions (Section 2.1.1). The detailed process of obtaining experimental conditions required for this study is explained in Section 3.2.1.

The representative elementary volume (REV) is a useful guide to design column experiments [Novakowski, 1992; Gilbert et al., 2014], where a REV has the same volume, shape, and orientation, regardless of location within the column. REV can extend up to 40 - 100 grain diameters [Mioska, 2012; Gilbert et al., 2014], with experiments for chemistry and microbiology requiring smaller REVs than flow experiments. In general, REV extension must be ≤ 40 grain diameters (for a chemical experiment). Therefore, the calculation of the column diameter, required to represent the porous media accurately, is as shown in Equation 2.12:

$$REV = \frac{d}{d_g} \tag{2.12}$$

Where:
d is the column diameter (cm)
d_g = grain size diameter of the sediment (cm)
REV is the representative elementary volume.

For the experiment used in this work, the $G_s = 0.1$ to $0.4cm$. Therefore, the REV for the grain size 0.1 cm ($REV_{0.1}$) and grain size 0.4 cm ($REV_{0.4}$) is as shown in Equation 2.13 and 2.14.

$$REV_{0.1} = \frac{3}{0.1} = 30 \tag{2.13}$$

$$REV_{0.4} = \frac{3}{0.4} = 7.5 \tag{2.14}$$

The REV is always $<$ 40 as required for chemical or biological experiments, even for the smallest grain size diameter of 0.1 cm. Therefore, the given column dimensions are representative of the given grain size and required study. In addition to the REV, another vital factor to be considered when designing columns is the length to diameter ratio. This is an important criterion to prevent preferential flow pathways, the ratio of the length of the column to its diameter must be at least 5 [Bergström, 2000; Fand and Thinakaran, 1990; Lewis and Sjöstrom, 2010; Novakowski, 1992]. Preventing preferential flow is especially important for the assumption of 1-D setups. Therefore, for a 1-D column, it is desirable to have a small diameter to prevent lateral flow from becoming an important process. However, if the column diameter is small compared to the column's length, this could cause sidewall flow (flow velocity is 1.11-1.45 times higher near the wall of the column than the centre [Sentenac et al., 2001]). For smaller diameters, this effect becomes dominant, thus causing effects that are unnecessary for the experiment.

The sediment was packed in the column using wet packing methods [Oliviera et al., 1996]. The packing was done to ensure homogeneity, reproducibility and eliminate any stratifying layers [Lewis and Sjöstrom, 2010; Oliviera et al., 1996]. A sterile spoon was used to deposit thin layers of the sediment into the column (Figure 2.8b). In addition, gentle vibration was provided intermittently with the sterile spatula to remove any entrapped bubbles during the packing process and ensure homogeneity of the deposited sediment. Oliviera et al., 1996 observed that this technique produced the highest

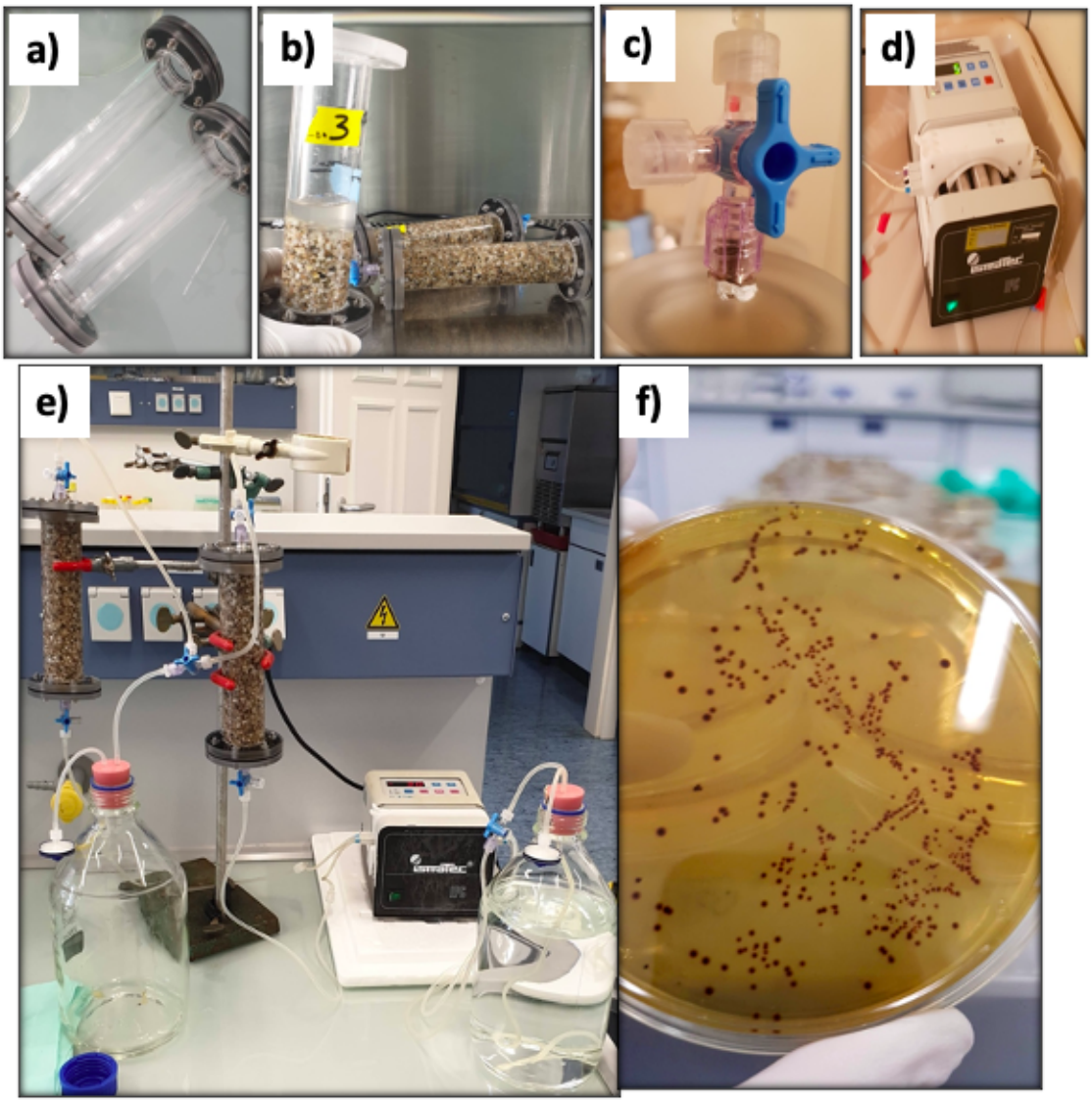

Figure 2.8: Experimental setup and materials used for the experimental setup a) acrylic glass columns, b) wet packing method used to fill the sediment in the column, c) three-way pipe used to regulate water flow before and after the experiments, d) peristaltic pump used to control mean flow velocities, e) the setup of the experiment (here shown only for condition C3), and f) plating of bacteria in m-Enterococcus agar, with the red colonies representing the bacteria colonies.

density of uniform packing without causing any lateral particle size segregation [Lewis and Sjöstrom, 2010]. The wet packing method ensures that the resulting packed sediment column is fully water-saturated, and each column layer is equal. Therefore, any effects observed from the contaminants are homogeneously distributed in the column, and it makes hydraulic calculations like bulk density, effective and total porosity more straightforward [Lewis and Sjöstrom, 2010].

During the packing process, the dry weight of the sediment was measured before and after the column packing. The dry sediment weight was used to measure the sediment-packed column's bulk density. The bulk density was calculated using the formula in Equation 2.15.

$$\rho_b = \frac{(W_i - W_f)}{\pi * d^2 * \frac{L}{4}} \tag{2.15}$$

Where:
ρ_b is the bulk density of the sediment packed column,
W_i is the weight of the container with the sediment before the column is packed (g),
W_f is the weight of the container with the sediment after the column is packed (g), and
d and L are the diameters and the length of the column respectively (cm).
Since the sediment is homogeneously packed, the bulk density values can be compared with typical values [Lewis and Sjöstrom, 2010] as represented in Table 2.1. Another standard measure that is related to the bulk density of the column is the total porosity (θ_t) of the sediment packed column [Lewis and Sjöstrom, 2010]. The θ_t of the media is calculated using the formula in Equation 2.16.

At the start of the experiments (before conducting the tracer tests), the bulk parameters of bulk density and total porosity were determined gravimetrically. The average bulk density and total porosity determined from all the experiments are 1.714 $g\ cm^{-3}$, and 34.9%, respectively. The values for these bulk parameters are verified using the values from Table 2.1 and Figure 2.4. The bulk density and total porosity values for soil characterised by a grain size diameter of 1 to 4 mm are 1.4 to 1.8, and 25 to 46% respectively (Table 2.1). The values of these bulk parameters obtained from the experiments are within this range, implying that the sediments are homogeneous and are well packed in the column.

$$\theta_t = \frac{\rho_b}{\rho_s} \tag{2.16}$$

Where:
ρ_s is the grain density = 2.63 gcm^{-3} [Rowell, 1994, Section 3.2.1].

Table 2.1: Average total porosity and bulk density ranges for each soil type, [Lewis and Sjöstrom, 2010]

Type of soils	**Total Porosity range (%)**	**Bulk density range** (gcm^{-3})
Coarse gravel	24 - 36	1.7- 2.0
Fine gravel	25 - 38	1.6 - 2.0
Coarse sand	31 - 46	1.4 - 1.8
Fine sand	26 - 53	1.2 - 2.0
Silt	34 - 61	1.0 - 1.7
Clay	34 - 60	1.0 - 1.7

All the components (including tubes, sediment, spoon, and fibreglass filters) were sterilized by autoclavation before packing the column to ensure no contamination during the experiments. The acrylic glass columns were sterilized separately at 70°C for at least 12 hours. All the column components were then assembled under a sterile hood, and packing (mentioned above) was also done under a sterile hood with sterile water. Upon assembly (Figure 2.8e), sterile de-oxygenated water is pumped through the setup from bottom to top for 2 to 3 days to achieve a steady-state for the flow velocity and ensure that any pre-entrapped bubbles were removed before the start of the experiment. The flow velocities were regulated using a peristaltic pump (Figure 2.8d) using tubes of differing diameters. At least 2 to 3 samples were collected during the acclimatisation of the setup. These samples were consequently plated to ensure that the setup was sterile before the start of the experiment. Flow rates were also measured regularly to ensure the smooth operation of the setup.

After the acclimatisation of the setup, the inlet solution is prepared, and the experiment is started. Based on the calculation of the total porosity and the Darcy velocity, the mean residence time of the water in the column is calculated using the Equation 2.17.

$$mean\ residence\ time = \frac{L}{v} \tag{2.17}$$

Where:
L is the length of the column (cm), and
v is the average linear flow velocity

The sampling times for each flow rate setup are then estimated so that at least four samples were collected for every pore volume. For every experiment, at least 20 samples were collected to ensure enough data was available to verify the model setup. The samples collected from the setup were then quantified using a combination of electrical conductivity meter (tracer experiments), fluorimeter (microsphere experiments), and plating on m-Enterococcus agar (Figure 2.8f, bacteria experiments). Some collected

samples were placed in dry ice at 4°C for 10 to 30 minutes before plating for the experiments with bacteria. This was only done for a few samples when the time between two sampling events was very short. In general, the samples were plated within minutes of acquisition. Therefore, placing it in ice for a short period ensured that the bacteria were preserved before plating. A detailed rendering of the quantification techniques and the stepwise approach used to determine the parameters can be found in the Figures 2.6, 2.7, and Figure 3.1.

2.4. Model setup

The system of partial differential equations (Equations 2.5 - 2.9) was implemented using the 'rodeo' package in R [R Core Team, 2020], which are in turn solved with the numerical method-of-lines approach [Kneis et al., 2017]. The primary objective of using this package was to provide a flexible modelling framework wherein various processes can be added or removed during various stages of model development [Kneis et al., 2017]. This separation of variables implies that the equations are fed in by separating variables, parameters, functions, processes, and their related stoichiometry [Kneis et al., 2017]. This method of separation of variables allows easy identification of redundant terms in the equation and facilitates visualization of the interaction between variables and the related processes. rodeo then generates an automatic code that allows the system of partial differential equations to be automatically translated into the source code for numerical integration [Kneis et al., 2017].

Once the model source code is generated, parameters relating to the specific processes are identified using the *"FME"* package [Soetaert and Petzoldt, 2010]. The cost function required for inverse parameterization is performed using the *"modCost"* function [Soetaert and Petzoldt, 2010], which calculates the sum of squared residuals for a given set of equations. The data fitting by unconstrained optimization is done using the *"modFit"* function wrapper. Function modFit is a wrapper funcrion and uses the functions from *optim*, *nls*, and function *nlminb*, from R's base packages [R Core Team, 2020] and the Levenberg-Marquardt algorithm from package *minpack.lm* [Elzhov et al., 2016; Soetaert and Petzoldt, 2010]. The resulting best fit parameter solutions are used to compare or transfer parameter values to the next stage of parameter fitting (Section 2.2, Equation 2.5-2.9).

Chapter 3

Reactive-transport modelling of *Enterococcus faecalis* JH2-2 passage through water saturated sediment columns

Aparna Chandrasekar[a,b], Martin Binder [a,c,d], Rudolf Liedl[a], Thomas U. Berendonk[b]

[a]Technische Universität Dresden, Institute of Groundwater Management, Bergstraße 66, 01069 Dresden, Germany

[b]Technische Universität Dresden, Institute of Hydrobiology, Zellescher Weg 40, 01217 Dresden, Germany

[c] Helmholtz-Centre for Environmental Research - UFZ, Department of Environmental Informatics, Permoserstraße 15, 04318 Leipzig, Germany

[d] Technische Universität Bergakademie Freiberg, Institute of Geology, Section of Hydrogeology and Hydrochemistry, Gustav-Zeuner-Str. 12, 09599 Freiberg, Germany

The following content has been originally published in the "Journal of Hazardous Materials, Special Issue: Micropollutants in water"

DOI: https://doi.org/10.1016/j.jhazmat.2021.125292

Keywords: Bacteria, Solute tracer, Microspheres, Column experiments, Dissolved oxygen

Highlights

- A stepwise experimental / modelling approach for microbial dynamics was developed.
- Implementation in *R* facilitates the addition or deletion of specific processes.
- The survival of *Enterococcus faecalis* is higher in oxygen rich environments.
- Straining is an important physical process.
- Microbial decay and growth are rate-limiting in the absence of dissolved oxygen.

Abstract

The reuse of treated wastewater (e.g. for irrigation) is a common practice to combat water scarcity problems world-wide. However, the potential spread of opportunistic pathogens and fecal contaminants like *Enterococci* within the subsoil could pose serious health hazards. Additional sources (e.g., leaky sewer systems, livestock farming) aggravate this situation. This study contributes to an understanding of pathogen spread in the environment, using a combined modelling and experimental approach. The impact of quartz sediment and certain wastewater characteristics on the dissemination of *Enterococcus faecalis* JH2-2 is investigated.

The transport processes of advection-dispersion and straining were studied by injecting conservative saline tracer and fluorescent microspheres through sediment packed columns, and evaluating resulting breakthrough curves using models. Similarly, simultaneously occurring reactive processes of microbial attachment, decay, respiration and growth were studied by injecting *Enterococcus faecalis* JH2-2 suspended in water with or without dissolved oxygen (DO) and nutrients through sediment, and evaluating resulting inlet and outlet concentration curves. The processes of straining, microbial decay and growth, were important when DO was absent. Irreversible attachment was important when DO was present. Sensitivity analysis of each parameter was conducted, and field scale behavior of the processes was predicted, to facilitate future work.

Graphical Abstract

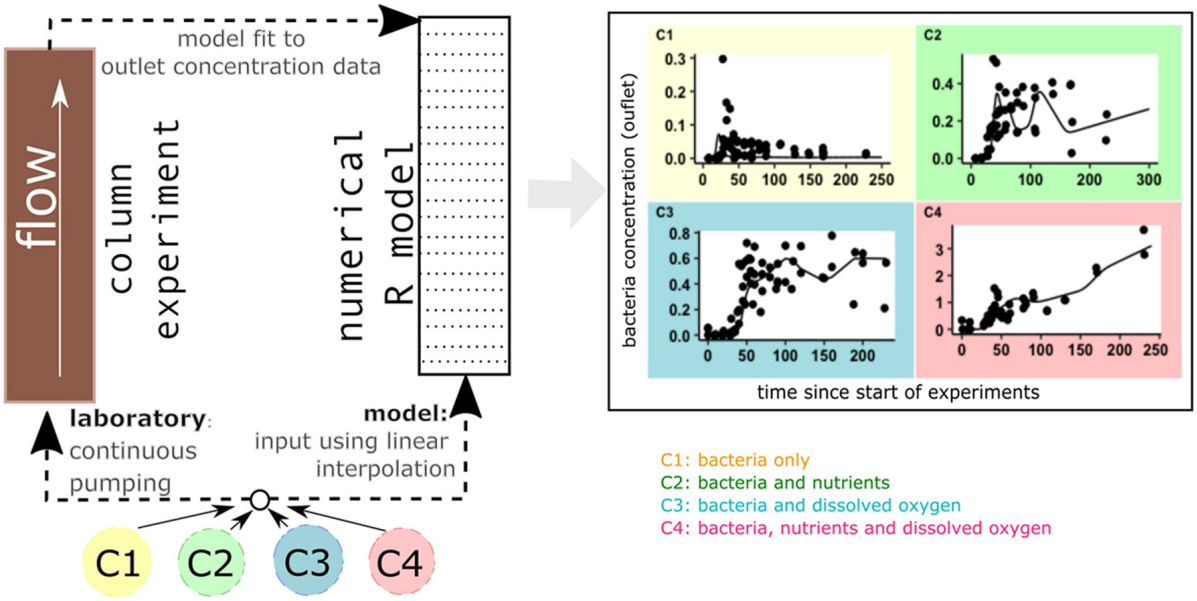

3.1. Introduction

The diminishing availability of safe drinking water around the world has created an urgent necessity to preserve and replenish freshwater sources such as lakes, rivers and groundwater. Groundwater and surface water together constitute more than 90% of raw water sources for drinking water purposes in Europe [van der Hoek et al., 2014]. In this context, the direct reuse of treated wastewater (TWW), for instance for irrigation purposes, has been adopted in many water scarce regions to provide nutrient-rich water for crops [Vergine, Salerno, et al., 2017].

However, this has raised concerns about exacerbating the spread of opportunistic pathogens (e.g. viruses, bacteria) to the subsoil and groundwater, rendering them unsafe for the use in drinking water [Hong et al., 2018]. Furthermore, urban wastewater treatment plants have been found to be hotspots for the emergence of antibiotic resistance (AR) in the environment [Cacace et al., 2019; Mishra et al., 2019; Rizzo et al., 2013]. In addition, leakages from the aging and, hence, partially failing wastewater infrastructure (e.g., European sewer networks that are partially older than 100 years: see, e.g., Ellis and Revitt, 2002) can lead to an uncontrolled recharge and diffuse contamination of urban aquifers including the spread of AR [Newton and McClary, 2019]. A clear understanding of the underlying physical, chemical, and biological processes in the subsoil environment is imperative to understand the spread of pathogenic bacteria in the subsoil environment.

Several combined experimental and modelling approaches have been previously used to isolate and study various subsoil processes [Balkhair, 2017; Feighery et al., 2013; Harter et al., 2000; Nielsen et al., 1986] The pool of software typically used for solving these reactive transport problems under one-dimensional (1-D) conditions (such as soil column setups) include HYDRUS-1D [Šimůnek et al., 1998], PhreeqC [Parkhurst, Appelo, et al., 2013], their combinations (e.g. HP1; [Jacques and Simunek, 2005]), as well as CXTFIT [Toride et al., 1995] and a large variety of other analytical solutions (e.g., Toride et al., 1993; Van Genuchten and Alves, 1984). HYDRUS-1D is effective in solving solute and colloid transport equations in the unsaturated environment, while PhreeqC focuses to a limited extend on hydro geo-chemical / biological equilibrium and non-equilibrium processes. HYDRUS is, however, not well suited for modelling fully water-saturated soil columns, and PhreeqC lacks the support for bacterial, i.e., colloidal transport. Eventually, CXTFIT is an analytical solution, consisting of linear models with limited number of processes providing finite capabilities in handling problems with variable boundary conditions. The same applies in principle to most other analytical solutions (e.g., Spitz

and Moreno, 1996). An easy-to-use and adaptable model algorithm focusing on the 1-D bacterial transport in porous media including physical and biological components is, to the knowledge of the authors, currently missing. For this reason, the present study constructs a flexible, 1-D numerical modeling framework using*R* software [Team et al., 2013]. The *R* packages "rodeo" [Kneis et al., 2017] and "FME" [Soetaert and Petzoldt, 2010] were employed for model construction and inverse parameterization, respectively. Since *R* is a widely applied and open source script language, development of this framework provides a flexible method to add and remove reactive transport processes in the soil-groundwater environment.

Physical processes that have been studied so far include filtration, kinetic attachment and detachment, [Bradford, Simunek, and Walker, 2006; Bradford et al., 2002; E. Smith and Hegazy, 2006; E. Smith and Badawy, 2008], colloidal straining and colloid-facilitated contaminant transport [Bradford, Simunek, and Walker, 2006; Bradford et al., 2002; Harter et al., 2000; Xu et al., 2006; Xu et al., 2008]. Corresponding model evaluations have been conducted based on laboratory-scale experiments where the migration behavior in natural soils and artificially mixed sediments was investigated under controlled (variably) saturated conditions [Dong et al., 2002; Gargiulo et al., 2008; Gargiulo et al., 2007; Levy et al., 2007; Pang and Šimůnek, 2006]. In addition to the aforementioned processes various other model equations have been formulated to determine the physical and biological processes associated with contaminant (specifically bacteria) transport in the subsoil environment [Abu-Ashour et al., 1994; Corapcioglu and Haridas, 1985; Matthess et al., 1988; Murphy and Ginn, 2000; Pekdeger and Matthess, 1983]. However, the aforementioned studies do not comprehensively consider the biological processes of microbial decay, respiration, growth, and the migration parameters associated with these processes. These processes are especially important in the context of TWW reuse.

The primary model species of bacteria employed in previous studies to study the aforementioned processes is *Escherichia coli* – a well-known indicator for fecal contaminations [Tallon et al., 2005]. However, *Enterococci* species (spp.) have recently been touted as better indicators of water quality [Boehm and Sassoubre, 2014], since *Enterococci* spp. and specifically *Enterococcus faecalis* are important members of the animal and human gut communities [Ateba and Maribeng, 2011; Harvey, 1997; Novais et al., 2005]. Furthermore, their high resilience to stressful environments including antibiotics like vancomycin and tetracycline [Novais et al., 2005], has facilitated their acceptance as indicators of fecal contamination [Newton and McClary, 2019], especially in the current context of spread of AR through TWW reuse. This study, therefore, uses *Enterococcus*

faecalis species as model bacteria, as opposed to *Escherichia coli*.

In the present study, we investigate the microbial attenuation (decay, attachment and respiration), and growth processes (in water phase and sediment phase) of *Enterococcus faecalis*, that occur due to changing dissolved oxygen (DO) and nutrient concentrations in the water. The reactive processes are built on top of the transport processes of advection, dispersion and straining, that have been previously well researched. We hypothesize, that by using a stepwise approach, to combine experimental results with corresponding model fitting, we can successfully isolate and identify the simultaneously occurring reactive processes. By doing so, we would like to clearly understand the impact of the TWW characteristics of DO and nutrients on bacteria migration in sandy sediments. The objective of the study is to:

1. provide an adequate model code in *R* to easily and adaptively activate or deactivate existing and new biological processes relating to *Enterococcus faecalis* (as a model species for other pathogens)
2. determine the important rate limiting processes involved in bacteria migration using a stepwise, combined experimental and modelling approach to isolate simultaneously occurring processes

3.2. Materials and methods

3.2.1. Experimental study

General setup, and stepwise approach for isolation of processes

To demonstrate the usage of the created framework, a series of six flow and transport experiments were designed. Sterile water was spiked with various components to distinguish the effects of transport and reactive processes. The six components used were: i. de-ionized sterile water spiked with solute tracers,i. de-ionized sterile water spiked with solute tracers, ii. fluorescent microspheres, iii. sterile water spiked with *E. faecalis* JH2–2 (DO = 0 mgL^{-1}, nutrients = 0 mgL^{-1}), iv. sterile water spiked with *E. faecalis* JH2–2 (DO = 0 mgL^{-1}, nutrients = 14.8 mgL^{-1}), v. sterile water spiked with *E. faecalis* JH2–2 (DO = 8.9 mgL^{-1} - i.e. near maximum saturation, nutrients = 0 mgL^{-1}), and vi. sterile water spiked with *E. faecalis* JH2–2 (DO = 8.9 mgL^{-1}, nutrients = 14.8 mgL^{-1}).

Synthetic water customized to these aforementioned characteristics (elaborated further in Table 3.1) was continuously injected into water-saturated, sterile quartz sediment

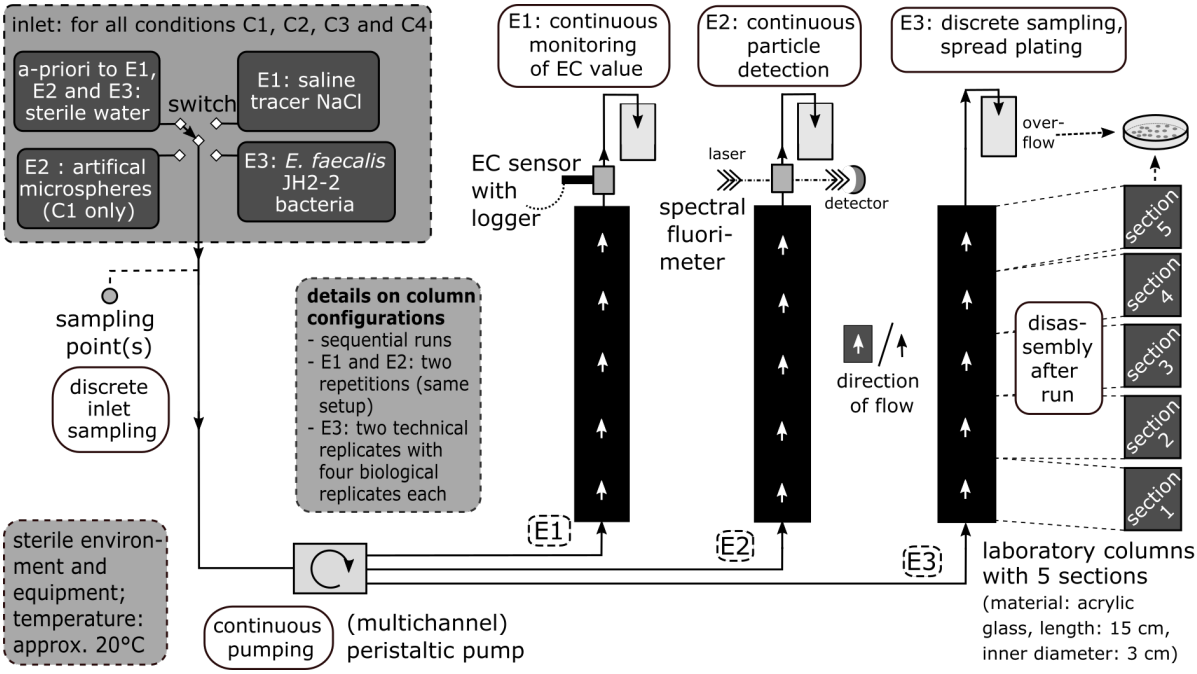

Figure 3.1: Lab-scale column experiment setup, along with details of the six experiments conducted and quantification methods used for each type of experiment. Setup is not to scale.

packed, acrylic glass columns (length: 15 cm, inner diameter: 3 cm, see Figure 3.1). This semi-natural porous medium (hereafter simply referred to as sediment) was characterized by a soil pH value of 5.4 [DIN EN 15933:2012–11, 2012], a grain density of $\sim 2.63\ gcm^{-3}$ ([DIN EN ISO 17892–3:2016–07, 2016], a column-averaged total porosity of $\sim 34\%$ and a loss on ignition of less than 0.1% [DIN 18128:2002–12, 2002]. The sediment was wet-packed into the columns along with intermittent vibration to ensure water-saturated conditions. The column was fitted with glass fiber filters in each end to prevent outflux of sediment grains from the column during the experiments. The components of the setup were sterilized separately and later assembled before each experiment under a sterile hood. All the components – except the columns – were subjected to wet autoclavation at $121°C$ for 20 minutes, before assembly of the set-up. The columns were sterilized by placing in an oven at $70°C$ overnight. The setup was operated after assembly, in a temperature-controlled room of $20 \pm 2°C$, to imitate the shallow groundwater temperature found in the Mediterranean regions (15-20$°C$, see Benz et al., 2017).

Upon assembly, the columns were saturated with sterile and de-oxygenated water for at least two days. The flow direction was set to a 'bottom-to-top' mode to ensure removal of possible pre-entrapped or entrapping air bubbles, thus maintaining water saturated conditions. Flowrates applied to the columns were adjusted to $\sim 1.0 \pm 0.1\ mL\ min^{-1}$ using a high-precision / low-pulsation multi-channel peristaltic pump (Co. Ismatec). This flow rate preserves laminar conditions (Darcy flow) at low Reynolds

numbers and was kept constant for all experiments to ensure comparability.

In general, the experimental setup was exposed to varying conditions of DO and nutrients. To enable effective isolation of the processes sterile de-ionized water spiked with explicitly defined DO (0 mgL^{-1} or 8.9 mgL^{-1}) and nutrients (0 mgL^{-1} or 14.8 mgL^{-1}) concentrations was used as proxy instead of TWW. This approached ensured that any change in the breakthrough curves of the bacteria originated from the changing water characteristics, thus enabling clear identification of processes. Experiment E1 (Table 3.1) was conducted before each experiment, when the column was repacked. Experiment E2 was conducted once before the E3 experimental series. Experiment E3 was conducted for approximately five pore volumes (approximately 240 minutes). Also note, that all E3 experiments included a regular manual measurement of the respective inlet and outlet concentrations of bacteria (around 12 measurements per experiment). The E3 experiment series were accompanied by a separate hydrophobicity determination (Subsection 3.2.1 - hydrophobicity determination).

Table 3.1: Overview on the flow and transport experiments: labels for experiments and the conditions that they were subjected to.

Experiment label	**Experimental foci / investigated processes**	**Applied substance and conditions (for ∼ 240 minutes per experiment)**	**Condition label(s)**
E1	Advection and dispersion	Solute tracer (sodium chloride dissolved in degassed water)	C1, C2, C3, C4
E2	Colloidal straining	Colloidal tracer (polystyrene microspheres in deionized sterile water)	Before experiments C1-C4
E3.1	Microbial decay and attachment	*E. faecalis* JH2-2 in degassed, sterile water without nutrients	C1
E3.2	Microbial growth	*E. faecalis* JH2-2 in degassed, sterile water with nutrients	C2
E3.3	Microbial respiration and attachment	*E. faecalis* JH2-2 in sterile water without nutrients	C3
E3.4	Microbial growth	*E. faecalis* JH2-2 in sterile water with nutrients	C4

Experiments E1 and E2: Transport experiments using solute and colloidal tracers

In E1, NaCl dissolved in degassed water (concentration: 8.5 $g\ L^{-1}$) was used as a conservative tracer to identify and quantify advection and dispersion in the columns [Eregno and Heistad, 2019]. The saline tracer concentration was measured indirectly using the sum parameter electrical conductivity (EC). Note that EC monitoring was realized con-

tinuously by employing a pre-calibrated sensor device (Figure 3.10, in the supplementary material) connected to a datalogger (both Co. WTW). The tracer breakthrough curves thus obtained were used to determine the effective porosity and dispersivity parameter coefficients.

In E2, artificial spherical polystyrene microspheres with pre-defined characteristics (1 μm diameter, yellow-green fluorescence, carboxyl-modified surfaces; Co. Sigma Aldrich) were used to determine the straining process. As the size of *Enterococci* spp. typically lie between 0.8 and 1 μm [Kokkinosa et al., 1998], the microsphere particles employed here aim to emulate the straining of *Enterococcus* bacteria in the sediment column, to obtain straining rate parameter coefficient and straining coefficient values. The microsphere concentration was quantified continuously using a pre-calibrated (Figure 3.11, in supplementary material 3.6) spectral fluorimeter (Co. Albilia, type GGUN-FL30). Note that this experiment was realized for one selected setup only due to logistical and technical limitations beyond the influence of the authors.

E3: Experiments with Enterococcus faecalis JH2-2

Enterococcus faecalis JH2-2 (*E. faecalis* JH2-2, a non-pathogenic opportunistic bacteria) was used as model bacteria in the experiments denoted E3.1 to E3.4. The bacteria were obtained in frozen aliquots (Laboratory of Physical Chemistry and Microbiology for the Environment, Team of Environmental Microbiology, University of Lorraine, Nancy, France), from which pure cultures were streaked in m-Enterococcus agar plates. The plates were stored at $4°C$ and renewed every month, to ensure the presence of viable bacteria for the experiments. At the start of each experiment a single colony was picked from these pure culture plates, using a sterile rod and suspended in a 1 mL vial containing Brain Heart Infusion (BHI) broth (Co. Sigma-Aldrich) media. The suspension was then incubated at $30°C$ (for maximum bacteria yield) for 18 h to allow them to reach their stationary growth phase (Figure 3.12, in supplementary material 3.6). Upon reaching the stationary growth phase, the suspension was centrifuged at $\sim$ 12000 x g for 10 minutes and washed twice with sterile 0.85% NaCl solution. Dilutions with sterile 0.85% NaCl solutions were made to adjust the concentration of the bacterial solution (used for continuous injection into the column) to approximately 1000 $CFU\ mL^{-1}$ (coliform units per mL). The procedure to adjust the inlet concentration involved an initial measurement of optical density of the bacterial suspension. This gave an instant estimate of the bacteria concentration, since the optical density value was converted to bacteria concentration in $CFU\ mL^{-1}$ using a pre-calibrated curve (Figure 3.13, in supplementary material 3.6). This concentration was later confirmed using standard spread plating method [Buck and Cleverdon, 1960].

In the E3 experimental series, *E. faecalis* JH2-2 were exposed to varying water characteristics (C1 to C4) as explained before. Each experiment had two technical replicates and four biological replicates (Figure 3.1). A technical replicate involved plating the same sample two times to determine the standard deviation of a single measurement (represented using error bar in the figures). A biological replicate represents the values obtained from repeating the experiment three times to confirm the reproducibility of the results. All the data points obtained from the biological replicates, have been normalized and combined in the results section. For experiments with inlet solutions devoid of DO (conditions C1 and C2), DO and other solved gases were removed from the water using a vacuum pump. To achieve this, sterilized and de-ionized tap water (with or without added nutrients) was subjected to vacuum degassing in a vacuum bottle for at least 30 minutes (target pressure within the bottle was approximately 34 mbar, the typical minimum value for this system). This solution was transferred to a sterile vacuum bag using nitrogen gas (overpressure method, total of 2 bar). For the experiments with DO (conditions C3 and C4), 0.85% NaCl solutions (with or without added nutrients) were sterilized in glass bottles sealed with a sterile rubber cork. The rubber cork contained two tubes (one connected to the peristaltic pump and one connected to a filter with 0.45 µm pore size) to regulate air pressure inside the bottle. For the conditions where DO was present, the concentration of the DO was measured to be approximately 8.9 $mg\ L^{-1}$ at 20 $°C$ (WTW FDO ®925). The viability of the bacteria at the highest possible concentration of DO at this temperature was aimed to be tested, this is why the DO concentration was left unchanged for the purpose of the experiments.

For the conditions with nutrients (C2 and C4), it was desired to have a concentration of nutrients to prevent excessive bacterial growth, which could result in biofilm formation inside the column. Growth rates of the bacteria using different concentrations of BHI were determined (Figure 3.14). Results indicate that the growth rate of the bacteria were significantly reduced for BHI concentration scenarios below 18.5 $mg\ L^{-1}$ (Figure 3.14). Thus, a nutrient solution with 14.8 $mg\ L^{-1}$ concentration was chosen for conducting the flow experiments.

At the end of each experiment the pore water was drained and the column was sectioned into five parts (3 cm for each section; see Figure 3.1). The sediment was carefully scraped out using a sterile spatula and transferred into a sterile petri dish, in a sterile environment. The sediment bacteria were quantified using methods described in Negreanu et al., 2012. 1 gram of sediment was suspended in 9 mL of sterile saline solution (0.85% NaCl) and vortexed (Co. Eppendorf MixMate) for 30 seconds and then shaken in an orbital shaker (Co. GFL) for 30 minutes. 100 μL of the decanted saline

solution was then pipetted into m-Enterococcus agar plates for quantification.

E. faecalis JH2-2 was quantified via standard spread plating methods using m-Enterococcus agar with 1% Triphenyltetrazoliumchloride (both Co. Sigma-Aldrich). Selective growth of *E. faecalis* JH2-2 was achieved by incubating the plates with samples at 41 $°C$ for 48 h (as per manufacturer's instructions). 100 μL of the samples were pipetted in freshly prepared agar plates; dilutions were made where concentrations were higher than 300 colonies per plate. The (dark) red colonies were counted (approximately 30 to 300 colonies) to determine the concentration.

Hydrophobicity determination

The hydrophobicity of the bacteria was determined using the 'bacteria adhesion to hydrocarbons' (BATH) method employing the procedure as described in Rosenberg, 1984. This experiment was conducted twice to reveal the hydrophobicity of *E. faecalis* JH2-2 to be 6.3% and 2.8%, respectively. The values indicate that *E. faecalis* JH2-2 are relatively hydrophilic and, hence, prefer the water phase.

3.2.2. Modeling and data analysis procedure

Framework basics and implementation

The employed model equation system (Table 3.2) merges the standard 1-D advection-dispersion equation (ADE), with a set of sub-models specifically related to microbial transport and reactive processes in the subsurface (colloidal straining, decay, respiration, (de)attachment, and microbial growth) that can be (de)activated separately. Two primary system variables are: water phase bacteria concentration (C) and sediment phase bacteria concentration (C_s), respectively. In the present study the model's differential equations (Table 3.2) were implemented into a newly designed computer-based algorithm employing the *R* package 'rodeo' [Kneis et al., 2017]. The package was chosen for the sake of computational efficiency of the optimization approach as 'rodeo' allows to realize selected functions to be written and compiled using FORTRAN [Adams et al., 1997]. The equations were solved using the method-of-lines approach included in the *R*-package 'deSolve' [Soetaert et al., 2010]. The 'FME' [Soetaert and Petzoldt, 2010] package was used for parameter estimation based on 'Port' [Gay, 1990] and 'bobyqa' [Powell, 2009] algorithm methods. Once the optimization routine converges, best-fit parameters for each of the given experimental data set are written to the output. The source code can be found at: https://github.com/aparna2306/bacteria_transport).

Table 3.2: Equations used to describe the processes (header) occurring for the water (first row) and sediment phase (second) bacteria. The experiment types used to determine the parameters are listed in the last row.

Change in storage	**Advection and dispersion**	**Colloidal straining [Xu et al., 2006]**	**Microbial decay, respiration, and de-/attachment [Bradford, Simunek, and Walker, 2006]**	**Microbial growth**
$\frac{\partial C}{\partial t}$	$-\frac{v_d}{\theta_e} * \frac{\partial C}{\partial x} + \alpha * \frac{v_d}{\theta_e} * \frac{\partial^2 C}{\partial x^2}$	$-k_{str} * C * e^{-C_s/\lambda}$	$-\mu_d * C - \mu_r * C - K_{att} * C$	$+\mu_g * C$
$\frac{\partial C_s}{\partial t}$		$+k_{str} * C * e^{-C_s/\lambda}$	$+K_{att} * C$	$+\mu_{gs} * C_s$
Experiment type	solute tracer experiment (E1)	microsphere experiment (E2)	bacteria experiment (E3) with conditions C1 and C3	bacteria experiment (E3) with conditions C2 and C4

Stepwise model fitting approach

To determine the transport parameters shown in Table 3.2, the process model components have to be fitted to the respective experimental data. A combined fitting of the complete model to all experimental data sets at the same time is, however, not feasible due to the large number of fitting parameters. To avoid model over-parameterization, the parameters were identified stepwise in this study ensuring that only one to two parameters were determined at the same time (refer Table 3.1).

First, Darcy velocities (v_d, $cm\ min^{-1}$) were directly obtained from the column setups (flow rate divided by flow area). Results from the solute tracer tests (E1) were used to determine both effective porosity (θ_e, dimensionless) and longitudinal dispersivity (α , cm) via the standard ADE. Hereby, initial estimates were obtained using the analytical-graphical method as described by Käss, 2004. Based on that, the colloidal straining rate (K_{str}, min^{-1}) and its coefficient (λ , particles per gram of soil) were determined in another step by fitting the straining model by Xu et al., 2006 to the breakthrough curves from the microsphere injection experiment E2 (while keeping θ_e and α fixed). The porosity and dispersivity values were also assumed to be the same as the tracer tests. It has been observed in similar studies (e.g. Xu et al., 2006), that the dispersivity of the colloids does not change greatly for lab-scale columns. These basic transport parameters are kept fixed for all further bacteria-related model fittings. Furthermore, since the grain diameter range used for all the experiments remain unchanged, it was reasonably assumed that the straining process rate is constant for all the experiments.

Microbial decay, respiration, attachment, and detachment are de-facto simultaneous processes with partially overlapping effects and were thus required to be fitted separately. This is a more complex step requiring controlled but varying biological and hydro chemical conditions. Microbial decay (μ_d, min^{-1}) and respiration (μ_r, min^{-1}) are determined using the bacteria concentrations measured at the inlet of the column in experiments E3.1 and E3.3 by exposing *E. faecalis* JH2-2 to the conditions C1 and C3, respectively. A 0-dimensional kinetic decay model was used to determine these parameters. Due to lower model complexity, these require lesser data points in general. Simultaneously, the attachment rate (K_{att}, min^{-1}) was determined for both C1 and C3. Microbial growth rates in both the water (μ_g, min^{-1}) and sediment phase (μ_{gs}, min^{-1}) were determined separately in experiments E3.2 and E3.4 by exposing the bacteria to the C2 and C4 conditions (i.e. without and with DO). This was done to analyze the impact of DO on the growth rate. Further information related to the parameter determination (especially for the bacteria-related part) is given at the respective sections of the result presentation. Also note that the experimental data (i.e. the breakthrough curves) was

evaluated in a normalized, i.e. dimensionless form, to allow for an inter-experiment and straightforward data comparison. Hereby, the input concentration (i.e. C_o) of a specific component at the inlet (i.e. $x = x_0 = 0\ cm$) and at starting time (i.e. $t = t_0 = 0\ min$) was used as scaling parameter for concentration axis (x-axis). Water phase concentrations are represented as $C_r = C/C_o$ and the sediment phase concentrations as $C_{rs} = C_s/C_o$. Since the inlet concentration is variable in the case of the E3 experiments (with conditions C1 to C4), the inlet concentration curves were considered as a function rather than a constant value. However, the input to the model was simplified by linear interpolation between the measured data points (see, "boundary.f95 file in the uploaded code). Time axis presentation (x-axis) was used unchanged from experimental data, without normalization.

In addition to the above, a prediction of bacteria migration in field-scale was conducted. To warrant a field scale prediction, the length of the column is increased from 15 cm to 150 cm. All other parameters were held constant, including the boundary conditions. The condition C4 is used as a case study. A range of fifty parameter values were generated, with equally incrementing values from a set minimum (2 orders of magnitude lower than determined parameter values), and maximum (2 orders of magnitude higher than determined parameter values) value. The actual parameter range are tabulated in Table 3.10, in the supplementary material 3.6. The function 'sensRange' [Soetaert and Petzoldt, 2010] included within the FME package, was used to calculate the model result for each generated parameter value. This study highlights the sensitivity of dispersivity values on the field scale prediction. A detailed sensitivity analysis of the impact of other parameters are shown separately in the supplementary material 3.6 (Figure 3.15). The resulting breakthrough curves are then compared to the observations from the lab scale experiment. The results comparing the lab-scale observation with that of the field scale prediction present dimensionless concentration (y-axis) and time (x-axis) axes, to facilitate interpretation of the results. The dimensionless concentration axis was scaled similarly to that of the lab-scale columns described previously. However, the time axis was scaled to the residence time of the water in the column and is represented in terms of pore volumes as $pv = \frac{(time*L)}{(v_d/\theta_e)}$, where L is the length of the column, and time is the x-axis variable.

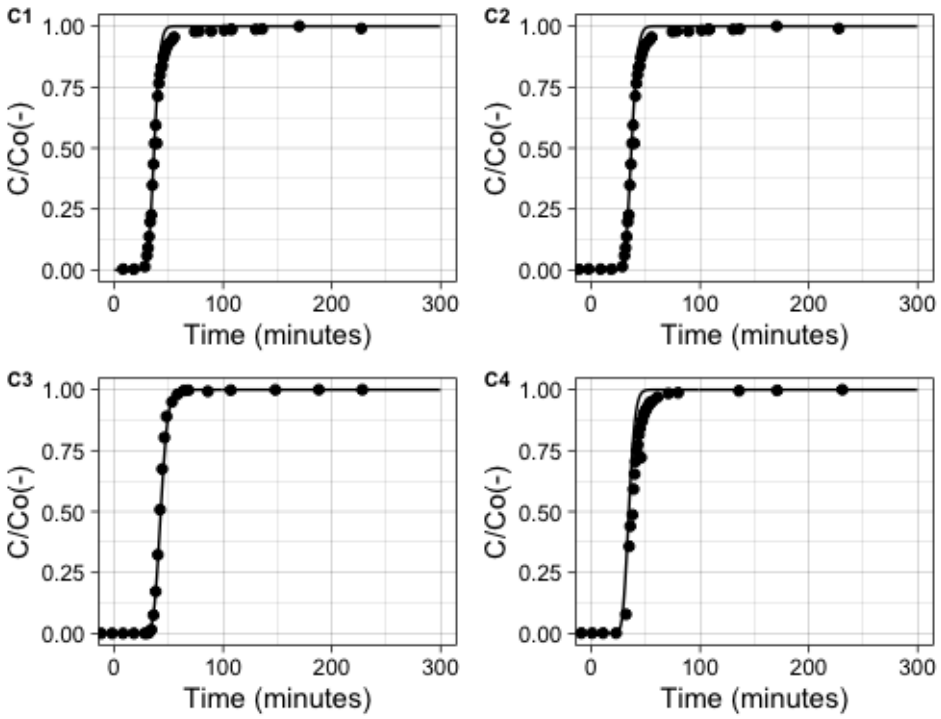

Figure 3.2: Experiment E1 – Normalized solute tracer breakthrough curves (C/C_o, circles) for conditions C1 to C4 with model fitting (ADE, solid line). C/C_o (-) is the normalized tracer concentration, i.e. ratio of measured tracer concentration to the inlet concentration of the tracer at the start of the experiment.

3.3. Results

3.3.1. Determination of hydraulic and non-reactive transport parameters (experiments E1 and E2)

The standard ADE was able to describe the dynamics of the breakthrough curves obtained from Experiment E1. Inverse modeling results obtained from fitting the non-modified ADE to the solute tracer test data (E1 series, see breakthrough curves, Figure 3.2) show θ_e between $\sim$ 34% and $\sim$ 39% (Table 3.3). These values are almost equal to the respective total porosities (total porosities were obtained gravimetrically, Table 3.3) indicating negligible immobile pore water amounts. Furthermore, the effective porosity as well as the dispersivity values do not vary greatly between each condition (Table 3.3) showing consistency in the column packing procedure. Specifically, the dispersivity values range from 0.5 to 1 mm. Since the length of the column is 15 cm, the effect of the dispersion process is minimal.

In the E2 experiment, the straining equation (Table 3.2) theorized by Xu et al., 2006 fit the data obtained from the continuous monitoring of the colloidal particles well

Table 3.3: Overview on the flow and transport experiments: labels for experiments and the conditions that they were subjected to.

Parameter (E1)	**Condition 1**	**Condition 2**	**Condition 3**	**Condition 4**
Parameters obtained using the optimization algorithm				
θ_e (-)	0.347 ± 0.008	0.342 ± 0.025	0.388 ± 0.041	0.365 ± 0.054
α (cm)	0.064 ± 0.022	0.080 ± 0.066	0.073 ± 0.025	0.093 ± 0.079
Known values (measured a-priori or given by boundary condition)				
Total porosity (-)	0.350 ± 0.044	0.342 ± 0.018	0.348 ± 0.006	0.350 ± 0.007
v_d (cm/min)	0.141 ± 0.004	0.138 ± 0.008	0.138 ± 0.004	0.157 ± 0.023
Parameter (E2)	**Condition 1**	**Condition 2**	**Condition 3**	**Condition 4**
K_{str} (min^{-1}	0.0378 ± 0.066	-	-	-
λ (particles / g-soil)	0.0728 ± 0.109	-	-	-

(Figure 3.3). Hereby, the previously obtained effective porosity and dispersivity parameter values were kept constant. The inlet concentration was constant, and continuously injected for the entire duration of the experiment. The model fits well with the experimental observations corroborating the use of the proposed straining model (residual standard error of fit is 0.023). The inversely determined colloidal straining (K_{str}) parameter value of $3.78 * 10^{-2}$ min^{-1} shows that straining is a process that is significant for particles of diameter $1\mu m$, and in sediments with grain sizes between 1 and 4 mm. This is corroborated by the Figure 3.3, where the outlet concentration is only 85% of the inlet concentration, even after three pore volume injections. As the rate of straining is of the order of magnitude of 10^{-2} min^{-1}, the straining process cannot be neglected for this set-up. The corresponding straining coefficient λ is $7.28 * 10^{-2}$ particles per gram-soil.

3.3.2. Determination of parameters related to the bacteria transport (E3 series)

Condition C1 – DO and nutrient-free conditions

In this condition the survival of the bacteria at both the inlet and the outlet of the column is the least. The bacteria show almost an instantaneous decrease in concentration (within 15 minutes from the start of the experiment) at the inlet of the column. The decay rate (μ_d) was determine using the concentration reduction occurring from 15 until 250 min. The decrease in concentration occurring in the first 15 minutes of the experiment was exponential and therefore is not considered for the fitting of this model. The parameters of microbial decay (μ_d) and attachment (K_{att} (C1)) are obtained using this condition. The decay rate – assumed to be non-related to the migration process through the porous medium – was determined by fitting the inlet bacteria concentration variation obtained

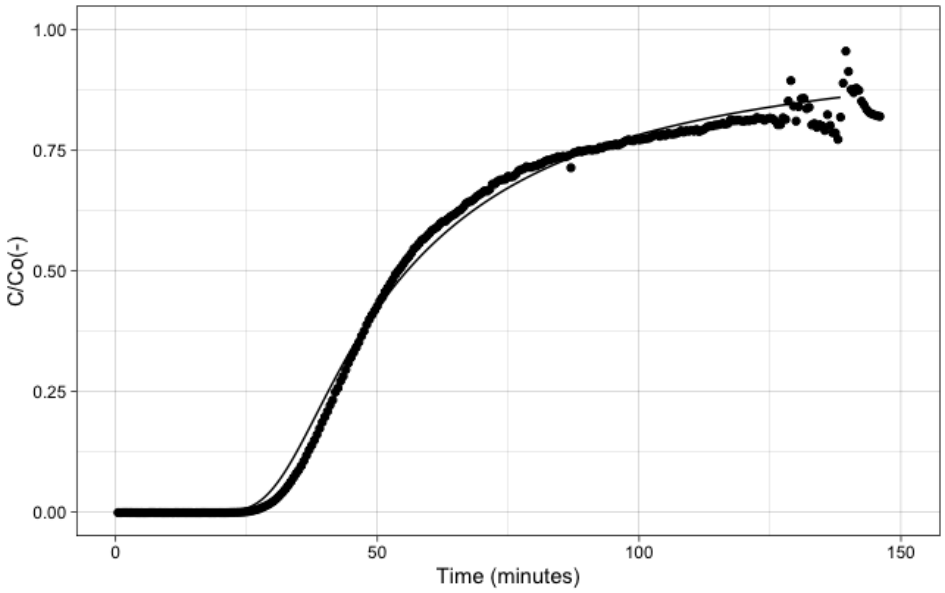

Figure 3.3: Experiment E2 – normalized microsphere breakthrough curves (C/C_o, black dots) with model fitting (solid line, strainingg model). C/C_o (-) is the normalized microsphere concentration, i.e. ratio of measured microsphere concentration to the inlet concentration of the microsphere at the start of the experiment.

in the E3.1 flow experiment (Figure 3.4a, black line shown in the first 30 minute section) to a first-order decay model (Table 3.2). The obtained rate is of the order of magnitude of 10^{-2} min^{-1} (Table 3.4), i.e. of the same order as the straining rate. This decay rate was used in the next step of the optimization algorithm to inversely determine the linear and irreversible attachment rate. The breakthrough curve obtained from the outlet of the column subjected to condition C1 conditions (Figure 3.4b) was used for model fitting. The obtained attachment rate is very low for the bacteria in condition C1 with a value of around 10^{-7} min^{-1} (Table 3.4), i.e., almost five orders of magnitude smaller than the decay or straining rate. The reduction in the concentration of the bacteria at both the inlet and the outlet is thus attributed to the decay processes rather than the attachment process.

Condition C2 – Nutrients available in DO-free water

This part of the experiment was designed to obtain two parameters: growth of the bacteria in the water and sediment phase (μ_g (C2), μ_{gs} (C2)). Owing to the absence of dissolved oxygen, both the decay and attachment processes recorded in C1 were assumed to occur for the condition C2. Therefore, both the decay and the attachment rates obtained from the condition C1 were kept fixed for condition C2. Based on this assumption, growth rates arising due to the addition of nutrients should be extractable from the C2 datasets. Here, the *E. faecalis* concentration at the inlet (Figure 3.5a)

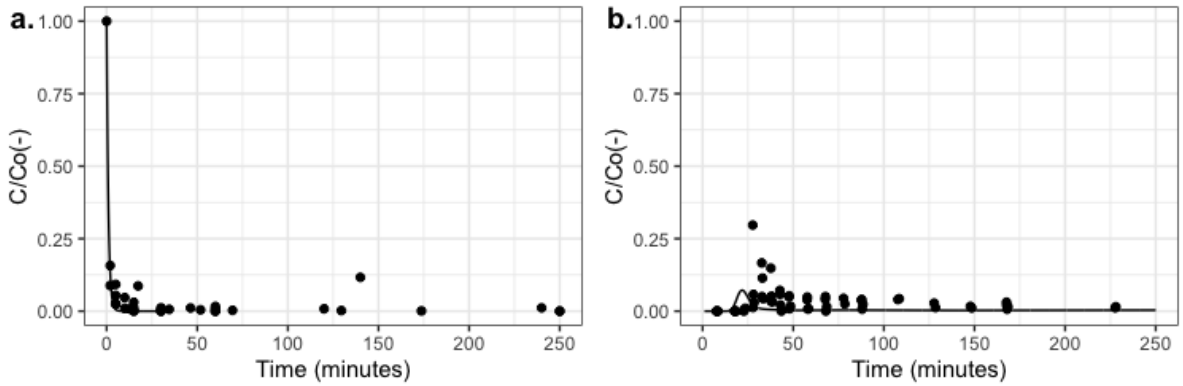

Figure 3.4: Experiment E3.1 – Normalized concentration curves (C/C_o, black dots) for E. faecalis JH2-2 exposed to condition C1 (nutrients: 0 $mg\ L^{-1}$, DO: 0 $mg\ L^{-1}$). Measured in water samples taken at the columns' a) inlet and b) outlet; including model fitting (solid line). C/C_o (-) is the normalized bacteria concentration, i.e. ratio of measured bacteria concentration – at both the inlet and outlet – to the inlet concentration of the tracer at the start of the experiment (at t = 0)

shows a decrease in concentration in the first few minutes of the experiment with exposure to condition C2, quite similar to that observed for C1 (as shown in Figure 3.4a). Nevertheless, contrary to C1, the bacteria show significant growth after approximately 100 minutes owing to the presence of nutrients. In addition to the growth of the bacteria in the inlet solution, microbial growth is also clearly visible in the breakthrough curve data obtained at the outlet of the column, i.e., after the passage through the porous media. The model fitting for C2 (Figure 3.5b) shows that the rate of growth is of the order of $10^{-2}\ min^{-1}$ (for both the water phase and sediment phase bacteria, Table 3.4). The outlet concentration, despite showing a consistent growth, is characterized by some fluctuations which are consistent with the fluctuations of the inlet boundary condition (Figure 3.5a). The growth rate parameter value is of the same order of magnitude as the straining rate (Table 3.3) and the decay rate parameters (Table 3.4).

Condition C3 – DO available, but no nutrients

The procedure used to fit the respiration rate and the rate of attachment (μ_r, K_{att} (C3)) was similar to that used in condition C1. The respiration rate was extractable from the variation of the inlet concentration (Figure 3.6a, black line represents the fit of the respiration model to the data). It was observed that the variation of the inlet concentration was low, when compared to that obtained in the conditions C1 and C2, where DO was absent. The apparent rate of $-2 * 10^{-4}\ min^{-1}$ (Table 3.4), was obtained by fitting a linear respiration rate constant to the data obtained in Figure 3.6a (black regression line). The μ_r value indicated that the contribution of the respiration process to the overall behavior is small. The respiration coefficient was then held constant, and the outlet breakthrough curve (Figure 3.6b) was used to determine the attachment rate

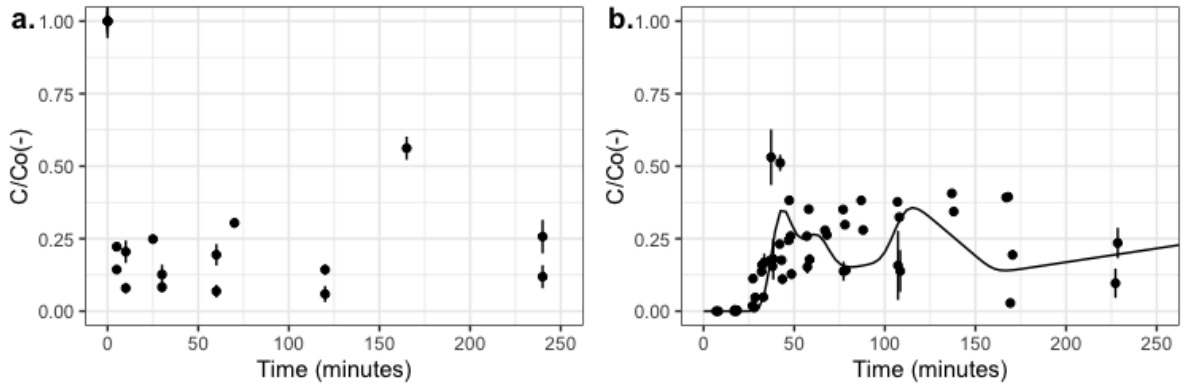

Figure 3.5: Experiment E3.2 – Normalized concentration curves (C/C_o, black dots) for *E. faecalis* JH2-2 exposed to condition C2 (nutrients: 14.8 $mg\ L^{-1}$, DO: 0 $mg\ L^{-1}$). Measured in water samples taken at the columns' a) inlet and b) outlet; the latter including model fitting (solid line). C/C_o (-) is the normalized bacteria concentration, i.e. ratio of measured bacteria concentration – at both the inlet and outlet – to the inlet concentration of the tracer at the start of the experiment (at t = 0).

parameter. Since the attachment rate obtained for this condition C3 was different from that obtained for the condition C1, the parameter was represented as K_{att} (C3) as seen in Table 3.4. The outlet breakthrough curve (Figure 3.6), show that after approximately 1 pore volume the bacteria reach an equilibrium concentration of 50% of the inlet solution. This indicated an additional attachment process, causing attenuation of bacteria within the column. Resulting attachment rate coefficient was of the order $10^{-3}\ min^{-1}$ (Table 3.4), which is four orders of magnitude higher than that obtained for C1. In addition, when compared to C2 (Figure 3.5b), the outlet concentration breakthrough curves show a higher survival of the bacteria in C3 (Figure 3.6b) for the investigated time frame. This indicated that the presence of DO is more favorable for the bacteria than nutrients. Quite similar to the previous steps, selected parameters, specifically the respiration rate and the attachment rate under aerobic conditions, are kept fixed during the optimization to allow the determination of the microbial growth rate for the water and sediment phase in the experiments with 'condition C4'.

Condition C4 – DO and nutrients available

The growth parameters for the bacteria in the water and sediment phase (μ_g , μ_{gs}) were determined using the dataset obtained from condition C4. This condition presented the highest survival of bacteria in both the inlet and the outlet of the column. Since both DO and nutrients were present in the water, a favorable condition for the bacteria was observed. Inlet concentration data (Figure 3.7a) show that the bacteria concentration gradually increase over time. Additionally, there seems to be further growth taking place during the transport through the sediment-packed column – as seen in the outlet concentrations. Towards the end of the experiment it was observed that the bacteria

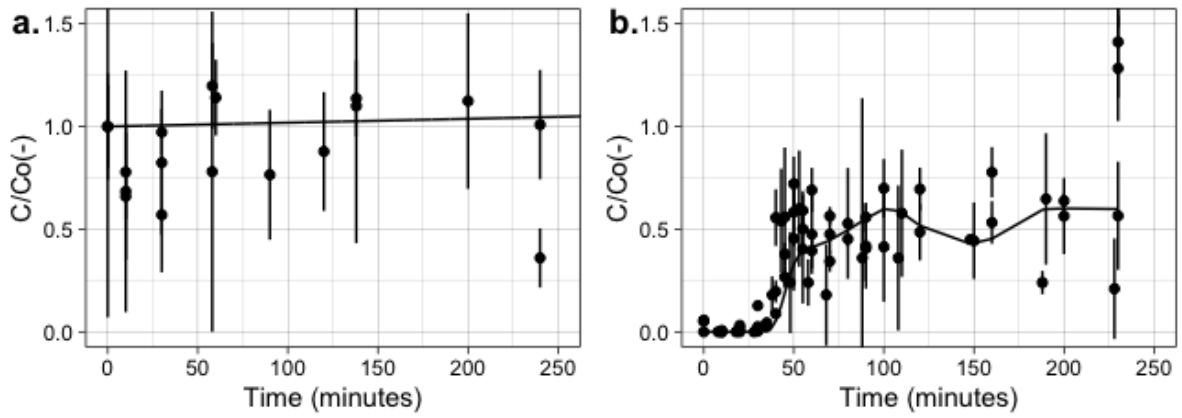

Figure 3.6: Experiment E3.3 – Normalized concentration curves (C/C_o, black dots) for *E. faecalis* JH2-2 exposed to condition C3 (nutrients: 0 $mg\ L^{-1}$, DO: 8.9 $mg\ L^{-1}$). Measured in water samples taken at the columns' a) inlet and b) outlet; including model fitting (solid line). C/C_o (-) is the normalized bacteria concentration, i.e. ratio of measured bacteria concentration – at both the inlet and outlet – to the inlet concentration of the tracer at the start of the experiment (at t = 0).

grow to reach a final concentration, three times higher than at the start of the experiment. The growth parameters could not be transferred directly from condition C2, as the growth rate was observed to be much lower for this condition. Therefore, to obtain a more accurate fit of the model, the growth rate coefficient was re-determined and notated as μ_g (C4), μ_{gs} (C4) in Table 3.4. The model fitting results show that water phase and sediment phase growth rates are of the order of $10^{-3}\ min^{-1}$ (Table 3.4), which are one order of magnitude lower than growth rate obtained from the experimental datasets under condition C2.

Summary of results, and prediction for field scale studies

The models were successfully fit to the data whereby the MSR and the standard error of the fit are at the most of the order of 10^{-2} (Table 3.4). Please note that the MSR and standard error values are obtained from the parameter estimation method. Furthermore, the flexible environment provided by the *R* software enabled us to adapt the model to have separate attachment, and growth rate coefficients for each of the conditions. The water phase bacteria showed highest survival for the condition C4, which contained both DO and nutrients.

The sediment-phase bacteria concentration was the highest for the condition C3 (Figure 3.8), and the lowest for the conditions C1 and C2. This result is consistent with the attachment parameters that were obtained for these conditions (Table 3.4), and corresponding model evaluations presented by M1, M2 and M3. The low attachment rates obtained for the conditions C1 and C2 are further corroborated by the model predictions (M1, M2). While the model successfully predicts the sediment-phase bacteria concen-

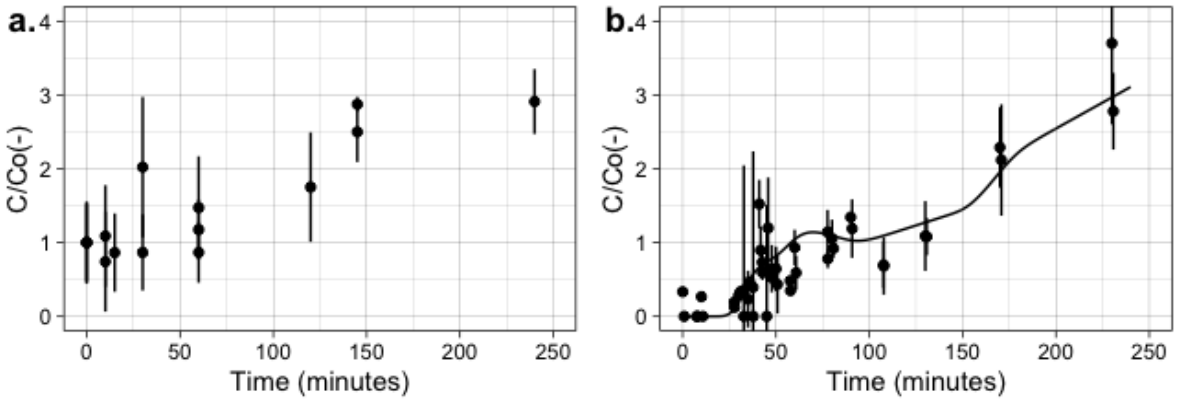

Figure 3.7: Experiment E3.4 – Normalized concentration curves (C/C_o, black dots) for *E. faecalis* JH2-2 exposed to condition C4 (nutrients: 14.8 $mg\ L^{-1}$, DO: 8.9 $mg\ L^{-1}$). Measured in water samples taken at the columns' a) inlet and b) outlet; including model fitting (solid line). C/C_o (-) is the normalized bacteria concentration, i.e. ratio of measured bacteria concentration – at both the inlet and outlet – to the inlet concentration of the tracer at the start of the experiment (at t = 0).

Table 3.4: Parameter values obtained from fitting bacteria breakthrough curves for conditions C1 - C4

Parameter (min^{-1})	**Estimated value**	**Standard Error**	**Mean squared residual of fit (MSR)**	**Comments**
μ_d	$6.16 * 10^{-2}$	$3.13 * 10^{-2}$	$2.12 * 10^{-4}$	Determined for C1 using Figure 3.4a
K_{att} $(C1)$	$1.75 * 10^{-7}$	$2.155 * 10^{-3}$	$3.23 * 10^{-3}$	Determined for C1 using Figure 3.4b
μ_g $(C2)$	$6.81 * 10^{-2}$	$3.55 * 10^{-4}$	$1.48 * 10^{-2}$	Determined for C2 using Figure 3.5b
μ_{gs} $(C2)$	$1.29 * 10^{-2}$	$3.57 * 10^{-4}$	$1.48 * 10^{-2}$	Determined for C2 using Figure 3.5b
μ_r	$1.84 * 10^{-4}$	$6.32 * 10^{-5}$	$2.82 * 10^{-2}$	Determined for C3 using Figure 3.6a
K_{att} $(C3)$	$1.37 * 10^{-2}$	$1.02 * 10^{-3}$	$2.87 * 10^{-2}$	Determined for C3 using Figure 3.6b
μ_g $(C4)$	$8.48 * 10^{-3}$	$1.29 * 10^{-3}$	$9.71 * 10^{-2}$	Determined for C4 using Figure 3.7b
μ_{gs} $(C4)$	$3.89 * 10^{-3}$	$9.42 * 10^{-3}$	$9.71 * 10^{-2}$	Determined for C4 using Figure 3.7b

tration for the conditions C1 and C2, the model over predicts the sediment retained bacteria concentration for the condition C3 and C4 (as shown by the lines M3 and M4).

The results, that have been obtained in the laboratory (condition C4), were used to make a prediction of the bacteria transport in small field-scale. The processes identified, i.e. advection-dispersion, straining, respiration, attachment, and growth, were implemented (based on the parameters values obtained in condition C4). The results

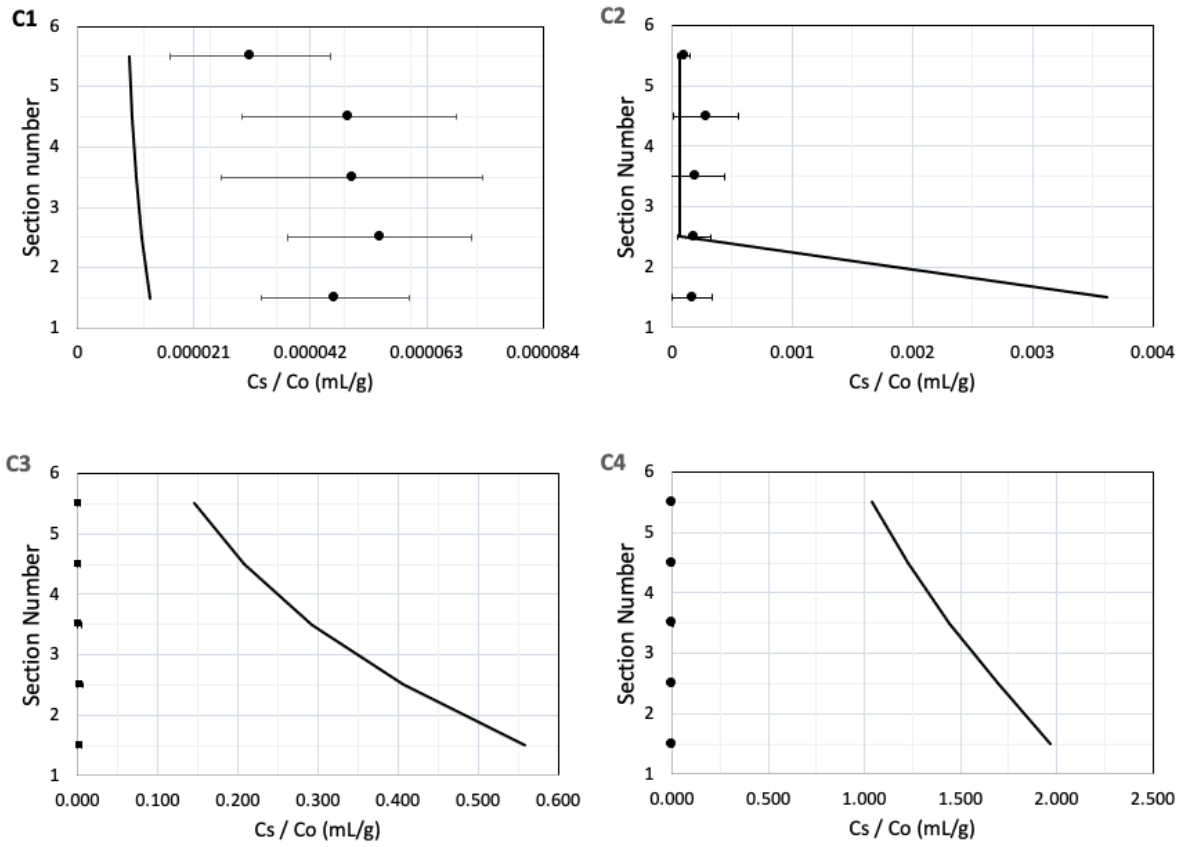

Figure 3.8: Observed concentration variation of soil bacteria in the aforementioned conditions (section 1 directly follows the inlet point, section 5 is next to the outlet point). Points represent the normalized measured concentration values (C_s/C_o) values for conditions C1 to C4 (solid black dots), with corresponding model evaluations represented by M1 to M4 (solid black line). C_s/C_o ($mL\ g^{-1}$) is the normalized sediment phase bacteria concentration, i.e. ratio of measured bacteria concentration at each sediment section, to the inlet concentration at the start of the experiment (at t = 0)

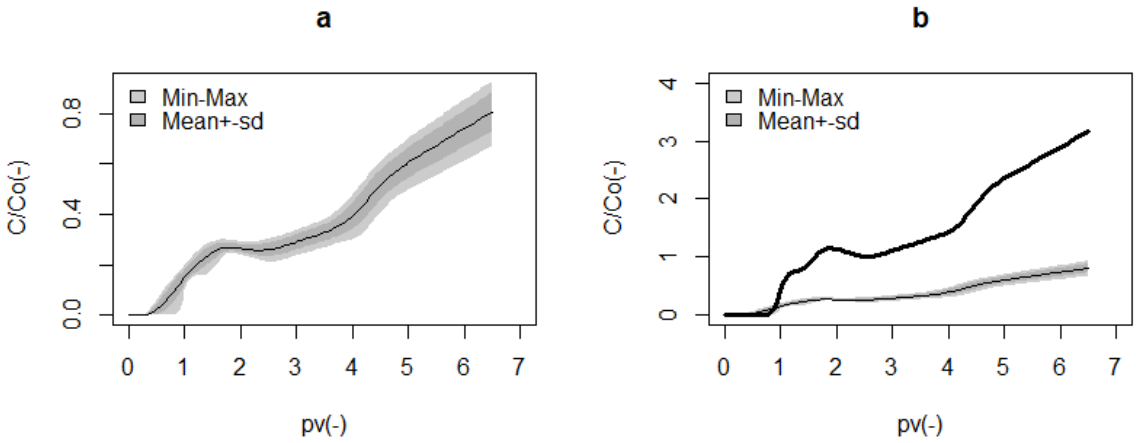

Figure 3.9: a) Sensitivity of the dispersivity parameter in field scale prediction, b) Model result for condition C4 (solid thick line) as compared to the same results that is predicted to occur in a 1.5m long field sediment columns (thin line within grey cone). C/C_o (-) is the normalized bacteria concentration, i.e. ratio of measured bacteria concentration – at both the inlet and outlet – to the inlet concentration of the tracer at the start of the experiment (at t = 0).

obtained compare the field scale result (grey cone, and solid thin black line) where the dispersivity value was incrementally distributed between 0.2 to 20 cm for 6.5 pore volumes (Figure 3.9), with the lab-scale experiment (solid line) and the field scale prediction. The dispersivity value are always different (mostly much higher) for field scale setups, compared to lab-scale. It is rightly observed that in general the fraction of bacteria reaching the outlet of the column is much smaller for the field-scale when compared to that obtained in the column. This is attributed to the larger straining process, causing a higher fraction of bacteria to be entrapped in the sediment, in the field scale. In addition, it is observed that the concentration of bacteria at the outlet is not very sensitive to the dispersivity parameter for the studied dispersivity length (0.2 - 20 cm). The shape of the curve remains the same for all the test parameter values indicating consistent boundary conditions. Therefore, the dispersivity value is used unchanged for further parameter sensitivity analysis (Figure 3.15, Table 3.5). A summary of the sensitivity analysis of the other parameter are shown in Figure 3.15, in the supplementary material, with the table of parameter range values in Table 3.5.

3.4. Discussion

3.4.1. Physical processes (E1 and E2)

Effective porosities (θ_e, Table 3.3) and dispersivity (α ,Table 3.3) values obtained were consistent with that expected for a water saturated column, packed with sediment of the grain size between 1 and 4 mm [Gibb et al., 1985]. The parameter values for dispersivity and effective porosities do not change greatly with repacking, showing consistency with packing methods. Furthermore, this ensures that the transport processes remain consistent, and enable us to build upon the model to determine reactive processes. The straining rate and straining coefficient parameters obtained in this study varied significantly from that obtained previously. Other studies have reported low straining rate coefficients (with values of de-facto 0 min^{-1} as seen in Xu et al., 2006) for flow setups characterized by a ratio between the colloidal particle diameter and the mean grain size diameter of the porous medium (i.e. d_p/d_g) of smaller than 10^{-4} (as chosen in this study). However, in the present experimental study we observe that straining contributes significantly to the fate of bacteria in the subsoil. This is most likely related to the much lower Darcy velocities used in our experiments (almost one third of the Darcy velocity used in the previous study of Xu et al., 2006). This, in turn, indicates that the relationship between the d_p/d_g ratio and straining rate is not valid for lower flowrates (as in this study).

3.4.2. Biological Processes (E3 series)

Condition C1 (E3.1.)

The inlet concentration of bacteria (Figure 3.4a) did not remain constant when subject to Condition C1. Although *E. faecalis* JH2-2 are facultative anaerobes, they show an instantaneous decrease in concentration upon contact with an environment devoid of DO (Figure 3.4). This could be because (a) no source of nutrients or comparable ions (like nitrates) is available to aid in its survival, therefore unfavorable survival conditions for the bacteria occur, or (b) *E. faecalis* transform into a viable but non-culturable (VBNC) state. Since the bacteria were grown and cultured in environments containing DO, a sudden unfavorable change in the condition could have caused the bacteria to transform into a VBNC state, thus undetectable using standard spread plate methods. Although the exact reason for the apparent concentration decrease is unknown, it can be observed that the absence of DO is an unfavorable condition for the bacteria. Previous studies

that have recorded transport of bacteria do not take the survival of bacteria in non-DO environments into account. The relatively low attachment rate indicate that the bacteria do not prefer to attach to the sediment in the absence of DO. Since *E. faecalis* JH2-2 were previously determined to be relatively hydrophilic, the low rate of attachment and low concentration of sediment-phase bacteria corroborate these results. The stepwise approach was able to successfully isolate the process of decay and attachment for this condition.

Condition C2 (E3.2.)

The condition is also characterized by a variable boundary condition similar to that observed in condition C1. The bacteria undergo both the decay and the growth process at the inlet and outlet of the column. The growth rate obtained in this condition C2 is of the same order of magnitude as the decay rate of bacteria that is obtained in the condition C1. This shows that the decay and the growth process simultaneously dominate the bacteria migration in the absence of DO, along with straining process. Since both the processes counteract each other, an equilibrium between the two processes is achieved. This is reflected in Figure 3.5, where the bacteria concentration curve at both the inlet and outlet of the column show a constant value after approximately 100 minutes of the experiment. The growth rate of the bacteria obtained from this condition is higher than that obtained from the batch growth rate of the bacteria (Figure 3.12). Since *E. faecalis* JH2-2 are facultative anaerobes, it is observed that their growth rate is much higher once they adapted to the DO free environment. The lower concentration of sediment retained bacteria obtained for this condition corroborate the lower attachment rate that was transferred from the condition C1. Growth of the sediment phase bacteria was, however, not significant although μ_{gs} (C2) parameter is relatively high ($\sim 10^{-2}$ min^{-1}). Since the concentration of sediment-phase bacteria is quite low, it could take much longer to see a significant impact of sediment-phase growth process. The stepwise modelling and experimental approach were thus successful in isolating the processes of decay, growth and attachment for the condition C1 and C2.

Condition C3 (E3.3.)

In this condition the absolute survival of the bacteria is much higher than for the condition C2 where the bacteria are suspended in an environment containing nutrients, further emphasizing the importance of DO for the survival of bacteria. Contrary to the conditions C1, C2 and C4, the variation of inlet concentration of the bacteria is not very high. A slight increase in the bacteria concentration at the inlet (Figure 3.6a), is observed possibly owing to the presence of trace nutrients, which were not stripped

off from the double washing of the bacteria before injection. The rate of attachment observed for the condition C3 was much higher than that obtained for the condition C1 indicating that the attachment process is more important in the presence of DO. This could be attributed to a) higher concentration of bacteria being present in the water phase available for attachment to the sediment thus leading to a higher rate of attachment or b) a change in the surface structure of the bacteria due to the presence of DO making it more suitable to attach to the sediment particles. Since the hydrophobicity tests (Section 3.2.1) indicate that *E. faecalis* JH2-2 are relatively hydrophilic, there is a higher possibility that the change in DO concentration causes a change in the surface structure of the bacteria leading to this difference in the attachment rate constant values. An overprediction of the model to the sediment-retained bacteria in observed in Figure 3.8. This could be attributed to an additional decay process that has not been accounted for in the current modelling approach. Since there were no additional data points for the sediment retained bacteria, further processes were not added to the sediment-phase. Further investigations should focus on getting kinetic data for the sediment retained bacteria to understand processes occurring in the sediment phase.

Condition C4 (E3.4.)

The bacteria survive the highest, in the presence of this condition. The boundary condition is not constant for this condition and shows an increase of bacteria concentration over time, which is indicative of growth. In addition to the growth of the bacteria in the inlet of the column, growth of the bacteria at the outlet of the column is also observed. The growth rate obtained from this condition is one order of magnitude smaller than that obtained for the condition C2. Despite this, it is seen that the absolute concentration of bacteria is the highest in this condition. This is attributed to the absence of a high decay rate that was associated with the condition C2. The growth rates obtained from this condition are consistent with that obtained from the batch growth rates (Figure 3.12.). For the condition with DO we see that the attachment of the bacteria to sediment, and straining is more dominant that the growth rate. A similar over prediction of the sediment-phase bacteria concentration is observed in this condition. Similar to condition C3, the presence of an additional decay process could explain this over prediction. The stepwise approach, and construction of a separate model in *R* software was successful in isolating the parameters of respiration, growth and attachment for the condition C3 and C4, and enabled comparison of the parameter values between the experiment E3.1-3.4.

Field scale prediction

The parameters that were obtained for the condition C4 were used to make predictions for the field scale result. The results indicate the change in dispersivity values from 0.2 cm to 20 cm only causes a change in the relative bacteria concentration from ~ 0.85 to ~ 0.5 (Figure 3.9a). Please note that the cell size used for the discretization was 0.5 cm, and the increments for dispersivity values for the sensitivity were 0.4. The Grid Peclet number is always below 2, thus eliminating the effects of numerical dispersion. The dispersivity does not cause a significant change in the outlet concentration of bacteria for the studied length and pore volume (Figure 3.9b). Since the attenuation processes of straining and attachment were more dominant for this condition, it is consistent that for longer travel lengths the outlet bacteria concentration is much lower. Results from this field scale prediction can be used to design sampling campaigns where the TWW are conditioned to similar DO and nutrients concentrations. The dispersivity length obtained from lab scale results are used in the field scale sensitivity analysis presented in the supplementary material in Figure 3.15. It is observed that the parameters of water-phase growth rate and respiration rate are very sensitive. Hence, determination of the same needs to be done carefully.

3.5. Conclusions and Outlook

The purpose of the combined experimental and model investigation was to isolate the processes and quantify the corresponding parameters that describe the impact of DO and nutrients on bacteria transport through sandy/gravel sediments. For this purpose, model evaluation was done using data from laboratory-scale experiments under constrained conditions. This study builds upon selected processes that are relevant for subsoil transport of bacteria. The stepwise approach was successful in isolating the simultaneous processes and thus obtain relevant parameters values corresponding to the proposed processes. Furthermore, the use of the flexible *R* software, enabled us to evaluate model parameters separately for each of the conditions. An understanding of these processes is relevant for the further investigation of bacteria spreading during reuse of TWW. In particular, it can be seen that changing important TWW characteristics of DO and nutrients exert a significant influence in biological processes namely microbial decay, respiration, attachment and growth of bacteria. It was determined that in the presence of dissolved oxygen, the attachment of bacteria to sediment was the most dominating process, whereas in the absence of dissolved oxygen microbial growth in the water phase was dominant. These processes add new knowledge into the research on the im-

pact of reuse of TWW in the spread of opportunistic bacteria (especially resilient species like *Enterococcus*), on the environment, and emphasizes the importance of research in this area. Furthermore, since *Enterococcus* is the preferred strain of bacteria used to determine fecal pollution, and there is a clear difference in the rate of attachment or decay when compared to *E. coli* (higher survival of *Enterococcus*) thus emphasizing that research with *Enterococci* species is imperative in the context of fecal pollution in the environment. This combined modelling and experimental approach can be used as a framework, upon which several processes can be added. This can be done step by step in a similar fashion as has been used in this study, where only one to two parameters are used for model fitting for a set of data. Addition of complexity, step by step can be used to develop a quantitative risk assessment model, where the risk of spread of certain bacteria and certain soil types can be predicted using the model. The risk assessment can prove to be instrumental in policy formulation and development for reuse of TWW in Europe and all over the world.

While this study adds on to knowledge about microbial processes in the subsoil environment, the results – obtained from experiments under well-defined and strictly controlled laboratory conditions – will most likely deviate when the experiment is repeated under more complex field conditions (with, for instance, spatiotemporally highly variable distributions of DO and nutrients). Adding complexity to hydraulic parameters (like variably saturated flow, presence of dead-end pores, and physically or chemically heterogeneous sediments) could help to create more realistic risk assessment models describing pathogen spread into soil and groundwater systems. Furthermore, the impact of external environmental triggers like temperature, water flowrate, grain size of sediments, and other types of bacteria (gram negative) and a combination of bacteria (as would be present in a real TWW sample) has not been covered in this study and should be investigated next. Addition of these processes upon the processes studied here will enable a holistic understanding of the various processes and the relative importance of the same when bacteria migrate through the subsoil.

3.6. Supplementary material

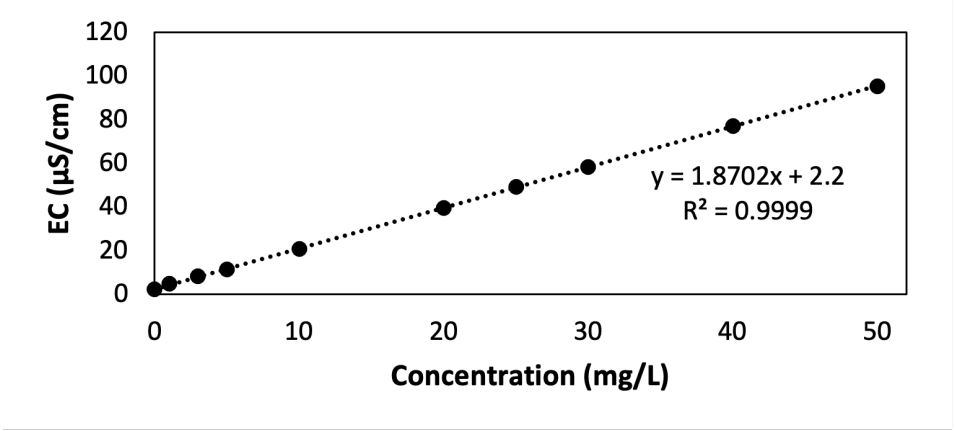

Figure 3.10: Calibration curve for tracer showing the relation between reading in the electrical conductivity meter with the concentration of tracer.

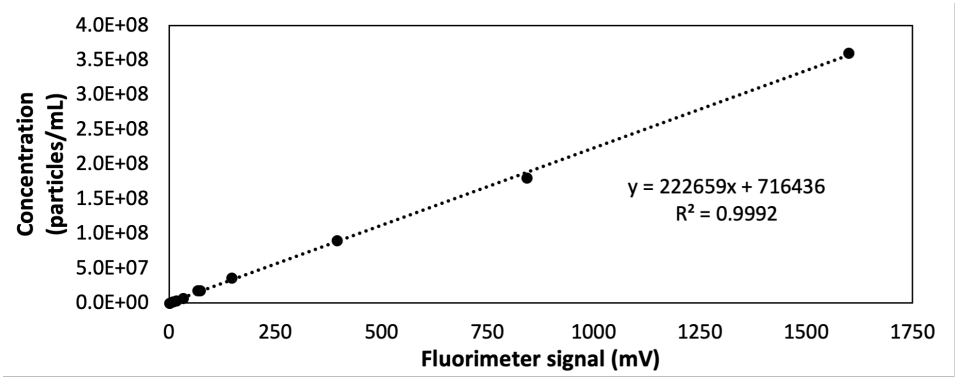

Figure 3.11: Calibration curve for the relation between spectral fluorimeter (reading in mV) and concentration of microspheres in particles/mL

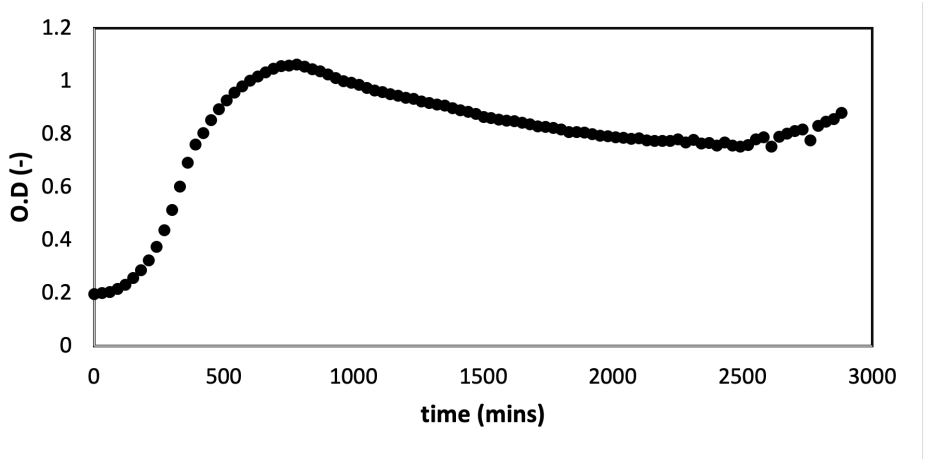

Figure 3.12: Curves representing the growth of bacteria, with nutrient concentration at 37 g/L as measured by the change in the optical density of the bacteria over time

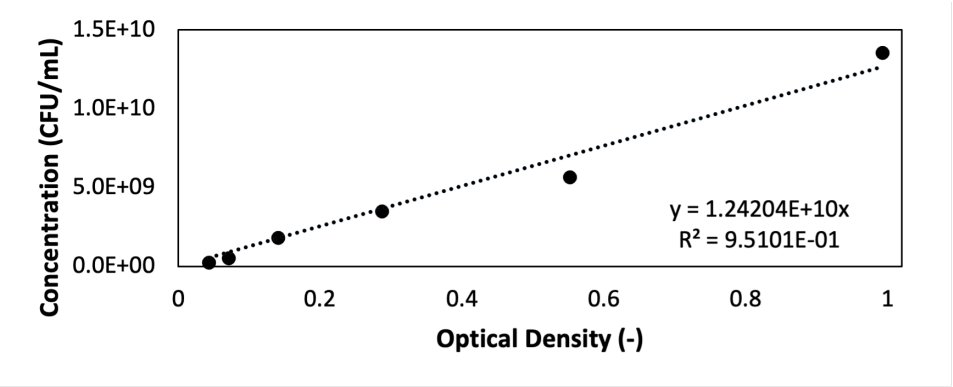

Figure 3.13: Calibration curve for the relation between bacterial concentration and optical density

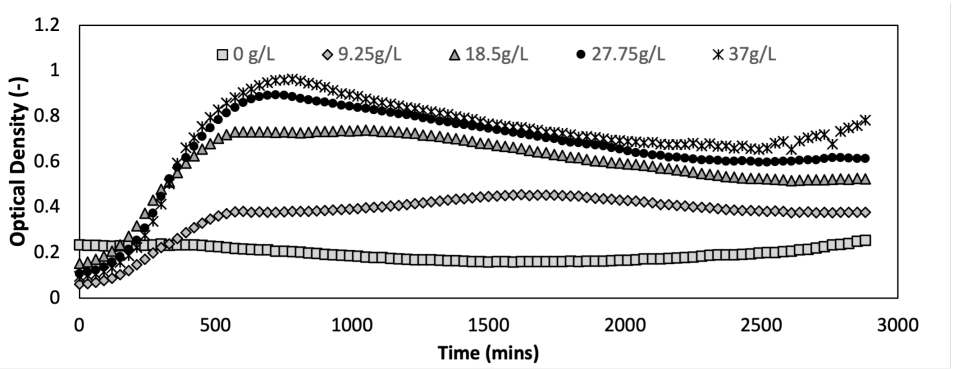

Figure 3.14: Curves representing the growth of bacteria, with nutrient concentration varying between 0-37g/L as measured by the change in the optical density of the bacteria over time

Table 3.5: List of parameters, with the values determined from the lab experiments and the minimum and maximum range to which they were changed for the sensitivity analysis.

Name of parameter	Value (from experiment)	min	max
μ_g (C4)	$8.48 * 10^{-3}$	$8.48 * 10^{-5}$	$8.48 * 10^{-1}$
μ_{gs} (C4)	$3.88 * 10^{-3}$	$3.88 * 10^{-5}$	$3.88 * 10^{-1}$
μ_r	$-2.00 * 10^{-4}$	$-2.00 * 10^{-6}$	$-2.00 * 10^{-2}$
K_{att}(C3)	$1.37 * 10^{-2}$	$1.37 * 10^{-4}$	1.37
D	$9.29 * 10^{-2}$	$2 * 10^{-1}$	$2.00 * 10^{1}$
θ_e	$3.65 * 10^{-1}$	$3.00 * 10^{-1}$	$3.70 * 10^{-1}$
k_o	$3.78 * 10^{-2}$	$3.78 * 10^{-4}$	3.78

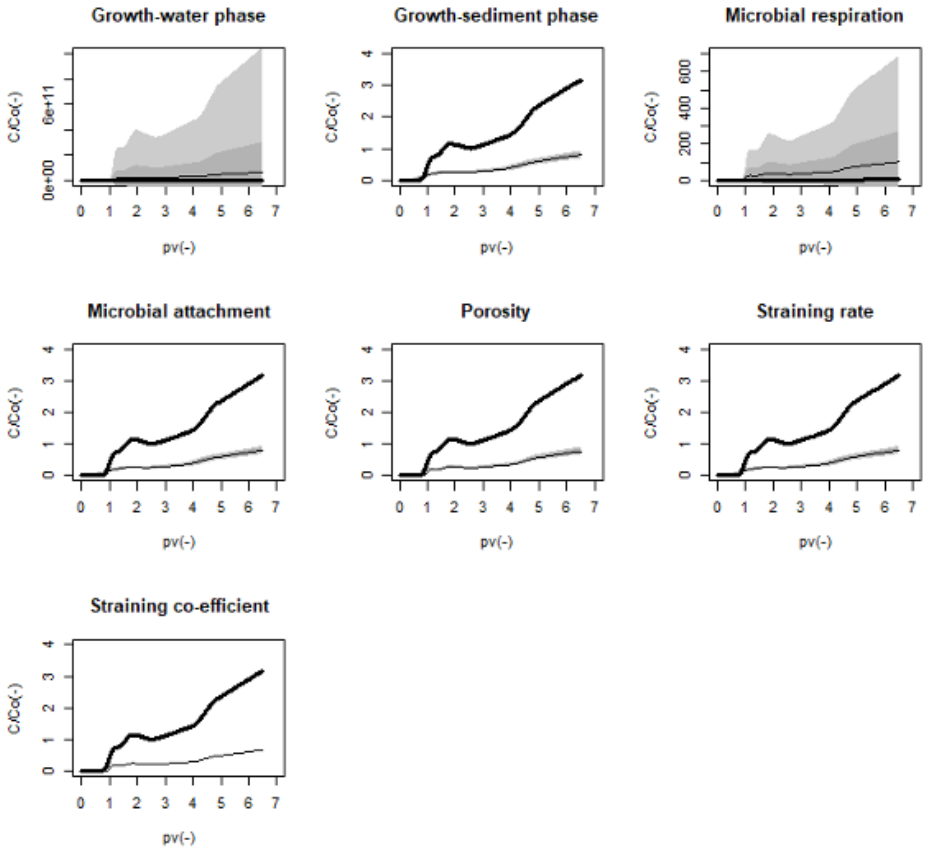

Figure 3.15: Sensitivity of all the parameters determined for the condition C4 (Grey cone with black thin line presenting the mean), for field scale (longer column length), when compared to the lab-scale observations (solid black line)

Chapter 4

Determining the impact of flow velocities on reactive processes associated with *Enterococcus faecalis JH2-2*

Aparna Chandrasekar[a,b], Martin Binder [c,d], Rudolf Liedl[b], Thomas U. Berendonk[a]

[a]Technische Universität Dresden, Institute of Hydrobiology, Zellescher Weg 40, 01217 Dresden, Germany

[b]Technische Universität Dresden, Institute of Groundwater Management, Bergstraße 66, 01069 Dresden, Germany

[c] Helmholtz-Centre for Environmental Research - UFZ, Department of Environmental Informatics, Permoserstraße 15, 04318 Leipzig, Germany

[d] Technische Universität Bergakademie Freiberg, Institute of Geology, Section of Hydrogeology and Hydrochemistry, Gustav-Zeuner-Str. 12, 09599 Freiberg, Germany

The following content has been originally published in the "Water Science and Technology" journal

DOI https://doi.org/10.2166/wst.2021.611

Keywords: bacteria transport, colloid transport, Damkoehler numbers, *Enterococcus*, process-based model

Highlights

- The influence of flow velocity on bacteria reactive processes like decay and growth was investigated.
- A combined experimental and modelling approach was employed to determine critical parameters.
- Dimensionless numbers (Peclet and Damkoehler numbers) were used to compare transport and reactive processes.
- Growth parameter indicated a dependency on flow velocity in the presence and absence of dissolved oxygen.

Abstract

This study focuses on the impact of infiltration rates on colloidal transport and reactive processes associated with *Enterococcus faecalis* JH2-2 using water-saturated sediment columns. The infiltration rates influence the physical transport of bacteria by controlling the mean flow velocity. This, in turn, impacts biological processes in pore water owing to the higher or lower residence time of the bacteria in the column. In the present study, continuous injection of *E. faecalis* (suspended in saline water with varying conditions of dissolved oxygen and nutrient concentrations) into a lab-scale sediment column was performed at flow velocities of 0.02 $cm\ min^{-1}$ and 0.078 $cm\ min^{-1}$, i.e., at residence times of 1–5 hours. The impact of residence times on reactive processes is significant for field scale setups. A process-based model with a first-order rate coefficient for each biological process was fitted for each obtained condition-specific dataset from the experimental observations (breakthrough curves). The coefficients were converted to a dimensionless form to facilitate the comparison of biological processes. These results indicate that the processes of attachment and growth were flow-dependent. The growth process in the absence of dissolved oxygen was the most dominant process, with a Damkoehler number of approximately 48.

4.1. Introduction

Reuse of treated wastewater is widely practised in water-scarce regions globally, with applications such as irrigation and managed aquifer recharge [Angelakis and Durham, 2008]. The important reactive processes in the saturated zone must be understood to assess the risk of contaminant transport to and within the groundwater. The high nutrient concentration present in urban wastewaters increases crop yield and may reduce the need for artificial fertilisation [Luprano et al., 2016]. Urban wastewater treatment plants act as hotspots for the emergence of antibiotic resistance [Cacace et al., 2019; Kampouris, Agrawal, et al., 2021; Rizzo et al., 2013]. This raises concerns regarding the spread of pathogens, antibiotic-resistant bacteria, and genes to groundwater. The processes, including filtration, microbial decay, and straining, have been studied primarily with colloids and *Escherichia coli*. For example, Bradford, Simunek, and Walker, 2006 investigated the impact of sediment grain size and flow velocity on the deposition behaviour of colloids while mimicking the shape and size of bacteria to study the physical processes that would occur during bacterial transport through sediments. It was observed that for larger grain sizes (710 μm) the flow velocity did not significantly impact the spatial distribution of colloids in the sediment, and the distribution became progressively varied with smaller grain sizes (150 μm). Especially for small grain sizes and low flow velocities (Darcy velocity of 0.051 $cm\ min^{-1}$), a higher percentage of the colloids were retained close to the inlet of a sediment-filled column, indicating a flow-dependent behaviour of the colloidal particles. Another study by E. Smith and Badawy, 2008 investigated the impact of flow velocities on various processes such as advection and dispersion, including the bacteria-related process of adsorption and filtration. It was observed that, at lower flow velocities (0.0783 $cm\ min^{-1}$), the reactive processes (e.g., adsorption) were rate-limiting, while a lower impact was determined for relatively higher flow velocities (1.1 $cm\ min^{-1}$). In addition, E. Smith and Badawy, 2008 recommended studying these processes in batch or column setups just prior to large-scale field investigations. Other studies have focused on the impact of parameters such as temperature [McCaulou et al., 1995], heterogeneous structures in the sediment [Harvey et al., 1993], cell size and morphology shape [Lehmann et al., 2018], and their impact on physical and biological processes occurring in the subsoil environment. Studies such as Huysmans and Dassargues, 2005 have analysed the impact of flow velocity on diffusion processes. However, a comparison of the reactive and transport processes has not been tested in detail. While the aforementioned studies elucidated the impact of flow rates, temperature, sediment heterogeneity, and cell size on biological processes such as filtration and adsorption, there is a lack of understanding of the relationship

between flow velocities and key reactive processes, namely decay, growth, and respiration. A recent study by Chandrasekar et al., 2021b investigated the impact of chemical wastewater characteristics such as dissolved oxygen (DO) and nutrients in wastewater using *Enterococcus faecalis* JH2-2. *E. faecalis* JH2-2 is a non-pathogenic, opportunistic bacterium. The aforementioned study was conducted using a single flow velocity of 0.14 $cm\ min^{-1}$; that is, the dependencies of varying flow velocities on the intensity of reactive processes were not investigated. However, in the broad context of wastewater reuse for irrigation a higher residence time associated with lower flow velocities could lead to certain reactive processes becoming more critical or rate-limiting conditions in the pore water. Furthermore, in crop fields, lower irrigation rates [Tideman, 1996] are more favourable to allow more time for crops to absorb water and nutrients [Ayers and Westcot, 1985]. However, this could lead to nutrients and bacteria accumulating in the soil with subsequent formation of biofilms and clogging of the sediment. Therefore, it is essential to understand the impact of low flow velocities on reactive processes, that is, velocities lower than those in previous studies.

The present study investigates the impact of flow velocity on the respective intensities of transport and reactive processes to close the existing gaps by employing Peclet and Damkoehler numbers. This study focuses on the processes of respiration, growth, and attachment of Enterococci species, specifically *E. faecalis* JH2-2.

It must be noted that on a larger scale, real-world studies with an expected de-facto continuous supply of nutrients and dissolved oxygen (e.g., during irrigation), the phenomenon of bacteria eventually clogging the pore channels should be considered. The accompanying changes in porosity, hydraulic conductivity, and permeability due to clogging must be considered [Kalwa et al., 2021]. Furthermore, the hydrological conditions found in larger scale setups are in general more complex with unsaturated or variably saturated soil conditions. The corresponding changes in porosity, hydraulic conductivity, and permeability due to clogging must be considered [Kalwa et al., 2021].

4.2. Materials and methods

4.2.1. Experimental setup

The experimental setup, sediment characteristics, sterilisation procedure, model species, methods to grow and quantify the bacteria, and calibration curves for saline and microsphere tracers were similar to those used by Chandrasekar et al., 2021b. The conditions were replicated to ensure comparability between the present and previous results.

Column setup including initial saline tracer experiments

Lab-scale column experiments were conducted using acryl glass columns of 15 cm in length and 3 cm in diameter (Figure 4.1). Two columns, running in parallel, were wet-packed using quartz sediment with a grain diameter of 1–4 mm, following the experimental concept used by Chandrasekar et al., 2021b. The ends of the columns were flanked with glass fibre filters to prevent an outflow of sediment particles. A multichannel peristaltic pump (Co. Ismatec) was used to adjust the flow velocities corresponding to flow velocities of 0.02 $cm\ min^{-1}$ (F_{slow}) and 0.078 $cm\ min^{-1}$ (F_{med}), respectively. A third flow velocity of 0.14 $cm\ min^{-1}$, hereafter referred to as F_{fast}, was previously evaluated by Chandrasekar et al., 2021b; therefore, this study focuses on the F_{slow} and F_{med} settings, while F_{fast} will be used as a reference. The flow velocities were monitored regularly and measured before each experiment.

Solute tracer experiments (breakthrough curves in Figure 3.10) were conducted using a saline tracer (sodium chloride, NaCl; concentration 8.5 $g\ L^{-1}$, in dissolved deionised water; Co. Sigma-Aldrich) to determine the basic transport parameters, effective porosity (η_e, unit: -), and longitudinal dispersivity length (α, unit: cm). The NaCl tracer was continuously injected for three pore volumes into the columns. The concentration of the components was indirectly measured at the outlet using a pre-calibrated electrical conductivity meter (Co. WTW, see also the Supplementary Material in Chandrasekar et al., 2021b). The flow was directed from the bottom to the top to remove the pre-entrapped air bubbles. The results from the tracer test, i.e., the transport parameters, were then used to determine the dimensionless time parameters used for normalisation of the time axis.

Experiments with microspheres and *E. faecalis* JH2-2

Analogous to the procedure described by Chandrasekar et al., 2021b, both microspheres and *E. faecalis* JH2-2 suspended in deionised water were subsequently injected into the laboratory-scale columns (Figure 4.1) to determine colloidal and bacteria-specific transport and reactive parameters.

Microspheres

Fluorescent microspheres (spherical shape, $1\mu m$ diameter, polystyrene surface, yellow-green fluorescence, Co. Sigma-Aldrich) were used in this experiment to imitate the shape and size of enterococci. Fluorescence of the microspheres was realized via internal labelling. The microspheres were continuously injected into the column at a concentration of approximately 10^9 particles mL^{-1}. The outlet concentration was continuously mea-

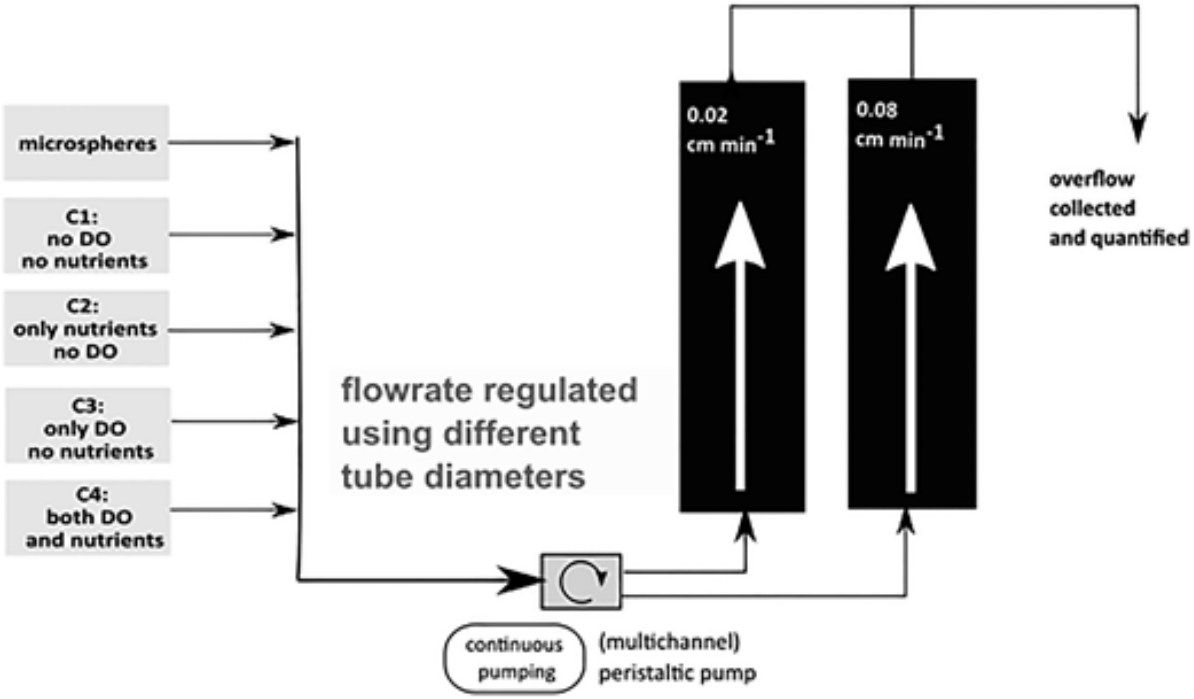

Figure 4.1: Experimental setup to study the transport of bacteria for varying flow velocities. Please note that the figure is purely representational and is not to scale.

sured using a pre-calibrated fluorimeter (Co. Albilia, type GGUN-FL30; Supplementary Material in Chandrasekar et al., 2021b). The breakthrough curve resulting from the microsphere injection experiment was used to determine the straining rate and straining coefficient, respectively.

Bacteria – E. faecalis JH2-2

E. faecalis JH2-2 used in this study was obtained from frozen aliquots (Laboratory of Physical Chemistry and Microbiology for the Environment, Team of Environmental Microbiology, University of Lorraine, Nancy, France). The pure cultures were streaked on m-Enterococcus agar plates, stored at $4°C$, and refreshed monthly to ensure the continuous presence of viable bacteria for the experiments. The bacteria were subjected to four conditions (C1 to C4) before and during the experiment (Table 4.1). Batch adsorption experiments were not conducted in the scope of this work. It has been previously concluded by, among others, E. Smith and Badawy, 2008 that adsorption parameters obtained from equilibrated batch experiments may not provide a suitable description of the adsorption kinetics taking place in column setups with typically more dynamic flow conditions. The reasoning and methodology regarding the DO and nutrient concentration variations, the procedure description for cultivating the bacteria for the experiments in Brain Heart Infusion media (Co. Sigma Aldrich), as well as a description of the plating method using selective plating media (m-Enterococcus agar) to quantify both the

Table 4.1: Matrix of the conditions to which bacteria were subjected, as well as flow velocity abbreviations

	Without Nutrients (0 $mg\ L^{-1}$)	**With Nutrients (14.8 $mg\ L^{-1}$)**
Without DO (0 $mg\ L^{-1}$)	Condition 1 (C1)	Condition 2 (C2)
With DO (8.9 $mg\ L^{-1}$)	Condition 3 (C3)	Condition 4 (C4)
Flow rate abbreviation	**Flow velocity**	
F_{fast}	0.14 $cm\ min^{-1}$ (reference only, data from Chandrasekar et al., 2021b)	
F_{med}	0.078 $cm\ min^{-1}$	
F_{slow}	0.02 $cm\ min^{-1}$	

inlet and outlet bacteria can be found in Chandrasekar et al., 2021b.

The final concentration of bacteria used at the inlet for the experiments was 10^3 to 10^4 $CFU\ mL^{-1}$ (coliform units per mL), which was then continuously injected into the inlet of the sediment columns (Heaviside function, approximately five pore volumes) using conditions C1 to C4 combined with flow velocities F_{med} and F_{slow}, respectively. At least two technical replicates were used for each sample, from which the average value was represented as the concentration of bacteria for the studied time point. In addition, four biological replicates were conducted for each experiment to ensure data reproducibility. Therefore, the data shown are combined/pooled data from all four biological replicates.

4.2.2. Model Setup

The equations used in this study (Table 4.2 and dimensionless form in Supplementary Material 4.6) facilitate comparing process rates for the different flow velocities studied. In the equations, the following symbology is used: v ($cm\ min^{-1}$) is the flow velocity, x (cm) is the travel distance (in this study: length of the sediment column), and t (min) is the time since the start of the experiment. C and C_s denote the observed concentrations of bacteria in the pore water and sediment phases, respectively. Units used in this study were CFU mL^{-1} and CFU g^{-1}, respectively. μ_d is the bacteria decay rate, and μ_d is the bacterial respiration rate, while K_{att} and $K_{att_{O2}}$ denote the bacterial attachment rates for C1 and C3, respectively. Finally, μ_g and $\mu_{g_{o2}}$ are the bacterial growth rates in the water under conditions C2 and C4, respectively. For all rate coefficients, the same unit (min^{-1}) was used.

The equations used for parameter fitting were then converted to the respective dimensionless forms to compare the flow velocities (Equations 4.19 and 4.20 in Appendix 4.6). The *R* software packages "rodeo" [Kneis et al., 2017] and "FME" [Soetaert and Petzoldt, 2010] were used for model formulation and inverse parameterisation, respectively.

The specific built-in functions used within the aforementioned packages were elucidated by Chandrasekar et al., 2021b. Finally, parameter fitting was performed using unconstrained optimisation using the "bobyqua" optimizer [Powell, 2009]. The source code can be found at https://github.com/aparna2306/bacteria_transport. The initial estimate used during parameter fitting for all rate coefficients was 0.001 min^{-1}.

The reactive processes occur simultaneously, and thus the parameters must be identified independently [Chandrasekar et al., 2021b]. To ensure parameter identifiability, the processes were isolated using varying concentrations of DO and nutrients (Table 4.1). Specifically, the parameters associated with microbial decay and respiration were determined by exposing *E. faecalis* JH2-2 to C1 and C3, respectively. These parameters were then assumed to remain unchanged when determining the parameters for the attachment process, using the outlet bacterial breakthrough curves in C1 and C3. The simultaneous processes of decay/respiration and attachment were fitted in the model using data from both the inlet and outlet of the column. Microbial growth rate constants were determined separately by exposing the bacteria to the C2 and C4 conditions (i.e., without and with DO). This was done to analyse the impact of DO on the growth rate. The parameters corresponding to advective-dispersive, straining, decay, respiration, and attachment were kept constant and were not used for model fitting in this step. The parameters relating to the growth processes occurring in the water phase were determined after this step while keeping the remaining parameters constant.

The parameters were then converted to the corresponding dimensionless numbers (Equations 4.1 and 4.2). The conversion to a dimensionless form for advective and dispersive transport processes was realised using the Peclet number (Equation 4.1).

$$Pe = \frac{L * \frac{v}{\theta_e}}{(\alpha * \frac{v}{\theta_e}) + D^*} \tag{4.1}$$

where Pe is the Peclet number and L is the length of the column (which, in this study, equals the previously described x in the equation system). D^* is the pore diffusion coefficient; it is neglected in the present study due to the large diameters of the employed microspheres and bacteria. Based on this assumption, a smaller Peclet number indicates that the dispersive process is stronger than the advective process and vice versa.

The comparison of the advective transport with reactive processes of straining, microbial decay, attachment, respiration, and growth are represented using the corresponding Damkoehler numbers (Equations 4.2 to 4.8; Da_{str}, Da_d, Da_{att} (for conditions C1 and C3), Da_r, and Da_g (for conditions C2 and C4)). Here, smaller Damkoehler numbers indicate that the contribution of the reactive processes is (relatively) less in-

Table 4.2: The system of partial differential equations can be obtained by adding all the terms with their respective signs. The term in column 1 is the left-hand side of the equation connected to the right-hand side using an '=' sign.

Change in storage	**Advection and dispersion**	**Straining [Xu et al., 2006]**	**Microbial decay / respiration [Bradford, Simunek, and Walker, 2006]**	**Attachment**	**Microbial growth**
$\frac{\partial C}{\partial t}$	$-v * \frac{\partial C}{\partial x} + \alpha * v * \frac{\partial^2 C}{\partial x^2}$	$-k_{str} * C * e^{-C_s/\lambda}$	$-\mu_d * C$ $-\mu_r * C$	$-K_{att} * C$ - $K_{att_{O2}} * C$	$+\mu_g * C$ $+\mu_{g_{O2}} * C$
$\frac{\partial C_s}{\partial t}$		$+k_{str} * C * e^{-C_s/\lambda}$		$+K_{att} * C_s$ $+ K_{att_{O2}} * C_s$	

tensive, i.e., the reactive process is "slower" than the transport processes. The resulting normalised equation system is presented in Supplementary Material, Appendix 4.6.

$$Da_d = \frac{\mu_d * L}{v} \tag{4.2}$$

$$Da_{att_{C1}} = \frac{K_{att} * L}{v} \tag{4.3}$$

$$Da_{g_{C2}} = \frac{\mu_{g_{C2}} * L}{v} \tag{4.4}$$

$$Da_r = \frac{\mu_r * L}{v} \tag{4.5}$$

$$Da_{att_{C3}} = \frac{K_{att_{O2}} * L}{v} \tag{4.6}$$

$$Da_{g_{C4}} = \frac{\mu_{g_{O2}} * L}{v} \tag{4.7}$$

$$Da_{str} = \frac{K_{str} * L * e^{-\frac{C_s}{\lambda}}}{v} \tag{4.8}$$

The results are presented in a normalised form, i.e., a dimensionless form, to facilitate data comparison. The input concentration (i.e. C_o) of a specific component at the inlet (i.e. x = x_o = 0 cm) and starting time (i.e., t = t_o = 0 min) was used as the scaling parameters for the concentration axis (y-axis). The water phase concentrations were represented as $C_r = C/C_o$. The "dimensionless time" variable is defined as the pore volume for that particular flow velocity as $t_r = t * v/L$.

4.3. Results and Discussion

4.3.1. Tracer and microsphere experiments

The results from the saline tracer experiment show that the residence time (i.e., the used dimensionless time scale reference) is approximately 80 min and 240 min for the flow velocities F_{med} and F_{slow}, respectively (Figure 4.6). In addition, the effective porosity and dispersivity values were 0.336 and 0.11 cm for F_{med} and 0.344 and 0.24 cm for F_{slow} (averaged values for all column setups; please refer to Table 4.3 for a complete list of parameters obtained using tracer tests for the conditions C1 to C4). The corresponding Peclet numbers show that the advective process is strongest for the highest flow velocity F_{fast} (as investigated in Chandrasekar et al., 2021b). The Peclet number for F_{slow} indicates an almost equal contribution of advective and dispersive processes. The Pe number is the lowest for the slow flow velocity F_{slow} owing to the slightly larger dispersivity value for this flow velocity (Table 4.3). Pe was always greater than 1, indicating that the advective process was always stronger than the dispersive process. The results from the microsphere experiments were obtained by continuously injecting spherical polystyrene colloids of $1\mu m$ diameter, suspended in deionised water, through sediment columns operating at various flow rates and automatically analysing the outflow concentration using a fluorimeter. The data obtained from the straining experiments indicate a flow-dependent behaviour, as seen in the parameter values of the clean-bed straining co-efficient and the straining rate (Table 4.4). The two values are clubbed into the Damkoehler number for straining (Da_{str}), which shows that collective straining is more dominant for the slow

flow velocity F_{slow} (see comparison graphs shown in Figure 4.5, Section 4.3.2). This is consistent with the observation (Figure 4.2), where only 50% of the injected microsphere concentration was reached at the column outlet for the flow velocity F_{slow} (as compared to nearly 80% for F_{med}). The longer residence time for the microsphere particles in the column for the slower flow velocity leads to a higher number of entrapped particles in the sediment matrix [Xu et al., 2006].

As explained before, there are two components to the Da_{str}, which comprise the clean bed straining coefficient and the straining rate. The straining rate was required to be set to a higher value for the flow velocity F_{slow} than for the flow velocity F_{med}. While the straining was a non-linear process for the flow velocity F_{med}, the exponential term (straining coefficient) was effectively reduced to 1 for the flow velocity F_{slow}, resulting in a linear behaviour. Additionally, the clean bed straining coefficient is one order of magnitude smaller for the F_{slow} flow velocity than for F_{med}. The difference in both cases is attributed to the water retention times, which is much higher for the flow velocity F_{slow}. The higher retention times allow for a higher interaction of the microspheres, leading to a much higher straining coefficient. Furthermore, the formation of aggregates in the sediments is possible. Both factors together contribute to a higher straining effect within the column for the slow flow velocity, as indicated by evaluating the Damkoehler numbers and the outlet breakthrough curves (Figure 4.2). In addition to determining the parameters, it was observed that for flow velocity F_{slow}, the microspheres arrived before the tracer. This indicates that because of the larger size of the microspheres, only the larger pore space (i.e. the centre of the respective pore flow channels) is occupied, through which water moves at a faster velocity than through the rest of the pore space, leading to an earlier breakthrough as compared to the tracer breakthrough. Therefore, our initial assumption of a constant dispersivity value does not hold to the full extent for the slow flow velocity. Regarding the latter, an extra diffusion parameter representing the diffusion of the microspheres may also be added to advection-dispersion equation equation (first equation in Table 4.2). However, this step was skipped in this case, and the equation was kept simple, as the focus was on studying reactive processes.

4.3.2. Bacteria experiments - comparison of processes

When comparing the reactive processes for condition C1, an instantaneous decay of the bacteria observed for both flow conditions at the inlet (Figure 4.3, Figure 4.4 – C1-in). The outlet concentration for the F_{med} flow velocity was 10% of the total bacteria and 0.2% for the F_{slow} flow velocity (Figure 4.3, Figure 4.4 – C1-out). This high reduction in bacterial concentration is attributed to cell lysis, due to the absence of nutrients,

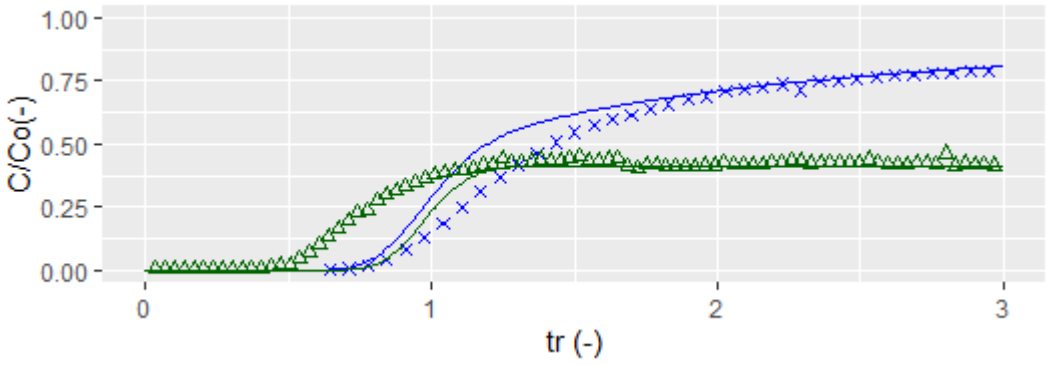

Figure 4.2: Breakthrough curves obtained from continuous injection of microspheres into the sediment column. Experimental observations are indicated by a blue "x" (F_{med}) or green "Δ" (F_{slow}), and the model fits are represented using solid lines with blue (F_{med}) and green (F_{slow}) colours.

dissolved oxygen, or electron acceptors in the water media where the bacteria are suspended. This rather complex microbiological process was mathematically implemented by assuming a simplified first-order decay rate of the bacteria. Here, the corresponding dimensionless Damkoehler number Dad is of the same order of magnitude for all the flow velocities (Figure 4.5). This is expected because the decay rate is obtained from the inlet concentration variation and does not change based on the flow velocity of the bacteria. Since the decay process is assumed to occur additionally in the column, the higher Damkoehler number (Figure 4.5) for decay is attributed to the higher residence time of the bacteria. This leads to a larger overall reduction in biomass; however, this is not represented by a larger decay rate constant. The attachment rates corresponding to C1 were determined to be of the same order of magnitude (Table 4.4), indicating no flow dependency. In addition, the attachment process was almost negligible for both flow velocities in the absence of DO (Figure 4.5). This is consistent with the small parameter values (Table 4.4), indicating that this process has no significant impact on even smaller flow velocities. Since the bacteria are relatively hydrophilic (4.5% hydrophobicity; Chandrasekar et al., 2021b), the anoxic environment could create an electrostatic barrier, reducing the tendency for the bacteria to attach [Hall et al., 2005]. The increase in residence time did not impact the attachment rate constant.

The inlet concentration (Figure 4.3, Figure 4.4 – C2-in) showed a reduction in the first pore volume for condition C2. Subsequently, biomass growth occurred at both the inlet and outlet of the column (Figure 4.3, Figure 4.4 – C2-out). The reduction in the inlet concentration during the first pore volume was attributed to the absence of DO. This could create an initial shock for the bacteria, thus leading to a loss of culturability or cell lysis. The mathematically simplified decay process parameters are obtained from condition C1. The growth parameter observed at the outlet of the column was quantified

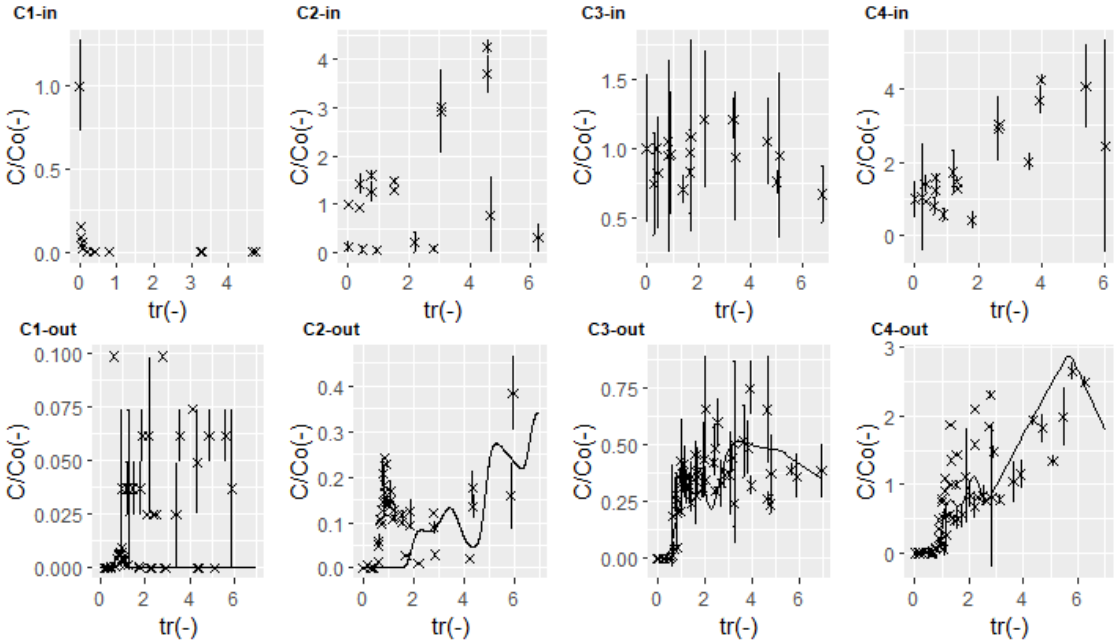

Figure 4.3: Concentration-time curves for the flow velocity F_{med}, where experimental observations are represented by an "x" with error bars at column inlet (upper row) and column outlet (lower row). Corresponding model fits are represented by a line. Please note that the y axis values vary for every subplot.

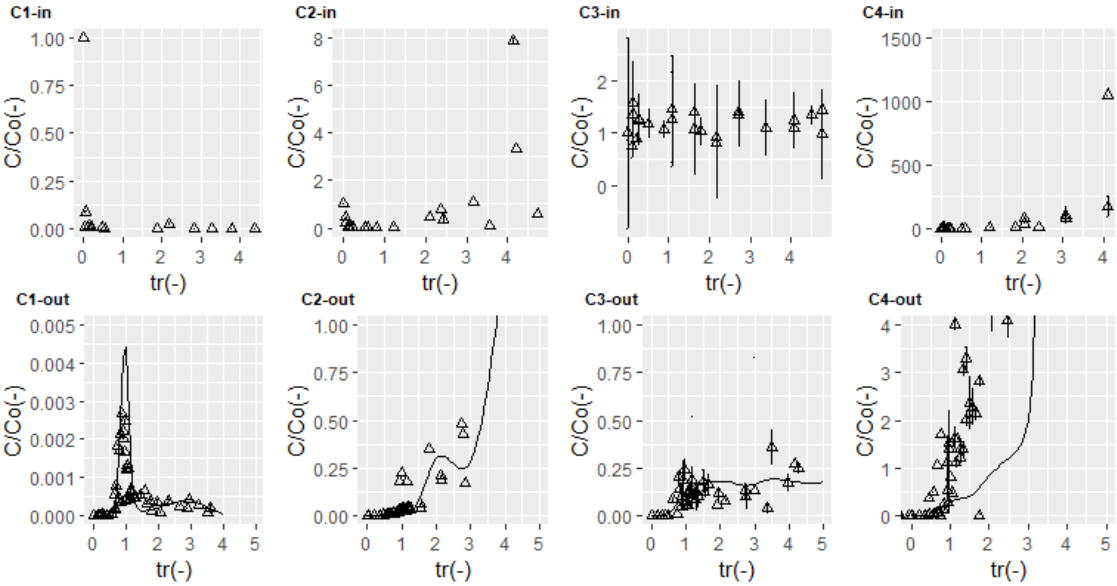

Figure 4.4: Concentration-time curves for the flow velocity F_{slow}, where experimental observations are represented by a "Δ" with error bars at column inlet (upper row), and column outlet (lower row). Corresponding model fits are represented by a line. Please note that the y axis values vary for every subplot.

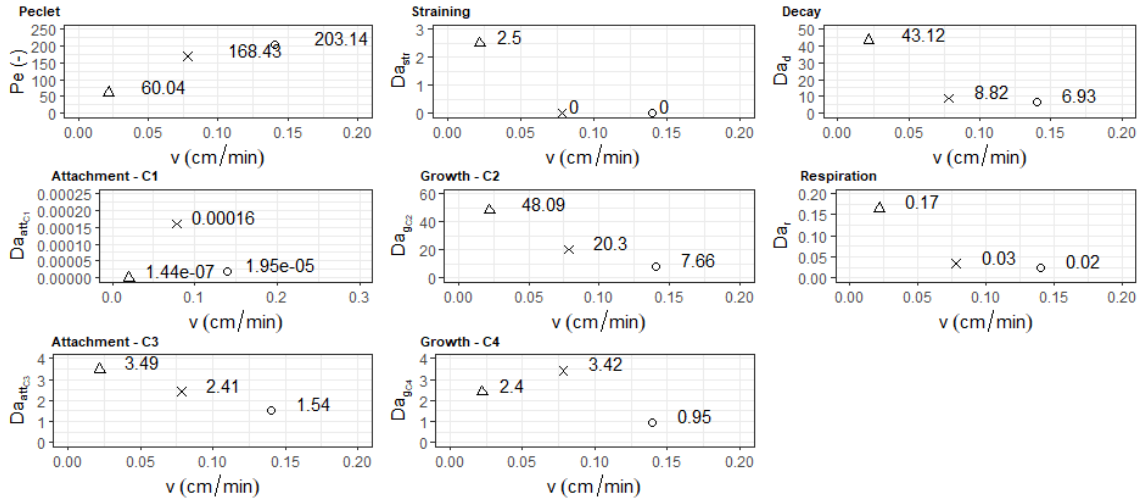

Figure 4.5: Relationship between the Peclet and Damkoehler numbers and flow velocities used in the scope of the study, compared with the values obtained in Chandrasekar et al., 2021b. Note that the "Δ" represents the Damkoehler numbers for the flow velocity F_{slow}, "x" represents the Damkoehler numbers for the flow velocity F_{med}, and the "o" represents the Damkoehler numbers obtained from the flow velocity F_{fast} in Chandrasekar et al., 2021b.

using the given set of data in Figure 4.3 and Figure 4.4 – C2-out. One pore volume delay was observed for the modelled breakthrough curves (Figure 4.3 – C2-out). Additionally, a wave-like pattern was also observed in the modelled outlet breakthrough curves. These observations are attributed to the initial decay process in the inlet and the variation in the bacterial inlet concentration. The inversely determined growth rate parameter was almost twice as large for F_{med}. However, the breakthrough curves at the outlet for the flow velocity F_{slow} showed a much higher increase after three pore volumes (Figure 4.4 – C2-out). This is due to the higher residence time of the bacteria for the flow velocity F_{slow}. The Damkoehler number ($Da_{g_{C2}}$) shows a linear decrease with increasing flow velocity (Figure 4.5).

For condition C3, the inlet concentration remains relatively unchanged for both the flow velocities, thus indicating that the respiration process is negligible for these flow velocities (Figure 4.3, Figure 4.4 – C3-in). The respiration rate parameters were of the same order of magnitude for all flow velocities studied (Table 4.4). It can also be seen in the inlet concentration that the concentration slightly decreased at the beginning of the experiment (Figure 4.3 – C3-in). However, there was no significant change in the concentration of bacteria at the inlet (Figure 4.3, Figure 4.4 – C3-in). The respiration rate values were then kept constant and were used to determine the attachment rate. The bacterial concentration recovered at the outlet of the column reached values of ∼ 25% of the injected bacteria for the F_{slow}, as opposed to ∼50% for the F_{med} (Figure 4.3, Figure 4.4 – C3-out). $Da_{att_{C3}}$ shows a linear dependence on the flow velocity. However,

the attachment parameter was one order of magnitude higher for the flow velocity F_{med} (Table 4.4). The Da_r, however, does not show a linear dependence with decreasing flow velocity, and the process is effectively much more intense for a slower flow velocity. Since the μ_r is determined in batch conditions, this effect must be tested in column setting before assuming a non-linear dependence to flow velocity.

A considerable growth of the bacteria was observed for both the flow conditions at the inlet (Figure 4.3, Figure 4.4 – C4-in) and the outlet (Figure 4.3, Figure 4.4 – C4-out) for condition C4. The concentration of bacteria recovered at the outlet for the flow velocity F_{slow} was much higher, owing to the longer residence time in the column, leading to biomass increase in the column. The Damkoehler numbers do not exhibit a linear effect with a decrease in the flow velocity. Instead, the growth parameter is observed to be much higher for the flow velocity F_{med} than for the lower flow velocity F_{slow} (Table A.2). This effect is also seen in the Damkoehler numbers, where $Da_{g_{C4}}$ is much higher for the flow velocity F_{med} (Figure 4.5). A similar effect was observed for condition C2, wherein the growth parameter was much higher for the flow velocity F_{med} than for F_{slow}. In general, a linear impact of the flow velocity on the Damkoehler numbers was observed within the context of the flow velocities and processes studied. They indicated a much faster reactive process effect for the slow flow velocity F_{slow} but a negligible impact for the higher flow velocities. The growth parameters C2 and C4 had higher values for the flow velocity F_{med}. This is interpreted as another non-linear effect, and $Da_{g_{C4}}$ shows that the growth process is the fastest for the medium flow velocity.

4.4. Conclusions and Future work

This study investigates the impact of flow velocity on the various reactive processes of *E. faecalis* JH2-2 during their transport through sandy sediments. The study shows that the growth and attachment processes are most affected by the change in flow velocity for the range of flow velocities studied. In general, the decay and the growth process (C2) were the fastest processes with Damkoehler numbers of 43.12 and 48.09 (Figure 4.5) for the flow velocity F_{slow}. The attachment process (C1) and respiration process were the slowest processes with Damkoehler numbers below 0.2, even for the slow flow velocity F_{slow}. These processes can be neglected in large-scale studies and relatively fast irrigation rates. The attachment process (C3) and growth process (C4) were significant, with Damkoehler numbers of ~ 3 for the relatively slow flow velocity F_{slow}. A threshold value was observed for Da_d and Da_r, which were determined from the parameters obtained from the inlet concentration. In addition, data suggest that in the absence of nutrients,

slower flow velocities favor the attenuation of bacteria and cause lower concentrations of bacteria to be leached from the soil. Conversely, when nutrients are present at higher flow velocities, a lower concentration of bacteria is leached into the groundwater. Please note that the parameters determined in this study using the stepwise approach (as well as the dimensionless numbers as aforementioned) are based on the mathematically 'best fit' solutions obtained for each step using the current solver. Other possible solutions with slightly worse objective functions have been neglected to reduce the degrees of freedom during optimization.

4.5. Supplementary material 1

Saline tracer tests conducted for all three flowrates and all the four conditions

Saline tracer tests were conducted by injecting 0.85% NaCl (8.5 gL-1 of NaCl in sterile deionized water) into the sediment packed column for 3 pore volumes. Since the columns were repacked after every experiment, tracer tests were conducted before the start of every experiment. The breakthrough curve obtained from the outlet was used to determine the effective porosity and the longitudinal dispersivity parameters for each of the flowrates and both parameters were used to determine the Peclet (Pe) number. The results from the experiments indicate that the residence time (time taken to reach 50% of the final concentration), is approximately 30 min, 80 min and 240 min for the flow velocities F_{fast}, F_{med}, and F_{slow} (Figure 4.6), which is approximately the residence time for the water inside the column (pv). The resulting Pe were greater than 1 (Figure 4.5 in main text, Table 4.6) for all the three flow conditions, indicating that the dispersive process did not dominate on the advective process. Furthermore, it was observed that the Pe became smaller with lower flowrates. This is expected as the advective process is stronger for faster flowrate. The systems are hydrologically similar, and the impact of the reactive processes can then be clearly studied. The results from these tracer tests are now transferred to study the impact of straining on the columns.

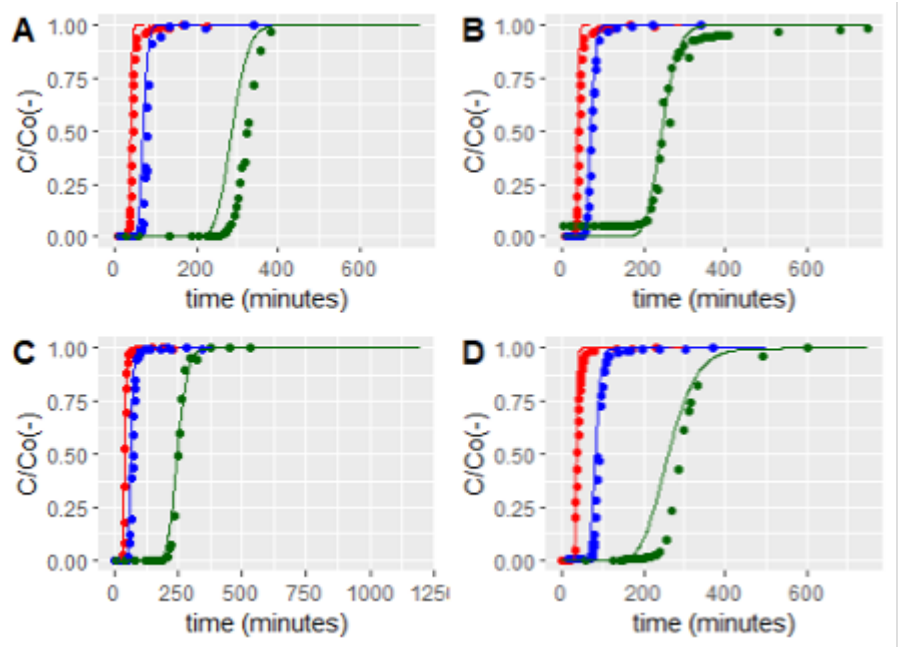

Figure 4.6: Tracer breakthrough curves for flow velocities F_{slow} (green), F_{med}(blue), and F_{fast} (red), for the conditions A) C1 B) C2 C) C3 D) C4.

Table 4.3: List of all relevant transport parameters (total porosity, effective porosity, longitudinal dispersivity, bulk density and Darcy velocity measure for all four conditions and all three flow velocities, based on the saline tracer tests. Values are given as averaged, i.e., mean values including standard deviations (sd). For F_{fast} please refer to the study Chandrasekar et al., 2021b

C1	F_{med}		F_{slow}	
	mean	sd	mean	sd
total porosity	0.348	0.007	0.344	0.016
effective porosity	0.330	0.033	0.346	0.033
dispersivity (cm)	0.100	0.016	0.053	0.013
bulk density ($g\ cm^{-3}$)	1.714	0.019	1.726	0.043
Darcy velocity ($cm\ min^{-1}$)	0.073	0.010	0.020	0.003
C2	F_{med}		F_{slow}	
	mean	sd	mean	sd
total porosity	0.336	0.029	0.357	0.060
effective porosity	0.158	0.065	0.537	0.695
dispersivity (cm)	0.360	0.013	0.355	0.012
bulk density ($g\ cm^{-3}$)	1.684	0.033	1.695	0.030
Darcy velocity ($cm\ min^{-1}$)	0.069	0.003	0.022	0.003
C3	F_{med}		F_{slow}	
	mean	sd	mean	sd
total porosity	0.303	0.025	0.314	0.037
effective porosity	0.097	0.028	0.104	0.047
dispersivity (cm)	0.347	0.005	0.349	0.014
bulk density ($g\ cm^{-3}$)	1.716	0.013	1.712	0.038
Darcy velocity ($cm\ min^{-1}$)	0.077	0.003	0.021	0.004
C4	F_{med}		F_{slow}	
	mean	sd	mean	sd
total porosity	0.375	0.037	0.359	0.034
effective porosity	0.091	0.016	0.248	0.213
dispersivity (cm)	0.341	0.011	0.347	0.005
bulk density ($g\ cm^{-3}$)	1.734	0.030	1.717	0.013
Darcy velocity ($cm\ min^{-1}$)	0.086	0.015	0.024	0.006

Table 4.4: List of parameters values with corresponding standard error (S.E.). The standard error was calculated using the summary package in R package 'FME'. The parameters K_{str} (straining rate), λ (straining coefficient), μ_d (decay rate), μ_r (respiration rate), K_{att} (attachment rate), and μ_g (growth rate) are as described in the main text

Flow velocity ($cm\ min^{-1}$)	λ ($particles\ mL^{-1}$)	Std. dev	k_{str} (min^{-1})	Std. dev
1.40 * 10^{-1}	7.28* 10^{-2}	1.09* 10^{-1}	3.78 * 10^{-2}	6.6 * 10^{-2}
7.84 * 10^{-2}	2.01* 10^{-2}	7.48 * 10^{-3}	3.33 * 10^{-2}	2.64 * 10^{-1}
2.19 * 10^{-2}	infinite	–	3.47· * 10^{-3}	3.85* 10^{-4}
Flow velocity ($cm\ min^{-1}$)	μ_d (min^{-1})	S. E.	$K_{att_{C1}}$ (min^{-1})	S. E.
1.40 * 10^{-1}	6.16 * 10^{-2}	3.13 * 10^{-2}	1.75 * 10^{-7}	2.155 * 10^{-3}
7.84 * 10^{-2}	4.39 * 10^{-2}	8.91 * 10^{-3}	1.13 * 10^{-6}	2.24 * 10^{-3}
2.19 * 10^{-2}	6.00 * 10^{-2}	1.52 * 10^{-2}	8.84 * 10^{-7}	1.81
Flow velocity ($cm\ min^{-1}$)	μ_r (min^{-1})	S. E.	$K_{att_{C3}}$ (min^{-1})	S. E.
1.40 * 10^{-1}	2.00 * 10^{-4}	6.32 * 10^{-5}	1.37 * 10^{-2}	1.02 * 10^{-3}
7.84 * 10^{-2}	1.67 * 10^{-4}	8.91 * 10^{-3}	1.20 * 10^{-2}	7.39 * 10^{-4}
2.19 * 10^{-2}	2.30 * 10^{-4}	6.60 * 10^{-5}	4.85 * 10^{-3}	5.23 * 10^{-4}
Flow velocity ($cm\ min^{-1}$)	$\mu_{g_{C2}}$ (min^{-1})	S. E.	$\mu_{g_{C4}}$ (min^{-1})	S. E.
1.40 * 10^{-1}	6.81 * 10^{-2}	3.55 * 10^{-4}	8.48 * 10^{-3}	1.29 * 10^{-3}
7.84 * 10^{-2}	1.01 * 10^{-1}	2.32 * 10^{-3}	1.70 * 10^{-2}	8.08 ·* 10^{-4}
2.19 ·* 10^{-2}	6.69* 10^{-2}	3.43 * 10^{-4}	3.35 * 10^{-3}	1.65 * 10^{-3}

Details on the parameter estimation procedure for the experiments employing *E. faecalis*

The fitted parameters to the model in the Table 2 of the manuscript are shown in Table 4.3 (part 1 and part 2). The shown flow velocity values ($1.40 * 10^{-1}$) $cm\ min^{-1}$, $7.84 * 10^{-2}$ $cm\ min^{-1}$ and $2.19 * 10^{-2}$ $cm\ min^{-1}$) are corresponding to F_{fast}, F_{med} and F_{slow}, respectively. As described in the main text, the parameter values corresponding to the F_{fast} have been obtained from Chandrasekar et al., 2021b.

4.6. Supplementary Material 2

Normalization procedure for comparison of processes

The modified advection dispersion equation (ADE) used for this study is shown in Equations 4.9 and 4.10.

$$\frac{\partial C}{\partial t} = -v*\frac{\partial C}{\partial x}+\alpha*v*\frac{\partial^2 C}{\partial x^2}-K_{str}*C*e^{-C_s/\lambda}-\mu_d*C-\mu_r*C-K_{att_{C1}/att_{C3}}*C+\mu_{g_{C2}/g_{C4}}*C \tag{4.9}$$

$$\frac{\partial C_S}{\partial t} = +K_{str}*C*e^{-C_s/\lambda}*\frac{\theta_e}{\rho}+K_{att_{C1}/att_{C3}}*C*\frac{\theta_e}{\rho} \tag{4.10}$$

The non-dimensionalization was applied to the concentration, length and time variables across the equations and the terms that were used for the non-dimensionalization are shown in the Equations 4.11 to 4.14.

$$C_R = C/C_o \tag{4.11}$$

$$C_{SR} = C_s/C_o*\frac{\rho}{\theta_e} \tag{4.12}$$

$$t_R = t*v/L \tag{4.13}$$

$$x_R = x/L \tag{4.14}$$

Where:

C_R, C_{SR}: Dimensionless concentration of bacteria in the water and sediment phase respectively (-, -).

C_o: Concentration of the bacteria at the inlet of the column at time t = 0, and x = 0 ($CFU\ mL^{-1}$)

t_R: non-dimensionalized time axis (-)

L: Length of the column (cm)

x_R: Non-dimensionalized length axis (-)

v: flow velocity ($cm\ min^{-1}$)

ρ : Bulk density ($cm\ m^{-3}$)

θ_e: effective porosity (-)

C, C_s: concentration of bacteria or particles in the water and sediment phase respectively ($CFU\ mL^{-1}$ or $particles\ mL^{-1}$, $CFU\ g^{-1}$)

t: time since start of the experiment (mins)

μ_d: bacteria decay rate (min^{-1})
μ_r: bacteria respiration rate (min^{-1})
$K_{att_{C1}/att_{C3}}$: bacteria attachment rate for the condition C1 and C3 respectively (min^{-1})
$\mu_{g_{C2}/g_{C4}}$: the bacteria growth rate in the water for the condition C2 and C4 respectively (min^{-1})

The aforementioned non-dimensionalization parameters for concentration and length are inputted into the modified ADE equation as shown in Equations 4.15 and 4.17 (based on 4.9) as well as in Equations 4.16 and 4.18 (based on Equation 4.10).

$$\frac{\partial C_R * C_o}{\partial(t_R * \frac{L}{v})} = \alpha * v * \frac{\partial^2(C_R * C_o)}{\partial(x_R * L)^2} - v * \frac{\partial C_R * C_o}{\partial x_R * L}$$

$$-K_{str} * (C_R * C_o) * e^{-C_{SR} * C_o/\lambda} - \mu_d * (C_R * C_o) - \mu_r * (C_R * C_o) \tag{4.15}$$

$$- K_{att_{C1}/att_{C3}} * (C_R * C_o) + \mu_{g_{C2}/g_{C4}} * (C_R * C_o)$$

The resulting equations are Equations 4.16 and 4.18.

$$\frac{\partial C_{SR} * C_o * \frac{\theta_e}{\rho}}{\partial(t_R * \frac{L}{v})} = +K_{str} * C_{SR} * C_o * e^{-C_s/\lambda} * \frac{\theta_e}{\rho} + K_{att_{C1}/att_{C3}} * C_{SR} * C_o * \frac{\theta_e}{\rho} \tag{4.16}$$

$$\frac{\partial C_R}{\partial t_R} = \frac{\alpha}{L}\frac{\partial^2 C_R}{\partial x_R^2} - \frac{\partial C_R}{\partial x_R}$$

$$-(\frac{K_{str} * L * e^{-C_{SR} * C_o/\lambda}}{v}) * C_R - (\frac{\mu_d * L}{v}) * C_R - (\frac{\mu_r * L}{v}) * C_R \tag{4.17}$$

$$-(\frac{K_{att_{C1}/att_{C3}} * L}{v}) * C_R + (\frac{\mu_{g_{C2}/g_{C4}} * L}{v}) * C_R$$

$$\frac{\partial C_{SR}}{\partial t_R} = +(\frac{K_{str} * L * e^{-C_{SR} * C_o/\lambda}}{v}) * C_{SR} + (\frac{K_{att_{C1}/att_{C3}} * L}{v}) * C_{SR} \tag{4.18}$$

By substituting the Peclet and Damkoehler numbers for the respective dimensionless parameters the normalized equations 4.19 and 4.20, used for comparison in section 3.2 of the manuscript, are obtained.

$$\begin{aligned}\frac{\partial C_R}{\partial t_R} = \frac{1}{Pe}\frac{\partial^2 C_R}{\partial x_R^2} - \frac{\partial C_R}{\partial x_R} - Da_{str} * C_R - Da_d * C_R \\ -Da_r * C_R - Da_{att_{C1}/att_{C3}} * C_R + Da_{g_{C2}/g_{C4}} * C_R\end{aligned} \tag{4.19}$$

$$\frac{\partial C_{SR}}{\partial t_R} = +Da_{str} * C_{SR} + Da_{att_{C1}/att_{C3}} * C_{SR} \tag{4.20}$$

Chapter 5

Synthesis

5.1. Discussion and conclusions

In this study a mechanistic modelling framework to verify biological processes occurring during pathogen transport through sandy sediment packed columns is developed. This was achieved using data from lab-scale, sediment packed, water-saturated column experiments. The broad application of the work is to understand pathogen transport through the subsoil during wastewater reuse. In this study, the impact of DO, nutrients and flow velocities on the processes involved with *Enterococci* were studied, using the combined experimental and modelling approach. The flexible modelling framework with eight reactive processes and three transport processes is implemented using *R* software, to allow for free access, easy addition and deletion of processes. These processes were studied under three flow velocities to evaluate the reproducibility of the same. The parameter values obtained from each of the flow velocities are compared using relevant dimensionless numbers.

The hydrological model was set up using three processes; advection, dispersion and straining. The processes were evaluated using results from continuous injection of saline water and microspheres, into the lab-scale column setup. Results from the tracer tests were used to evaluate the parameters of effective porosity and dispersivity. The average effective porosity values determined from all the experiments were determined to be 34.7% (Range: 30.3% - 38.8%). The parameters of effective and total porosity were almost identical. Since the column is fully water-saturated, this indicates the absence of major dead end pore spaces and absence of immobile pore water. The dispersivity value for all the experiments conducted ranged from 0.5 - 5 mm (Average value 1.41 mm). This indicates that the effects of mechanical dispersion account for 1 mm. Since the column is 15 cm long, the mechanical dispersion accounts for $< 1\%$ of the column length. Dispersivity is usually less significant for small scale setups [Ewing, 2005] as observed in this study.

Previous studies [Bradford et al., 2004; Bradford and Torkzaban, 2008; Bradford, Simunek, Bettahar, Van Genuchten, and Yates, 2006; Dıaz et al., 2010; Foppen et al., 2007; Xu et al., 2006; Xu et al., 2008; Xu and Saiers, 2009] on straining process indicate that this is a significant process occurring during contaminant transport through soils. These studies determined the impact of colloid sizes, shape, grain diameters, bacteria strain types, and effect of dead end pores on the straining process. Xu et al., 2006 indicate that the process of straining can be ignored for columns where the particle diameter (or colloid diameter) to grain diameter ratio are lesser than 0.005 . In this study this ratio is 0.0004. Nevertheless, it was found that straining impacts bacteria kinetics in soil and cannot be ignored for sediments with larger grain sizes, like coarse sand - fine gravel. The straining model description by Xu et al., 2006 fit well with the data obtained from the microsphere experiment for the given sediment. The straining processes showed a variation with flow velocity whereby the straining equation was simplified to a linear model representing straining rate as for the "slow" flow velocity. Furthermore, it is observed that the process of straining is more significant for the "slow" flow velocity. One possible explanation for this could be that due to the higher residence time of the microspheres (which are neutrally charged and relatively hydrophilic), electrostatic forces between the sediment grain and the microsphere begin to occur. These forces cause higher retention of microspheres in the sediment. A detailed discussion of the impact of flow velocity on the straining parameters is elaborated in Section 4.3.1 in Chapter 4. The aforementioned processes of advection, dispersion, and straining form the basis of the hydrological model. The reactive (biological) processes are built on this hydraullic model.

The first hypothesis presented in the study emphasised the role of dissolved oxygen for facultative anaerobes. The results presented in Chapter 3 confirmed the hypothesis. DO has an impact on growth and attachment of facultative anaerobes and opportunistic bacteria like *E. faecalis* JH2-2. The bacteria were continuously injected into sediment packed columns in environments that contained and were devoid of DO. In the absence of dissolved oxygen, *E faecalis* JH2-2 showed a considerable loss of culturability. This loss of culturability is associated with a decay parameter that is of the order of $10^{-2}\ min^{-1}$. The respiration rate constant for the bacteria in DO rich environments was of the order of $10^{-4}\ min^{-1}$ indicating that bacteria prefer environments that contain dissolved oxygen. The attachment rate also showed a significant difference in DO's presence and absence. While the attachment parameters were almost $10^{-7}\ min^{-1}$ in DO-free environments, they were more significant (parameter of the order of $10^{-2}\ min^{-1}$) for the environments rich in DO. One reason for this difference in the parameter rates could be associated with the absolute numbers of the bacteria. Since the concentration of bacteria is significantly

smaller for the DO-free environments, the bacteria have lesser opportunities to interact with the sediment. The growth parameter was one order of magnitude larger for the experiments without DO, as compared to those with DO. This indicates that the bacteria grow better in the absence of DO, despite the significantly larger concentration of bacteria found in the outlet of the columns subject to condition C4, as compared to C2. A similar trend was observed for all the flow velocities studied (Table 4.4). Putting into context, the relative importance of the processes under varying DO conditions (Figure 4.5), the processes of decay and growth were significant in non-DO environments. While attachment was more significant in DO-rich environments - a.k.a. the highest $Da_{att_{C3}}$ was still lower than the lowest Da_d or $Da_{g_{C2}}$. In the context of developing larger scale models, and risk assessment frameworks, the processes of decay and growth in DO-free environments are more significant than growth in a DO-rich zone. Furthermore, slower flow velocities are associated with a higher Damkoehler number (as expected), indicating a greater significance of these processes under slower flow conditions.

The second hypothesis was rejected by the results presented in the Chapters 3 and 4. The concentration of nutrients used in this experiments is 18.5 $mg\ L^{-1}$. As seen in the Figure 3.14, at this concentration, there is a limited growth of bacteria (Optical Density at maximum growth is 0.7 as compared to Optical Density 1 at 37 $g\ L^{-1}$). The parameter related to the growth processes in DO-free environments were of the order $10^{-2}\ min^{-1}$. The growth rate in the presence of DO was found to be of the order of $10^{-3}\ min^{-1}$. Based on the results from Figure 4.5, the $Da_{g_{C2}}$ is as significant as the decay process (as seen by Da_d), and in the presence of DO, $Da_{g_{C4}}$ is as significant as the attachment process $Da_{att_{C3}}$. The bacteria grow both in the inlet and the outlet of the column, and for the condition with and without DO. For the condition C2 (no DO), the absolute numbers of the bacteria only 50% of the initial concentration value for all the flow velocities at the outlet of the column. However, there is significant growth for the flow velocities F_{med} and F_{slow} at the inlet of the column wherein the bacteria are present at almost 4-8 times more than the concentration present at the start of the experiment. This means that there is a high concentration of bacteria entering the column. Since the attachment parameter under no DO conditions (C1 and C2) are also quite small, this could mean that most of the bacteria entering the column, come out the outlet, and additionally grow inside the column. Therefore, for higher time periods this growth process could mean a significant concentration of bacteria exiting from the column. This can be found further in the Figure 4.4 - C2-out, where for pore volumes greater than 4 there is a very high concentration of bacteria that exits the column. A similar observation is seen for the condition C4, where significantly high concentrations for bacteria are seen in the inlet and the outlet of the column. For this condition C4, the attachment parameter

does cause a reduction in the bacteria exiting the column. However with time (as seen in Figure 4.4 - C4-in and C4-out) the concentration of bacteria at both the inlet and outlet of the column is almost 150 times the concentration of bacteria present at the start of the experiment. This bacteria concentration could possibly mean that growth of bacteria is faster than exponential, and the linear growth rate law does not provide a satisfactory fit for estimating the growth rate of the bacteria. Assessing the role of nutrients in risk assessment models, we must keep in mind that the growth of bacteria in the subsoil environment (where the soil is devoid of nutrients), nutrient concentration in the water alone, could lead to a significant amount of bacteria reaching the lower soil layers, and subsequently leach into the groundwater. In addition, it can be seen that the growth parameter is very influential (Figure 3.5), and careful measurement of this parameter is required for field scale setups. In addition, the respiration rate must be carefully measured owing to the high sensitivity associated with changes in the parameter.

It is noteworthy that for the F_{med} the growth and attachment parameters were one order of magnitude higher than those for the F_{fast} and F_{slow} flow velocities. This, combined with the poor fitting of the linear model to describe the growth process for the "slow" flow velocity in condition C4, disproves the third hypothesis. Furthermore, Chapter 4 clearly shows that the variation of the Damkoehler numbers is not always proportional to the flow velocities. This indicates that parameter values need to be carefully studied for each flow velocity, especially for the growth and attachment processes; these parameter values could not be transferred within flow velocities. A time-dependent parameter could describe the process more accurately.

This work adds significant knowledge on the impact of various water quality characteristics on biological processes under varying flow conditions. This work successfully separated processes relating to attachment, straining, decay and respiration. Since these processes usually occur simultaneously, it is difficult to separate the processes and determine the impact of each process individually on the transport of bacteria within the subsoil region. Additionally, comparing the time scales of the various processes, it can be seen that all the processes studied are significant. A general ranking of the processes (across the various flow velocities studied) can be seen in the Chapter 4, where the Damkoehler numbers of the reactive processes were determined. This gives us an estimation on how significant the processes are in isolation, and their effect in combination can be predicted. For example, in a combined environment, the process of attachment can be neglected for environments that are devoid of DO, and an equilibrium model could be used for the decay process, since the process occurs very quickly within the time scale in this study.

5.2. Critical review, pathways towards future work

While, the current work provides a small insight into developing a modelling framework to understand bacteria transport through saturated sediments, a more extensive model encompassing varying effects would be more accurate for conducting quantitative risk assessment studies. For example building biological processes using unsaturated flow models could be a more accurate description of the bacteria dynamics in real-world scenarios. Therefore, this model can be considered a starting point for developing more complex models. Another improvement on the current modelling approach would be to combine statistical modelling with the process models (with possible non-linear rate laws, where necessary). This could be instrumental in understanding the correlation between the various parameters in larger scale models. These parameters include temperature, pH, antibiotic stress, variable microbial community, presence of heavy metals, to name a few.

Moving back to the lab-scale results, in the absence of DO *Enterococci* show almost a fast decay. While the decay rate was consistent with the order of $10^{-2}\ min^{-1}$, it must be noted that *Enterococcus faecalis* JH2-2 is a facultative anaerobe. Facultative anaerobes generally survive as good or better in environments devoid of oxygen. While the absence of any electron acceptors and nutrition source could contribute towards the cell lysis of the bacteria in the column, the statement must be corroborated with microscopy results, or live dead bacteria kit. These quantitative techniques will provide better insights into the exact process of 'decay' that the bacteria have undergone. Therefore, we can understand if the bacteria have simply become uncultivable or the bacteria undergo lysis due to the harsh conditions. In addition, if the bacteria undergo cell lysis, then the possible transfer of genetic material from the dead cells into the bacterial community (transformation) must be analysed within the context of antibiotic resistance. Furthermore, the decay and respiration processes have parameters obtained from the inlet concentration variation, i.e. from a non-flow setup. These parameters could be exaggerated, and especially for translating to field-scale setup, these parameters require cautious measurement in flow setup (especially considering the respiration parameter shows high sensitivity in scaled up field predictions).

In this study, the variation of DO concentration in the length of the column was not measured. While the DO concentration may not vary significantly for a column of length 15 cm the concentration could show significant variation when using more enormous columns. This means an additional process accounting for the loss of DO concentration must be added to the set of equations. This in turn will lead to a dynamic variation in the

process rate though the length of the column, which has not been accounted for in this study. DO could be measured using optical sensors connected using a fibre optic cable in the column without removing the sample. The same applies for the measurement of nutrient concentration at regular intervals within the column (or at least at the inlet and the outlet of the column, at various points in time). These data could provide an enhanced understanding on how nutrients are consumed during the flow of bacteria, and how their consumption impacts the kinetics and dynamics of bacteria concentration. The concentration profile of nutrients and DO through the length of the column are imperative to understand, especially when doing a mass balance for the concentration of the *Enterococci* in the column. The presence of limiting concentrations of nutrient or dissolved oxygen could warrant the use of a non-linear model (e.g. Monod equation) to describe the bacterial kinetics in larger-scale setups. The model shows poor-fitting with the sediment bacteria (Chapter 3). Therefore the growth rate of the bacteria in the sediment must be validated using kinetic data of the sediment bacteria. Additional processes occurring in the sediment phase like 'decay' (cell lysis) and detachment of the bacteria from the sediment must also be considered. Sediment bacteria can be kinetically measured at various points in the sediment column by drilling small holes in the column, and procuring small amounts of sediment (without having a significant impact on the total sediment mass of the column). Another important factor that has not been included in this study is the error propagation of parameter values. One of the shortcomings of using a stepwise combined experimental and modelling approach is that the error value associated with one parameter gets carried over in the next step of the model fitting procedure. This means that an erroneous parameter value used early on in the model fitting procedure could get translated into the subsequent steps, deeming any other parameter values unreliable. It is therefore important to obtain accurate parameter fittings early on in the model fitting steps, to ensure that processes and parameters built on these are accurately determined. While the aforementioned shortcomings must be acknowledged, this modelling framework can be used to understand the optimal sampling point and sampling times for further studies in this field, or larger scale studies. The results can provide considerable insights into assessing the optimal number of samples that must be procured for model validation in more complex environments. As more processes are studied, and the impact of various environmental factors can be considered, the processes and the correlation between environmental parameters and the bacteria concentration can be understood. This data provides a critical pathway to developing a decision support framework or tool that can be used by policymakers to understand the minimum water quality standard that can be used for irrigation or managed aquifer recharge.

Bibliography

Abu-Ashour, J., Joy, D. M., Lee, H., Whiteley, H. R., & Zelin, S. (1994). Transport of microorganisms through soil. *Water, Air, & Soil Pollution*, *75*(1), 141–158. https://doi.org/10.1007/BF01100406

Adams, J. C., Brainerd, W. S., Martin, J. T., Smith, B. T., & Wagener, J. L. (1997). *Fortran 95 handbook: Complete iso/ansi reference*. MIT press.

Alcalde-Sanz, L., & Gawlik, B. M. (2017). *Minimum quality requirements for water reuse in agricultural irrigation and aquifer recharge - towards a water reuse regulatory instrument at EU level* (tech. rep. EUR 28962 EN) [JRC109291]. Luxembourg, Publications Office of the European Union, https://doi.org/10.2760/887727

Angelakis, A. N., Monte, M. H. M. D., Bontoux, L., & Asano, T. (1999). The status of wastewater reuse practice in the mediterranean basin: Need for guidelines. *Water Research*, *33*, 2201–2217. https://doi.org/10.1016/S0043-1354(98)00465-5

Angelakis, A., Asano, T., Bahri, A., Jimenez, B. E., & Tchobanoglous, G. (2018). Water reuse: From ancient to modern times and the future. *Frontiers in Environmental Science*, *6*, 26.

Angelakis, A., & Durham, B. (2008). Water recycling and reuse in eureau countries: Trends and challenges [AQUAREC 2006 CHEMECA 2006]. *Desalination*, *218*(1), 3–12. https://doi.org/https://doi.org/10.1016/j.desal.2006.07.015

Angelakis, A., & Gikas, P. (2014). Water reuse: Overview of current practices and trends in the world with emphasis on eu states. *Water Utility Journal*, *8*(67), e78.

Arthur, M., & Saffer, D. (2022). *EARTH 111: Water: Science and society* [Darcy's experiments and darcy's law]. https://www.e-education.psu.edu/earth111/node/926

Asano, T. (2005). Urban water recycling. *Water Science and Technology*, *51*(8), 83–89. https://doi.org/10.2166/wst.2005.0232

Asano, T. (1993). Proposed california regulations for groundwater recharge with reclaimed municipal wastewater. *Water Science and Technology*, *27*(7-8), 157–164.

Asano, T., & Levine, A. D. (1996). Wastewater reclamation, recycling and reuse: Past, present, and future. *Water Science and Technology*, *33*, 1–14. https://doi.org/10.2166/wst.1996.0656

Assembly, G. (2015). *Resolution adopted by the general assembly on 11 september 2015* (tech. rep.). A/RES/69/315 15 September 2015. New York: United Nations.

Ateba, C. N., & Maribeng, M. D. (2011). Detection of enterococcus species in groundwater from some rural communities in the mmabatho area, south africa: A risk analysis. *African Journal of Microbiology Research*, *5*(23), 3930–3935. https://doi.org/10.5897/AJMR11.645

Ayers, R., & Westcot, D. (1985). *Water quality for agriculture* (Vol. 29). Food; Agriculture Organisation of the United Nations.

Bahri, A., & Brissaud, F. (1996). Wastewater reuse in tunisia: Assessing a national policy. *Water Science and Technology*, *33*, 87–94. https://doi.org/10.2166/wst.1996.0665

Bai, H., Cochet, N., Pauss, A., & Lamy, E. (2016). Bacteria cell properties and grain size impact on bacteria transport and deposition in porous media. *Colloids and Surfaces B: Biointerfaces*, *139*, 148–155. https://doi.org/10.1016/j.colsurfb.2015.12.016

Balkhair, K. S. (2017). Modeling fecal bacteria transport and retention in agricultural and urban soils under saturated and unsaturated flow conditions. *Water research*, *110*, 313–320. https://doi.org/10.1016/J.WATRES.2016.12.023

Benz, S. A., Bayer, P., & Blum, P. (2017). Global patterns of shallow groundwater temperatures. *Environmental Research Letters*, *12*(3), 034005. https://doi.org/10.1088/1748-9326/aa5fb0

Berendonk, T. U., Manaia, C. M., Merlin, C., Fatta-Kassinos, D., Cytryn, E., Walsh, F., Bürgmann, H., Sørum, H., Norström, M., Pons, M.-N., et al. (2015). Tackling antibiotic resistance: The environmental framework. *Nature Reviews Microbiology*, *13*(5), 310–317. https://doi.org/10.1038/nrmicro3439

Beretta, G. P., & Stevenazzi, S. (2018). Specific yield of aquifer evaluation by means of a new experimental algorithm and its applications [Number: 1]. *Acque Sotterranee - Italian Journal of Groundwater*, *7*(1). https://doi.org/10.7343/as-2018-325

Bergström, L. (2000). Leaching of agrochemicals in field lysimeters : A method to test mobility of chemicals in soil. *Pesticide/Soil Interactions*, 279.

Bixio, D., De Heyder, B., Cikurel, H., Muston, M., Miska, V., Joksimovic, D., Schäfer, A. I., Ravazzini, A., Aharoni, A., Savic, D., & Thoeye, C. (2005). Municipal wastewater reclamation: Where do we stand? an overview of treatment technology and management practice. *Water Science and Technology: Water Supply*, *5*(1), 77–85. https://doi.org/10.2166/ws.2005.0010

Bixio, D., Thoeye, C., Wintgens, T., Ravazzini, A., Miska, V., Muston, M., Chikurel, H., Aharoni, A., Joksimovic, D., & Melin, T. (2008). Water reclamation and reuse: Implementation and management issues. *Desalination*, *218*, 13–23. https://doi.org/10.1016/j.desal.2006.10.039

Bixio, D., Thoeye, C., De Koning, J., Joksimovic, D., Savic, D., Wintgens, T., & Melin, T. (2006). Wastewater reuse in europe. *Desalination*, *187*(1-3), 89–101. https://doi.org/10.1016/j.desal.2005.04.070

Boehm, A. B., & Sassoubre, L. M. (2014). Enterococci as indicators of environmental fecal contamination. in: Enterococci: From commensals to leading causes of drug resistant infection. [PMID: 24649503]. *Massachusetts Eye and Ear Infirmary*.

Bourgeois-Nicolaos, N., Moubareck, C., Mangeney, N., Butel, M.-J., & Doucet-Populaire, F. (2006). Comparative study of *vanA* gene transfer from *Enterococcus faecium* to *Enterococcus faecalis* and to *Enterococcus faecium* in the intestine of mice. *FEMS microbiology letters*, *254*(1), 27–33. https://doi.org/10.1111/j.1574-6968.2005.00004.x

Bradford, S. A., & Bettahar, M. (2006). Concentration dependent transport of colloids in saturated porous media. *Journal of contaminant hydrology*, *82*(1-2), 99–117. https://doi.org/10.1016/j.jconhyd.2005.09.006

Bradford, S. A., Bettahar, M., Simunek, J., & Van Genuchten, M. T. (2004). Straining and attachment of colloids in physically heterogeneous porous media. *Vadose Zone Journal*, *3*(2), 384–394. https://doi.org/10.2113/3.2.384

Bradford, S. A., Simunek, J., Bettahar, M., Van Genuchten, M. T., & Yates, S. R. (2003). Modeling colloid attachment, straining, and exclusion in saturated porous media. *Environmental science & technology*, *37*(10), 2242–2250. https://doi.org/10.1021/es025899u

Bradford, S. A., Simunek, J., & Walker, S. L. (2006). Transport and straining of e. coli o157: H7 in saturated porous media. *Water Resources Research*, *42*(12). https://doi.org/10.1029/2005WR004805

Bradford, S. A., & Torkzaban, S. (2008). Colloid Transport and Retention in Unsaturated Porous Media: A Review of Interface-, Collector-, and Pore-Scale Processes and ModelsAll rights reserved. No part of this periodical may be reproduced or transmitted in any form or by any means, electronic or mechanical, including photocopying, recording, or any information storage and retrieval system, without permission in writing from the publisher. *Vadose Zone Journal*, *7*(2), 667–681. https://doi.org/10.2136/vzj2007.0092

Bradford, S. A., Yates, S. R., Bettahar, M., & Simunek, J. (2002). Physical factors affecting the transport and fate of colloids in saturated porous media. *Water resources research*, *38*(12), 63–1. https://doi.org/10.1029/2002WR001340

Bradford, S. A., Simunek, J., Bettahar, M., Van Genuchten, M. T., & Yates, S. (2006). Significance of straining in colloid deposition: Evidence and implications. *Water Resources Research*, *42*(12). https://doi.org/10.1029/2005WR004791

Brissaud, F. (2008). Criteria for water recycling and reuse in the mediterranean countries. *Desalination*, *218*, 24–33. https://doi.org/10.1016/j.desal.2006.07.016

Buck, J. D., & Cleverdon, R. C. (1960). The spread plate as a method for the enumeration of marine bacteria 1, 2. *Limnology and Oceanography*, *5*(1), 78–80. https://doi.org/10.4319/lo.1960.5.1.0078

Cacace, D., Fatta-Kassinos, D., Manaia, C. M., Cytryn, E., Kreuzinger, N., Rizzo, L., Karaolia, P., Schwartz, T., Alexander, J., Merlin, C., et al. (2019). Antibiotic resistance genes in treated wastewater and in the receiving water bodies: A pan-european survey of urban settings. *Water research*, *162*, 320–330. https://doi.org/10.1016/j.watres.2019.06.039

Chanan, A., & Woods, P. (2006). Introducing total water cycle management in sydney: A kogarah council initiative. *Desalination*, *187*, 11–16. https://doi.org/10.1016/j.desal.2005.04.063

Chandrasekar, A., Binder, M., Liedl, R., & Berendonk, T. U. (2021a). Determining the impact of flow velocities on reactive processes associated with enterococcus faecalis JH2-2. *Water Science and Technology*, *85*(1), 485–495. https://doi.org/10.2166/wst.2021.611

Chandrasekar, A., Binder, M., Liedl, R., & Berendonk, T. U. (2021b). Reactive-transport modelling of enterococcus faecalis JH2-2 passage through water saturated sediment columns. *Journal of Hazardous Materials*, *413*, 125292.

Chang, D., & Ma, Z. (2012). Wastewater reclamation and reuse in beijing: Influence factors and policy implications. *Desalination*, *297*, 72–78. https://doi.org/10.1016/j.desal.2012.04.019

Chen, G., & Walker, S. L. (2012). Fecal indicator bacteria transport and deposition in saturated and unsaturated porous media. *Environmental Science & Technology*, *46*(16), 8782–8790. https://doi.org/10.1021/es301378q

Cipolletta, G., Ozbayram, E. G., Eusebi, A. L., Akyol, Ç., Malamis, S., Mino, E., & Fatone, F. (2021). Policy and legislative barriers to close water-related loops in innovative small water and wastewater systems in europe: A critical analysis. *Journal of Cleaner Production*, *288*. https://doi.org/10.1016/j.jclepro.2020.125604

Consoli, S., Licciardello, F., Aiello, R., Giuffrida, F., Leonardi, C., & Cirelli, G. (2012). Treated municipal wastewater reuse in vegetable production. *Agricultural Water Management*, *104*, 163–170. https://doi.org/10.1016/j.agwat.2011.12.011

Corapcioglu, M. Y., & Haridas, A. (1985). Microbial transport in soils and groundwater: A numerical model. *Advances in Water Resources*, *8*(4), 188–200. https://doi.org/10.1016/0309-1708(85)90063-6

Cunningham, A. B., Sharp, R. R., Caccavo, F., & Gerlach, R. (2007). Effects of starvation on bacterial transport through porous media. *Advances in Water Resources*, *30*(6), 1583–1592. https://doi.org/10.1016/j.advwatres.2006.05.018

Darcy, H. (1856). The public fountains of the city of dijon. *Victor Dalmont, Paris, France*.

Deen, W. (2012). *Analysis of transport phenomena*. Oxford University Press.

DIN 18128:2002–12. (2002). Soil - investigation and testing - determination of ignition loss.

DIN EN 15933:2012–11. (2012). Sludge, treated biowaste and soil-determination of ph. german version.

DIN EN ISO 17892–3:2016–07. (2016). Geotechnical investigation and testing - laboratory testing of soil - part 3: Determination of particle density (iso 17892–3:2015, corrected version 2015–12-15); german version en iso 17892–3:2015.

Ding, D. (2010). Transport of bacteria in aquifer sediment: Experiments and modeling. *Hydrogeology journal*, *18*(3), 669–679. https://doi.org/10.1007/s10040-009-0559-3

Dıaz, J., Rendueles, M., & Dıaz, M. (2010). Straining phenomena in bacteria transport through natural porous media. *Environmental Science and Pollution Research*, *17*(2), 400–409. https://doi.org/10.1007/s11356-009-0160-2

Dong, H., Rothmel, R., Onstott, T. C., Fuller, M. E., DeFlaun, M. F., Streger, S. H., Dunlap, R., & Fletcher, M. (2002). Simultaneous transport of two bacterial strains in intact cores from oyster, virginia: Biological effects and numerical modeling. https://doi.org/10.1128/AEM.68.5.2120-2132.2002

Eckis, R. (1934). *South coastal basin investigation: Geology and ground water storage capacity of valley fill*. State of California, Department of Public Works.

Ellis, J., & Revitt, D. (2002). Sewer losses and interactions with groundwater quality. *Water Science and Technology*, *45*(3), 195–202. https://doi.org/10.2166/wst.2002.0079

Elzhov, T., Mullen, K., Spiess, A., Bolker, B., & Mullen, M. (2016). Minpack.lm: R interface to the levenberg-marquardt nonlinear least-squares algorithm found in minpack, plus support for bounds. https://CRAN.R-project.org/package=minpack.lm

Eregno, F., & Heistad, A. (2019). On-site treated wastewater disposal systems – the role of stratified filter medias for reducing the risk of pollution. *Environment International*, *124*, 302–311. https://doi.org/10.1016/j.envint.2019.01.008

European Commission and Directorate-General for Environment. (2009). *Groundwater protection in europe : The new groundwater directive : Consolidating the eu regulatory framework*. Publications Office. https://doi.org/10.2779/84304

Ewing, R. (2005). Scaling | transport processes. In D. Hillel (Ed.), *Encyclopedia of soils in the environment* (pp. 477–485). Elsevier. https://doi.org/10.1016/B0-12-348530-4/00570-1

Fand, R., & Thinakaran, R. (1990). The influence of the wall on flow through pipes packed with spheres. *112*(1), 84–88. https://doi.org/10.1115/1.2909373

Fawell, J., Corre, K. L., & Jeffrey, P. (2016). Common or independent? the debate over regulations and standards for water reuse in europe. *International Journal of Water Resources Development*, *32*, 559–572. https://doi.org/10.1080/07900627.2016.1138399

Feddes, R. A., de Rooij, G. H., & van Dam, J. C. (Eds.). (2004). *Unsaturated-zone modeling: Progress, challenges and applications* (Vol. 6). Kluwer Academic Publishers.

Feighery, J., Mailloux, B. J., Ferguson, A., Ahmed, K. M., van Geen, A., & Culligan, P. J. (2013). Transport of e. coli in aquifer sediments of bangladesh: Implications for widespread microbial contamination of groundwater. *Water resources research*, *49*(7), 3897–3911. https://doi.org/10.1002/wrcr.20289

Fontes, D. E., Mills, A. L., Hornberger, G. M., & Herman, J. S. (1991). Physical and chemical factors influencing transport of microorganisms through porous media. *Applied and Environmental Microbiology*. https://doi.org/10.1128/aem.57.9.2473-2481.1991

Foppen, J. W., Van Herwerden, M., & Schijven, J. (2007). Measuring and modelling straining of escherichia coli in saturated porous media. *Journal of contaminant hydrology*, *93*(1-4), 236–254. https://doi.org/10.1016/j.jconhyd.2007.03.001

Gargiulo, G., Bradford, S., Simunek, J., Ustohal, P., Vereecken, H., & Klumpp, E. (2008). Bacteria transport and deposition under unsaturated flow conditions: The role of water content and bacteria surface hydrophobicity. *Vadose Zone Journal*, *7*(2), 406–419. https://doi.org/10.2136/vzj2007.0068

Gargiulo, G., Bradford, S., Šimůnek, J., Ustohal, P., Vereecken, H., & Klumpp, E. (2007). Transport and deposition of metabolically active and stationary phase deinococcus radiodurans in unsaturated porous media. *Environmental science & technology*, *41*(4), 1265–1271. https://doi.org/10.1021/es062854a

Gay, D. M. (1990). Usage summary for selected optimization routines. *Computing science technical report*, *153*, 1–21.

Ghermandi, A., Bixio, D., & Thoeye, C. (2007). The role of free water surface constructed wetlands as polishing step in municipal wastewater reclamation and reuse. *Science of The Total Environment*, *380*(1), 247–258. https://doi.org/10.1016/j.scitotenv.2006.12.038

Ghermandi, A., Bixio, D., Traverso, P., Cersosimo, I., & Thoeye, C. (2007). The removal of pathogens in surface-flow constructed wetlands and its implications for water reuse. *Water Science and Technology*, *56*(3), 207–216. https://doi.org/10.2166/wst.2007.511

Gibb, J., Barcelona, M., Ritchey, J., & LaFaivre, M. (1985). Effective porosity of geologic materials.

Gilbert, O., Hernández, M., Vilanova, E., & Cornellà, O. (2014). Guidelining protocol for soil-column experiments assessing fate and transport of trace organics. *Demeau, Brussels, Belgium*, *3*, 54.

Gilmore, M. S., Clewell, D. B., Courvalin, P., Dunny, G. M., Murray, B. E., Rice, L. B., et al. (2002). *The enterococci: Pathogenesis, molecular biology, and antibiotic resistance* (Vol. 10). ASM press Washington, DC.

Hall, J. A., Mailloux, B. J., Onstott, T. C., Scheibe, T. D., Fuller, M. E., Dong, H., & DeFlaun, M. F. (2005). Physical versus chemical effects on bacterial and bromide transport as determined from on site sediment column pulse experiments. *Journal of contaminant hydrology*, *76*(3-4), 295–314. https://doi.org/10.1016/j.jconhyd.2004.11.003

Harter, T., Wagner, S., & Atwill, E. R. (2000). Colloid transport and filtration of cryptosporidium parvum in sandy soils and aquifer sediments. *Environmental science & technology*, *34*(1), 62–70. https://doi.org/10.1021/es990132w

Haruvy, N. (1998). Wastewater reuse—regional and economic considerations. *Resources, Conservation and Recycling*, *23*(1-2), 57–66.

Harvey, R. W., Kinner, N. E., MacDonald, D., Metge, D. W., & Bunn, A. (1993). Role of physical heterogeneity in the interpretation of small-scale laboratory and field observations of bacteria,

microbial-sized microsphere, and bromide transport through aquifer sediments. *Water Resources Research*, *29*(8), 2713–2721. https://doi.org/10.1029/93WR00963.

Harvey, R. W. (1997). Microorganisms as tracers in groundwater injection and recovery experiments: A review. *FEMS Microbiology Reviews*, *20*(3-4), 461–472. https://doi.org/10.1111/j.1574-6976.1997.tb00330.x

Helmecke, M., Fries, E., & Schulte, C. (2020). Regulating water reuse for agricultural irrigation: Risks related to organic micro-contaminants. *Environmental Sciences Europe*, *32*(1), 4. https://doi.org/10.1186/s12302-019-0283-0

Holden, P. A., & Fierer, N. (2005). Microbial processes in the vadose zone. *Vadose Zone Journal*, *4*(1), 1–21. https://doi.org/10.2113/4.1.1

Hong, P.-Y., Julian, T. R., Pype, M.-L., Jiang, S. C., Nelson, K. L., Graham, D., Pruden, A., & Manaia, C. M. (2018). Reusing treated wastewater: Consideration of the safety aspects associated with antibiotic-resistant bacteria and antibiotic resistance genes. *Water*, *10*(3), 244. https://doi.org/10.3390/w10030244

Hornberger, G. M., Mills, A. L., & Herman, J. S. (1992). Bacterial transport in porous media: Evaluation of a model using laboratory observations. *Water Resources Research*, *28*(3), 915–923. https://doi.org/10.1029/91WR02980

Huertas, E., Salgot, M., Hollender, J., Weber, S., Dott, W., Khan, S., Schäfer, A., Messalem, R., Bis, B., Aharoni, A., & Chikurel, H. (2008). Key objectives for water reuse concepts. *Desalination*, *218*(1), 120–131. https://doi.org/https://doi.org/10.1016/j.desal.2006.09.032

Huysmans, M., & Dassargues, A. (2005). Review of the use of péclet numbers to determine the relative importance of advection and diffusion in low permeability environments. *Hydrogeology Journal*, *13*(5), 895–904. https://doi.org/10.1007/s10040-004-0387-4

Issaadi, N., Aït-Mokhtar, A., Belarbi, R., & Hamami, A. (2018). *8 - effect of variability of porous media properties on drying kinetics: Application to cement-based materials* (F. Nicot & O. Millet, Eds.). Elsevier. https://doi.org/https://doi.org/10.1016/B978-1-78548-278-6.50008-6

Jacques, D., & Simunek, J. (2005). *User manual of the multicompenent variably-saturated flow and transport model hp1 (version 1.0, sck cen-blg-998),waste and disposal, sck cen, mol, belgium* (tech. rep.). Department of Environmental Sciences, University of California, Riverside, USA.

Jamieson, R., Gordon, R., Sharples, K., Stratton, G., & Madani, A. (2002). Movement and persistence of fecal bacteria in agricultural soils and subsurface drainage water: A review. *Canadian biosystems engineering*, *44*(1), 1–9.

Janosova, B., Miklankova, J., Hlavinek, P., & Wintgens, T. (2006). Drivers for wastewater reuse: Regional analysis in the czech republic. *Desalination*, *187*, 103–114. https://doi.org/10.1016/j.desal.2005.04.071

Jiménez, B., & Asano, T. (2008). *Water reuse: An international survey of current practice, issues and needs* (Vol. 15). IWA Publishing. https://doi.org/10.2166/9781780401881

Johnson, W. P., Blue, K. A., Logan, B. E., & Arnold, R. G. (1995). Modeling bacterial detachment during transport through porous media as a residence-time-dependent process. *Water Resources Research*, *31*(11), 2649–2658. https://doi.org/10.1029/95WR02311

Kalwa, F., Binder, M., Händel, F., Grüneberg, L., & Liedl, R. (2021). Biological and physical clogging in infiltration wells: Effects of well diameter and gravel pack. *Groundwater*. https://doi.org/10.1111/gwat.13104

Kampouris, I. D., Agrawal, S., Orschler, L., Cacace, D., Kunze, S., Berendonk, T. U., & Klümper, U. (2021). Antibiotic resistance gene load and irrigation intensity determine the impact of wastewater irrigation on antimicrobial resistance in the soil microbiome. *Water Research*, *193*, 116818. https://doi.org/https://doi.org/10.1016/j.watres.2021.116818

Kampouris, I. D., Klümper, U., Agrawal, S., Orschler, L., Cacace, D., Kunze, S., & Berendonk, T. U. (2021). Treated wastewater irrigation promotes the spread of antibiotic resistance into subsoil pore-water. *Environment International*, *146*, 106190. https://doi.org/10.1016/j.envint.2020.106190

Käss, W. (2004). Geohydrologische markierungstechnik.

Kellis, M., Kalavrouziotis, I., Gikas, P., et al. (2013). Review of wastewater reuse in the mediterranean countries, focusing on regulations and policies for municipal and industrial applications. *Global NEST Journal*, *15*(3), 333–350.

Khan, S. J., & Anderson, R. (2018). Potable reuse: Experiences in australia. *Current Opinion in Environmental Science and Health*, *2*, 55–60. https://doi.org/10.1016/j.coesh.2018.02.002

Kneis, D., Petzoldt, T., & Berendonk, T. U. (2017). An r-package to boost fitness and life expectancy of environmental models. *Environmental Modelling & Software*, *96*, 123–127. https://doi.org/10.1016/j.envsoft.2017.06.036

Kokkinosa, A., Fasseas, C., Eliopoulos, E., & Kalantzopoulos, G. (1998). Cell size of various lactic acid bacteria as determined by scanning electron microscope and image analysis. *Le Lait*, *78*(5), 491–500. https://doi.org/10.1051/lait:1998546

Lavrnić, S., Zapater-Pereyra, M., & Mancini, M. L. (2017). Water scarcity and wastewater reuse standards in southern europe: Focus on agriculture. *Water, Air, and Soil Pollution*, *228*. https://doi.org/10.1007/s11270-017-3425-2

Lazarova, V., Levine, B., Sack, J., Cirelli, G., Jeffrey, P., Muntau, H., Salgot, M., & Brissaud, F. (2001). Role of water reuse for enhancing integrated water management in Europe and Mediterranean countries. *Water Science and Technology*, *43*(10), 25–33. https://doi.org/10.2166/wst.2001.0571

Leal, L. G. (1992). *Laminar flow and convective transport processes - scaling principles and asymptotic analysis* (Vol. 251). Boston: Butterworth-Heinemann. https://doi.org/10.1016/C2009-0-26910-8

Lehmann, K., Schaefer, S., Babin, D., Köhne, J. M., Schlüter, S., Smalla, K., Vogel, H.-J., & Totsche, K. U. (2018). Selective transport and retention of organic matter and bacteria shapes initial

pedogenesis in artificial soil - a two-layer column study. *Geoderma*, *325*, 37–48. https://doi.org/https://doi.org/10.1016/j.geoderma.2018.03.016

Levy, J., Sun, K., Findlay, R., Farruggia, F., Porter, J., Mumy, K., Tomaras, J., & Tomaras, A. (2007). Transport of escherichia coli bacteria through laboratory columns of glacial-outwash sediments: Estimating model parameter values based on sediment characteristics. *Journal of contaminant hydrology*, *89*(1-2), 71–106. https://doi.org/10.1016/j.jconhyd.2006.08.006

Lewis, J., & Sjöstrom, J. (2010). Optimizing the experimental design of soil columns in saturated and unsaturated transport experiments. *Journal of contaminant hydrology*, *115*(1-4), 1–13. https://doi.org/10.1016/j.jconhyd.2010.04.001

Luprano, M. L., De Sanctis, M., Del Moro, G., Di Iaconi, C., Lopez, A., & Levantesi, C. (2016). Antibiotic resistance genes fate and removal by a technological treatment solution for water reuse in agriculture. *Science of The Total Environment*, *571*, 809–818. https://doi.org/https://doi.org/10.1016/j.scitotenv.2016.07.055

Manning, J. C. (2016). *Applied principles of hydrology: Third edition*. Waveland Press.

Matthess, G., Pekdeger, A., & Schroeter, J. (1988). Persistence and transport of bacteria and viruses in groundwater—a conceptual evaluation. *Journal of Contaminant Hydrology*, *2*(2), 171–188. https://doi.org/10.1016/0169-7722(88)90006-X

McCaulou, D. R., Bales, R. C., & Arnold, R. G. (1995). Effect of temperature-controlled motility on transport of bacteria and microspheres through saturated sediment. *Water Resources Research*, *31*(2), 271–280. https://doi.org/https://doi.org/10.1029/94WR02569

McCaulou, D. R., Bales, R. C., & McCarthy, J. F. (1994). Use of short-pulse experiments to study bacteria transport through porous media. *Journal of Contaminant Hydrology*, *15*(1), 1–14. https://doi.org/10.1016/0169-7722(94)90007-8

Menon, E. S. (2014). *Transmission pipeline calculations and simulations manual*. Gulf Professional Publishing.

Mioska, M. J. (2012). *A column experiment for groundwater remediation post-mine closure at the wolverine mine, yukon*. Royal Roads University (Canada).

Mishra, S., Kneis, D., Berendonk, T. U., & Aubeneau, A. (2019). Optimum positioning of wastewater treatment plants in a river network: A model-based approach to minimize microbial pollution. *Science of the Total Environment*, *691*, 1310–1319. https://doi.org/10.1016/j.scitotenv.2019.07.035

Mizyed, N. R. (2013). Challenges to treated wastewater reuse in arid and semi-arid areas. *Environmental Science and Policy*, *25*, 186–195. https://doi.org/10.1016/j.envsci.2012.10.016

Molinos-Senante, M., Hernández-Sancho, F., & Sala-Garrido, R. (2011). Cost-benefit analysis of water-reuse projects for environmental purposes: A case study for spanish wastewater treatment plants. *Journal of Environmental Management*, *92*, 3091–3097. https://doi.org/10.1016/j.jenvman.2011.07.023

Monod, J. (1942). Recherches sur la croissance des cultures bacteriennes.

Murphy, E. M., & Ginn, T. R. (2000). Modeling microbial processes in porous media. *Hydrogeology Journal*, *8*(1), 142–158. https://doi.org/10.1007/s100409900043

Nagashima, A. (1977). Viscosity of water substance—new international formulation and its background. *Journal of Physical and Chemical Reference Data*, *6*(1133). https://doi.org/10.1063/1.555562

Negreanu, Y., Pasternak, Z., Jurkevitch, E., & Cytryn, E. (2012). Impact of treated wastewater irrigation on antibiotic resistance in agricultural soils. *Environmental science & technology*, *46*(9), 4800–4808. https://doi.org/10.1021/es204665b

Newton, R. J., & McClary, J. S. (2019). The flux and impact of wastewater infrastructure microorganisms on human and ecosystem health. *Current opinion in biotechnology*, *57*, 145–150. https://doi.org/10.1016/j.copbio.2019.03.015

Nielsen, D., Th. Van Genuchten, M., & Biggar, J. (1986). Water flow and solute transport processes in the unsaturated zone. *Water resources research*, *22*(9S), 89S–108S. https://doi.org/10.1029/WR022i09Sp0089S

Nimmo, J. R. (2006). Unsaturated zone flow processes. *Encyclopedia of hydrological sciences*.

Novais, C., Coque, T. M., Ferreira, H., Sousa, J. C., & Peixe, L. (2005). Environmental contamination with vancomycin-resistant enterococci from hospital sewage in portugal. *Applied and Environmental Microbiology*, *71*(6), 3364–3368. https://doi.org/10.1128/AEM.71.6.3364-3368.2005

Novakowski, K. S. (1992). An evaluation of boundary conditions for one-dimensional solute transport: 2. column experiments. *Water Resources Research*, *28*(9), 2411–2423. https://doi.org/10.1029/92WR00592

Ogata, A., & Banks, R. B. (1961). *A solution of the differential equation of longitudinal dispersion in porous media: Fluid movement in earth materials*. US Government Printing Office.

Oliviera, I., Demond, A., & Salehzadeh, A. (1996). Packing of sands for the production of homogeneous porous media. *Soil Science Society of America Journal*, *60*(1), 49–53. https://doi.org/10.2136/sssaj1996.03615995006000010010x

Pang, L., & Šimůnek, J. (2006). Evaluation of bacteria-facilitated cadmium transport in gravel columns using the hydrus colloid-facilitated solute transport model. *Water resources research*, *42*(12). https://doi.org/10.1029/2006WR004896

Paranychianakis, N. V., Salgot, M., Snyder, S. A., & Angelakis, A. N. (2015). Water reuse in eu states: Necessity for uniform criteria to mitigate human and environmental risks. *Critical Reviews in Environmental Science and Technology*, *45*, 1409–1468. https://doi.org/10.1080/10643389.2014.955629

Parkhurst, D. L., Appelo, C. et al. (2013). *Description of input and examples for phreeqc version 3—a computer program for speciation, batch-reaction, one-dimensional transport, and inverse geochemical calculations* (tech. rep. A43). US Geological Survey Reston, VA, USA.

Pekdeger, A., & Matthess, G. (1983). Factors of bacteria and virus transport in groundwater. *Environmental Geology*, *5*(2), 49–52. https://doi.org/10.1007/BF02381095

Porubcan, A. A., & Xu, S. (2011). Colloid straining within saturated heterogeneous porous media. *Water research*, *45*(4), 1796–1806. https://doi.org/10.1016/j.watres.2010.11.037

Powell, M. J. (2009). The bobyqa algorithm for bound constrained optimization without derivatives. *Cambridge NA Report NA2009/06, University of Cambridge, Cambridge*, *26*.

R Core Team. (2020). *R: A language and environment for statistical computing*. R Foundation for Statistical Computing. Vienna, Austria. https://www.R-project.org/

Radcliffe, J. C. (2006). Future directions for water recycling in australia. *Desalination*, *187*, 77–87. https://doi.org/10.1016/j.desal.2005.04.069

Ricart, S., & Rico, A. M. (2019). Assessing technical and social driving factors of water reuse in agriculture: A review on risks, regulation and the yuck factor. *Agricultural Water Management*, *217*, 426–439. https://doi.org/10.1016/j.agwat.2019.03.017

Rizzo, L., Manaia, C., Merlin, C., Schwartz, T., Dagot, C., Ploy, M., Michael, I., & Fatta-Kassinos, D. (2013). Urban wastewater treatment plants as hotspots for antibiotic resistant bacteria and genes spread into the environment: A review. *Science of the total environment*, *447*, 345–360. https://doi.org/10.1016/j.scitotenv.2013.01.032

Rizzo, L., Krätke, R., Linders, J., Scott, M., Vighi, M., & de Voogt, P. (2018). Proposed EU minimum quality requirements for water reuse in agricultural irrigation and aquifer recharge: SCHEER scientific advice. *Current Opinion in Environmental Science & Health*, *2*, 7–11. https://doi.org/10.1016/j.coesh.2017.12.004

Rosenberg, M. (1984). Bacterial adherence to hydrocarbons: A useful technique for studying cell surface hydrophobicity. *FEMS Microbiology Letters*, *22*(3), 289–295. https://doi.org/10.1111/j.1574-6968.1984.tb00743.x

Rowell, D. (1994). Laboratory methods for studying mineralization. *Soil science: Methods and Applications. Longman Scientific and Technical, Longman Group UK Ltd., Longman House, London, England*.

Runkel, R. L. (1996). Solution of the advection-dispersion equation: Continuous load of finite duration. *Journal of Environmental Engineering*, *122*(9), 830–832. https://doi.org/10.1061/(ASCE)0733-9372(1996)122:9(830)

Salgot, M., & Folch, M. (2018). Wastewater treatment and water reuse. *Current Opinion in Environmental Science and Health*, *2*, 64–74. https://doi.org/10.1016/j.coesh.2018.03.005

Schäfer, A., Ustohal, P., Harms, H., Stauffer, F., Dracos, T., & Zehnder, A. J. (1998). Transport of bacteria in unsaturated porous media. *Journal of contaminant Hydrology*, *33*(1-2), 149–169. https://doi.org/10.1016/S0169-7722(98)00069-2

Selim, H. M., & Ma, L. (1998). *Physical nonequilibrium in soils: Modeling and application*. Ann Arbor Press.

Sen, T. K., Das, D., Khilar, K. C., & Suraishkumar, G. (2005). Bacterial transport in porous media: New aspects of the mathematical model. *Colloids and Surfaces A: Physicochemical and Engineering Aspects*, *260*(1-3), 53–62. https://doi.org/10.1016/j.colsurfa.2005.02.033

Sentenac, P., Lynch, R., & Bolton, M. (2001). Measurement of a side-wall boundary effect in soil columns using fibre-optics sensing. *International Journal of Physical Modelling in Geotechnics*, *1*(4), 35–41. https://doi.org/10.1680/ijpmg.2001.010404

Shoushtarian, F., & Negahban-Azar, M. (2020). Worldwide regulations and guidelines for agricultural water reuse: A critical review. *Water*, *12*, 971. https://doi.org/10.3390/w12040971

Silliman, S., Dunlap, R., Fletcher, M., & Schneegurt, M. (2001). Bacterial transport in heterogeneous porous media: Observations from laboratory experiments. *Water Resources Research*, *37*(11), 2699–2707. https://doi.org/10.1029/2001WR000331

Šimůnek, J., Šejna, M., & Van Genuchten, M. T. (1998). *The hydrus-1d software package for simulating the one-dimensional movement of water, heat, and multiple solutes in variably-saturated media.* Int. Ground Water Model. Cent.

Šimůnek, J., & van Genuchten, M. T. (2016). Contaminant transport in the unsaturated zone: Theory and modeling. *The handbook of groundwater engineering* (pp. 221–254). CRC Press.

Šimůnek, J., & Bradford, S. A. (2008). Vadose zone modeling: Introduction and importance. *Vadose Zone Journal*, *7*(2), 581–586. https://doi.org/10.2136/vzj2008.0012

Smith, E., & Hegazy, S. (2006). E. coli transport in soil columns: Implications for reuse of treated wastewater in irrigation. *Water science and technology*, *54*(11-12), 175–182. https://doi.org/10.2166/wst.2006.851

Smith, E., & Badawy, A. (2008). Modelling e. coli transport in soil columns: Simulation of wastewater reuse in agriculture. *Water Science and Technology*, *57*(7), 1123–1129. https://doi.org/10.2166/wst.2008.205

Smith, K., Liu, S., Liu, Y., & Guo, S. (2018). Can china reduce energy for water? a review of energy for urban water supply and wastewater treatment and suggestions for change. *Renewable and Sustainable Energy Reviews*, *91*, 41–58. https://doi.org/10.1016/j.rser.2018.03.051

Soetaert, K., & Petzoldt, T. (2010). Inverse modelling, sensitivity and monte carlo analysis in R using package FME. *Journal of Statistical Software*, *33*(3), 1–28. https://doi.org/10.18637/jss.v033.i03

Soetaert, K., Petzoldt, T., & Setzer, R. W. (2010). Solving differential equations in R: Package deSolve. *Journal of Statistical Software*, *33*(9), 1–25. https://doi.org/10.18637/jss.v033.i09

Spitz, K., & Moreno, J. (1996). *A practical guide to groundwater and solute transport modeling.* University of Texas Press.

Stevik, K. T., Kari, A., Ausland, G., & Fredrik Hanssen, J. (2004). Retention and removal of pathogenic bacteria in wastewater percolating through porous media: A review. *Water Research*, *38*(6), 1355–1367. https://doi.org/10.1016/j.watres.2003.12.024

Stokes, G. G. et al. (1851). On the effect of the internal friction of fluids on the motion of pendulums. *9*, 1–141.

Stuart, C. H., Schwartz, S. A., Beeson, T. J., & Owatz, C. B. (2006). *Enterococcus faecalis*: Its role in root canal treatment failure and current concepts in retreatment. *Journal of endodontics*, *32*(2), 93–98. https://doi.org/10.1016/j.joen.2005.10.049

Tallon, P., Magajna, B., Lofranco, C., & Leung, K. T. (2005). Microbial indicators of faecal contamination in water: A current perspective. *Water, air, and soil pollution*, *166*(1), 139–166. https://doi.org/10.1007/s11270-005-7905-4

Team, R. C. et al. (2013). R: A language and environment for statistical computing.

Thomann, R. V., & Mueller, J. A. (1987). *Principles of surface water quality modeling and control*. Harper & Row Publishers.

Tideman, E. (1996). *Watershed management : Guidelines for indian conditions*. Omega Scientific Publishers.

Toride, N., Leij, F., Van Genuchten, M. T., et al. (1995). *The cxtfit code for estimating transport parameters from laboratory or filed tracer experiments* (Vol. 2). U. S. Salinity Laboratory Agricultural Research Service. U. S. Department of Agriculture, Riverside, California.

Toride, N., Leij, F. J., & van Genuchten, M. T. (1993). A comprehensive set of analytical solutions for nonequilibrium solute transport with first-order decay and zero-order production. *Water Resources Research*, *29*(7), 2167–2182. https://doi.org/10.1029/93WR00496

van der Hoek, J. P., Bertelkamp, C., Verliefde, A., & Singhal, N. (2014). Drinking water treatment technologies in europe: State of the art–challenges–research needs. *Journal of Water Supply: Research and Technology—AQUA*, *63*(2), 124–130. https://doi.org/10.2166/aqua.2013.007

Van Genuchten, M. T., & Alves, W. (1984). *Analytical solutions of the one-dimensional convective-dispersive solute transport equation*. US Department of Agriculture, Agricultural Research Service.

Vergine, P., Lonigro, A., Salerno, C., Rubino, P., Berardi, G., & Pollice, A. (2017). Nutrient recovery and crop yield enhancement in irrigation with reclaimed wastewater: A case study. *Urban Water Journal*, *14*(3), 325–330. https://doi.org/10.1080/1573062X.2016.1141224

Vergine, P., Salerno, C., Libutti, A., Beneduce, L., Gatta, G., Berardi, G., & Pollice, A. (2017). Closing the water cycle in the agro-industrial sector by reusing treated wastewater for irrigation. *Journal of Cleaner Production*, *164*, 587–596. https://doi.org/10.1016/j.jclepro.2017.06.239

Weiss, T. H., Mills, A. L., Hornberger, G. M., & Herman, J. S. (1995). Effect of bacterial cell shape on transport of bacteria in porous media. *Environmental Science & Technology*, *29*(7), 1737–1740. https://doi.org/10.1021/es00007a007

World Health Organisation. (2006). *WHO Guidelines for the safe use of wastewater, excreta and greywater - Volume 4* (tech. rep.). World Health Organization.

Xu, S., Gao, B., & Saiers, J. E. (2006). Straining of colloidal particles in saturated porous media. *Water Resources Research*, *42*(12). https://doi.org/10.1029/2006WR004948

Xu, S., Liao, Q., & Saiers, J. E. (2008). Straining of nonspherical colloids in saturated porous media. *Environmental science & technology*, *42*(3), 771–778. https://doi.org/10.1021/es071328w

Xu, S., & Saiers, J. E. (2009). Colloid straining within water-saturated porous media: Effects of colloid size nonuniformity. *Water resources research*, *45*(5). https://doi.org/10.1029/2008WR007258

Note on the commencement of the doctoral procedure

1. I hereby assure that I have produced the present work without inadmissible help from third parties and without aids other than those stated; ideas taken directly or indirectly from external sources are identified as such.

2. When selecting and evaluating the material and also when producing the manuscript, I have received support from the following persons: Prof. Dr. rer. nat. habil. Thomas U. Berendonk, Prof. Dr. habil. Rudolf Liedl, Dr.-Ing. Martin Binder, and Dr. David Kneis.

3. No further persons were involved in the intellectual production of the present work. In particular, I have not received help from a commercial doctoral adviser. No third parties have received monetary benefits from me, either directly or indirectly, for work relating to the content of the presented dissertation.

4. The work has not previously been presented in the same or a similar format to another examination body in Germany or abroad, nor has it - unless it is a cumulative dissertation - been published.

5. If this concerns a cumulative dissertation in accordance with §10 Section 2, I assure compliance with the conditions specified there.

6. I confirm that I acknowledge the doctoral regulations of the Faculty of Environmental Sciences of the Technische Universität Dresden.

.....
Place, Date

.....
Signature (Aparna Chandrasekar)

Übereinstimmungserklärung

Übereinstimmungserklärung:

Die Übereinstimmung dieses Exemplars mit dem Original der Dissertation zum Thema: „Transport of *Enterococcus faecalis* JH2-2 through sandy sediments“ wird hiermit bestätigtbereinstimmungserklärung:

****

I hereby confirm the accordance of this copy with the original dissertation on the topic: "Transport of *Enterococcus faecalis* JH2-2 through sandy sediments"

.....
Place, Date

.....
Signature (Aparna Chandrasekar)

List of conference presentations and journal publications

Conference Participations

1. A. Chandrasekar, T. U. Berendonk, I. Kampouris, D. Cacace, D. Kneis, M. Binder, R. Liedl, “Empirically Evaluate the Impact of Certain Water Quality Parameters on the Fate of Enterococcus faecalis JH2-2 transport in Sandy Sediments”, 20- 24 October 2019, 11th Micropol and Ecohazard Conference, Seoul, Republic of Korea (Poster Presentation)

2. A. Chandrasekar, D. Kneis, M. Binder, S. Krenek, T.U. Berendonk, R. Liedl, “A combined modelling and experimental approach to study relevant bacterial subsoil processes”, 10-12 October 2018, XENOWAC II, Challenges and Solutions related to Xenobiotics and Antimicrobial Resistance in the Framework of Urban Wastewater Reuse: Towards a Blue Circle Society Limassol, Cyprus (Oral Presentation)

3. A. Chandrasekar, D. Kneis, R. Liedl, "Modelling subsurface transport of bacteria in the context of wastewater reuse: Hydrodynamic processes", 3-7 June 2018, Computational Methods in Water Resources XXII, Bridging gaps between data, models and predictions, Saint-Malo, France (Poster presentation)

4. A. Chandrasekar, D. Kneis, R. Liedl, "Modelling the transport of antibiotic resistant bacteria in the subsurface", 21-24 March 2018, 26th Meeting of the German Association for Hydrogeology 2018, Bochum, Germany (Poster presentation)

Journal Publications

1. Chandrasekar, A., Binder, M., Liedl, R., & Berendonk, T. (2021). Determining the impact of flow velocities on reactive processes associated with *Enterococcus faecalis* JH2-2. *Water Science and Technology*, 85(1), 485–495. https://doi.org/10.2166/wst.2021.611 (**Chapter 3**)

2. Chandrasekar, A., Binder, M., Liedl, R., & Berendonk, T. U. (2021). Reactive-transport modelling of *Enterococcus faecalis* JH2-2 passage through water saturated sediment columns. *Journal of Hazardous Materials*, 413, 125292. https://doi.org/10.1016/j.jhazmat.2021.125292 (**Chapter 4**)

Proportion of own contributions in Journal Publications and thesis

- Idea and conception - 70%
- Literature research - 90%
- Planning of laboratory experiments - 70%
- Data collection (execution of experiments / sample analyses) - 100%
- Evaluation of the measured data in laboratory experiments and model fitting - 80%
- Writing the initial version of the manuscripts - 70%
- Revision and finalization of the manuscripts - 90%

I received support services in the selection and evaluation of the material as well as in the production of the manuscript. In particular, this took place in the preparation of the peer-reviewed technical articles that are part of this cumulative dissertation. My own contribution to the peer-reviewed articles, as well as the individuals also involved, are indicated above. Apart from this, the model setup, and experiment planning (Chapter 2), were scientifically supported in parts by Dr. David Kneis. In addition, I received support from Dr. David Kneis in writing the initial versions of the two manuscripts. Furthermore, I received help from Dr. Norbert Kreuzinger during my research stay at the Institute for Water Quality, Resources and Waste Management, Technische Universität Wien. He primarily guided me on set up for column experiments, and quantification of bacteria.

Acknowledgements

"If I have seen further it is by standing on the shoulders of Giants".
-Sir. Isaac Newton

The journey of my Doctoral degree has only been possible through the content guidance of many giants of this field. They have not only provided me with their valuable time, knowledge, expertise and resources; but also invaluable emotional support and guidance. **To all the supervisors, reviewers, and mentors, I hope that I will be able to achieve great heights and hold the torch for the progress of this field like you have.**

Prof. Dr. habil. Rudolf Liedl, whose support and guidance as my PhD supervisor is incalculable. He guided me on the modelling aspect of my work. Furthermore, he has helped me to critically evaluate and interpret my experimental results. In addition, he always encouraged me to attend various conferences and training events through the course of my PhD. His positive encouragement and constant support has invariably shaped my thinking and approach to my work. His belief in my abilities has deeply impacted my outlook on myself, and my life.

Prof. Dr. rer. nat. habil. Thomas. U. Berendonk whose ideas and creative thought have provided me support on working with two prestigious EU funded research projects, with a large and excellent network of scientists and researchers. As my PhD supervisor, he has guided me at key junctions in my PhD, and helped me with my experimental methodology and design. He has (directly and indirectly) introduced me to various brilliant researchers, and scientists from all over the world. The communications with these researchers has provided various fruitful outcomes - whether it was just to obtain data, exchange ideas, or dance at the end of the conference. His positive support, friendly advises and constant encouragement for excellence enabled me to push my boundaries, and work harder and achieve my goals.

I have been very lucky to have such supportive supervisors for my Thesis work. They have constantly encouraged me to test and push my own boundaries. I couldn't have asked for a better start towards my career.

Prof. Dr. Despo Fatta-Kassinos has constantly helped me and pushed me to achieve my goals, despite being geographically far away in Cyprus. She has invested a lot of effort into positively motivating me into reaching the best of my abilities. Your experience and energy has inspired me to reach further than I ever imagined I could.

I would like to specifically thank **Prof. Dr. Traugott Scheytt and Prof. Dr. Gertjan Medema** who have spent considerable time and energy in reviewing my thesis and providing me their valuable comments to improve my thesis. In addition, I would also like to thank all the **anonymous reviewers who have been involved in reviewing my publications**. Your stringent reviews have helped me significantly improve the quality of my papers.

Dr.-Ing. Martin Binder, your help with my work, your detailed comments and scientific expertise, have shaped my critical thinking skills and increased my scientific aptitude. For this I will be ever grateful.

Through the course of my PhD I have been lucky to be involved with two huge EU funded project and be able to network with the intelligent scientists and researchers associated with the projects. I would like to thank **the entire network of ANSWER and DSWAP projects**, for the support and opportunities that have elevated my career as an early stage researcher. In addition, I would like to thank **all my colleagues from the Institute of Hydrobiology and Institute of Groundwater Management**. My colleagues, and friends who have helped me for setup of laboratory equipment, formulating models, writing my paper, or even just grabbing a cup of coffee - thank you for all the pleasant memories.

I would like to send my thanks to my **family: mother, father, sisters and husband**. Their incredible emotional support has helped me push through the hard days, and celebrate the good days. Their constant encouragement and strength during hard times has been my source of comfort, and with them lies my happy place. Thank you for everything that you have done for me.

Last but not the least I would like to thank the funding sources: the European Union's Horizon 2020 Research and Innovation Programme under the Marie Skłodowska-Curie grant agreement No 675530, and the PRIMA program supported by the European Union under grant agreement No. 1822.